DEVELOPMENTAL REQUIREMENT AND REGULATION OF THE DROSOPHILA HOMOLOG OF *MCPH1*, A HUMAN MICROCEPHALY GENE

By

Jamie Lyn Rickmyre

Dissertation

Submitted to the Faculty of the

Graduate School of Vanderbilt University

in fulfillment of the requirements

for the degree of

DOCTOR OF PHILOSOPHY

in

Cell and Developmental Biology

August, 2010

Nashville, Tennessee

Approved:

Laura Lee

Kathleen Gould

David Cortez

Ethan Lee

For my family

ACKNOWLEDGEMENTS

I am in deep gratitude to many people, without whom this accomplishment would never be possible. First and foremost, I am indebted to my mentor, Laurie Lee, for providing guidance and "grinding my beans" every step of the way. Thank you for introducing me to the world of Drosophila and for teaching me how become a scientist, but mostly, thank you for your generosity. I won't forget how you provided shelter for me when I was homeless (for three weeks). Ethan Lee, the co-leader of the lab, was always there to provide advice and exciting new ideas, but also to introduce us all to the world of Tribbles. I want to thank my all of my committee members, Chris Hardy, Kathy Gould, Daniela Drummond-Barbosa, Dave Cortez, and Ethan Lee for keeping me on my toes.

I have been fortunate to work with many people during my time in the Lee labs. Julie Merkle, I'm unable to express how much I appreciate her friendship. She always lent an ear for my problems and seemingly shared my thoughts. Curtis Thorne introduced me to Bob, Frank, and the Pancakes House. I look forward to the day he can match my mad MarioKart skills. To Kristin, Michael, and Curtis, my classmates who joined at the same time as I, I'm thankful that we were all guinea pigs together as the first students in the Lee labs. To Ali, Jeanne, and Kelly, I have two words: Woo woo! The rest of the members, past and current, have always made the lab an interesting place to work.

I'm thankful for my family and friends; they've always had faith in me. My mom and dad have always been supportive and available for advice, and I've been

blessed to have my brother living in the same city for the past seven years. I hope I will continue to make you all proud. My wonderful group of friends outside of the science world have kept me laughing along the way, and I will continue letting them think I know everything about every natural occurrence in the world.

Last but not least, to my best friend, Chris Cselenyi. Your friendship over the past several years has meant more to me than you'll know. Few people know how to put me in my place like you, and even fewer can make me laugh. I look forward to watching you establish your career and hope to remain your friend for a lifetime.

TABLE OF CONTENTS

Page:

LIST OF TABLES

LIST OF FIGURES

CHAPTER I

INTRODUCTION

Introduction

DNA is the code of life responsible for the production of all proteins, from bacteria to the animal kingdom. The entire genome is made up of a code consisting of only four different nucleotides, the basic building blocks of DNA structure, and gives rise to genes and regulatory sequences that determine the proteins to be made within the cell. The genes are transcribed into messenger RNA that, when fully processed, can be translated into proteins, which compose the majority of cellular contents and account for enzymatic reactions within the cell. Genetic mutations affecting protein structure or production, and that result in greater fitness and overall cell survival, have been occurring since the first cell was formed billions of years ago. Spontaneous mutations that do not lead to positive changes, however, are responsible for a vast number of diseases, including cancer, an out-of-control growth of cells that most often arises from genetic instability and failure to properly repair DNA.

It is here in this dissertation that I present my research, all aimed to understand the role of MCPH1, a protein required for genomic stability in multicellular organisms. I begin by describing the consequence of a null mutation of *mcph1* and the genomic catastrophe that occurs in developing Drosophila embryos. Next, I present the cell-cycle regulation of MCPH1 by the Anaphase Promoting

Complex, a multi-subunit structure that targets proteins for ubiquitin-mediated degradation. Finally, I present a screen for binding partners of Drosophila MCPH1 in an effort to place the protein within a molecular framework.

The cell cycle

All cells arise from other cells. Daughter cells must inherit cellular components that will ensure their survival and in the case of organisms, to function as part of a whole. Cellular contents such as organelles, proteins, and structural components are produced throughout the cell cycle and are distributed to daughter cells during cell division (Morgan, 2007). DNA in the form of chromosomes exists in two copies and must be precisely replicated before being equally divided into daughter cells. Canonical cell cycles consist of four stages: an initial gap phase or G1 which allows for growth, DNA replication during the synthesis or S phase, a secondary growth period or G2, and finally M phase which consists of mitosis, in which duplicated chromosomes are equally divided, and cytokinesis, the actual cell division into two daughter cells (Figure 1.1). The term interphase is used to describe the period of time between mitoses.

The G1 and G2 gap phases give the cell the time it needs to allow for duplication of cellular components that will eventually be divided into the daughter cells, and in a canonical cell cycle, account for more than 50% of the time. Furthermore, at the end of the gap phases, checkpoints are in place to ensure the cell is ready to proceed to the next phase (to be described in more detail later).

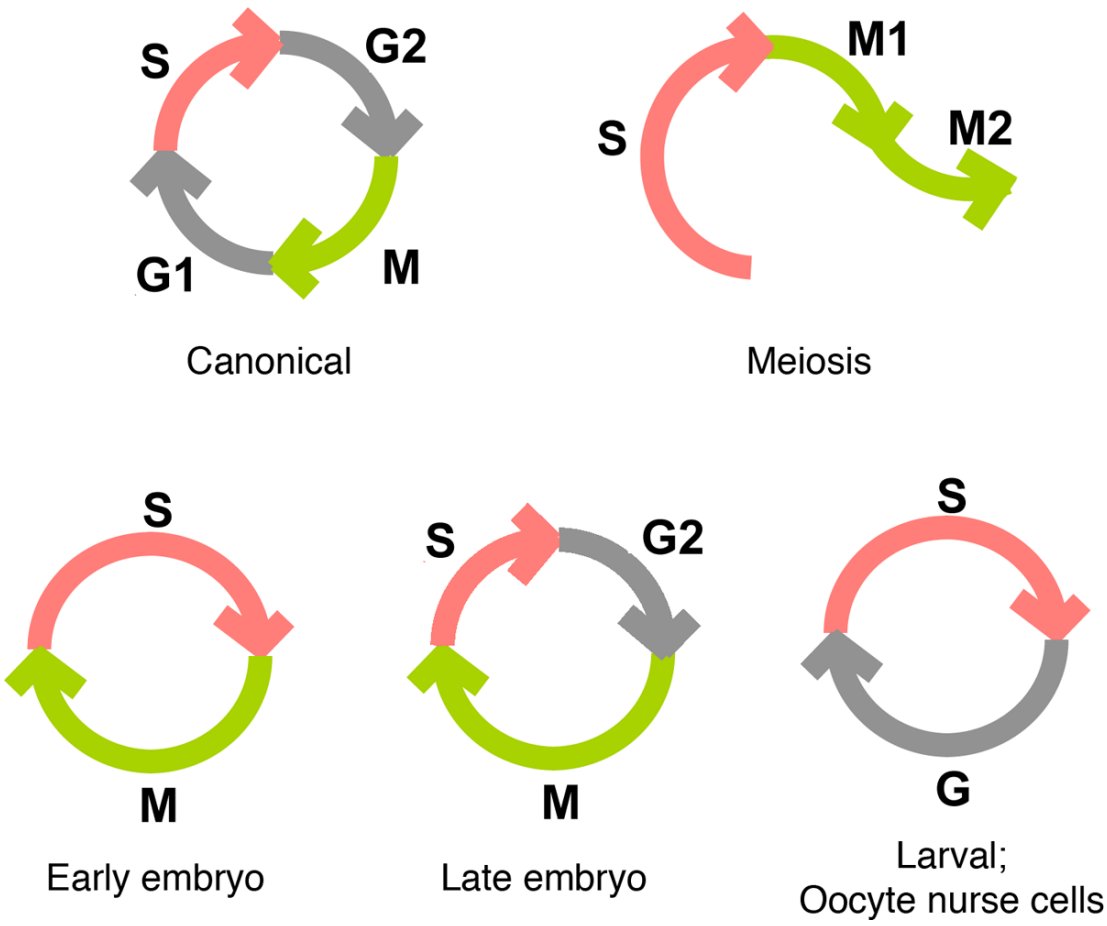

Figure 1.1. Variations of the cell cycle during Drosophila development. Cartoon depicting the types of cell cycles found in Drosophila.

Briefly, prior to replicating DNA during S phase, a DNA damage checkpoint ensures the cell will not begin replicating damaged chromosomes. Checkpoints at the G2/M transition also ensure chromosomes are not damaged and that the cells have duplicated other components prior to the start of cell division.

Variations of the canonical cell cycles exist depending on the needs of particular types of cells (Lee and Orr-Weaver, 2003). For example, during meiosis, germ cells replicate chromosomes once producing 4n copies. This is followed by two divisions, meiosis I and meiosis II, with the result of a single chromosome in each germ cell (Figure 1.1). Expedited cycles lacking gap phases exist for some developing organisms to ensure survival (Figure 1.1). Other cells may require repeated rounds of replication without division, also known as endocycles, and function as transcriptional powerhouses to provide mRNAs and proteins for neighboring cells (Figure 1.1). This is the case during larval development in Drosophila as well as in oocyte development.

Cell-cycle control

Progression through the cell cycle is controlled by Cyclin Dependent Kinase or Cdk activity. In Drosophila and vertebrates, four Cdk complexes exist which are important for cell cycle control and are activated when bound to a Cyclin (Morgan, 1997). Cdk2/Cyclin E promotes entry into S phase while Cdk2/Cyclin A is required for its completion. Additionally, Cdk1/Cyclin A activity is required for entry into mitosis, promoting activation of Cdk1/Cyclin B which is required during early

mitosis for proper spindle formation and alignment of chromosomes along the metaphase plate. Cdk4/Cyclin D functions during G1 to promote growth.

Control over Cdk/Cyclin activity is mediated by inhibitory phosphorylation of the Cdk by Wee1 kinase, which is reversed by the phosphatase Cdc25 (Morgan, 1997). In addition, Cdk activating kinases and Cdk inhibitor proteins further regulate Cdk activity but will not be discussed in detail. Another mechanism controlling Cdk activity is ubiquitin-mediated proteolysis of cyclins (King et al., 1996). In the cell, addition of ubiquitin moieties to proteins promotes a wide variety of cellular processes, including proteolysis. The addition of ubiquitin occurs in three steps. First, ubiquitin is covalently attached to the ubiquitin-activating enzyme, E1, and is then transferred to an E2, ubiquitin-conjugating enzyme. Finally, an E3 ubiquitin ligase recognizes substrates to be ubiquitylated and allows the transfer of ubiquitin from the E2 to a lysine, K, residue on the substrate. In ubiquitin-mediated proteolysis, this process is repeated creating a chain where successive moieties are added to the lysine 48 of the previous ubiquitin. These ubiquitin chains are recognized by the 26S proteasome and substrates are subsequently degraded (Figure 1.2).

Two multi-subunit E3 ubiquitin ligases are involved in promoting ubiqutin-mediated degradation of cell cycle components. The SCF complex degrades phosphorylated substrates during S phase and G2 including Cyclin E in addition to other cell-cycle regulators (Cardozo and Pagano, 2004). At the metaphase to anaphase transition and during G1, The Anaphase Promoting Complex, or APC,

another multi-subunit E3 ubiquitin ligase targets substrates for degradation and is described in more detail in the next section (Harper et al., 2002).

The Anaphase Promoting Complex

The APC consists of approximately 12 subunits and includes a RING (really interesting new gene) finger subunit, APC11, which binds the E2, and a subunit with a Cullin homology domain, APC2, that acts as a scaffold to allow for proper ubiquitin ligase activity (Thornton and Toczyski, 2006). APC must be activated by one of its two effectors, Cdc20 and Cdh1. Cdc20 activates APC at the metaphase to anaphase transition where it first triggers the ubiquitylation of Securin as well as the mitotic cyclins. Degradation of Securin allows Separase to cleave cohesion bonds between sister chromatids, promoting the onset of anaphase. At the end of mitosis, APC is activated by Cdh1, further targeting Cyclin B for degradation to ensure the inactivity of Cdk1, and other substrates such as the Aurora and Polo-like kinases as well as Cdc20.

APC recognizes its substrates with the aid of its activators (Figure 1.2). Both APC-Cdc20 and APC-Cdh1 recognize substrates with functional destruction or D boxes (Thornton and Toczyski, 2006). The D box sequence consists of an arginine, two amino acids, and a leucine, or RXXL, and is a common motif found in many proteins; therefore, it should not alone be used to identify APC substrates and must be confirmed experimentally. A second common motif, the KEN box is recognized only by APC-Cdh1. In many cases, the lysine, glutamic acid, and asparagine of the KEN sequence is followed by one to three amino acids and a proline (Feine et al.,

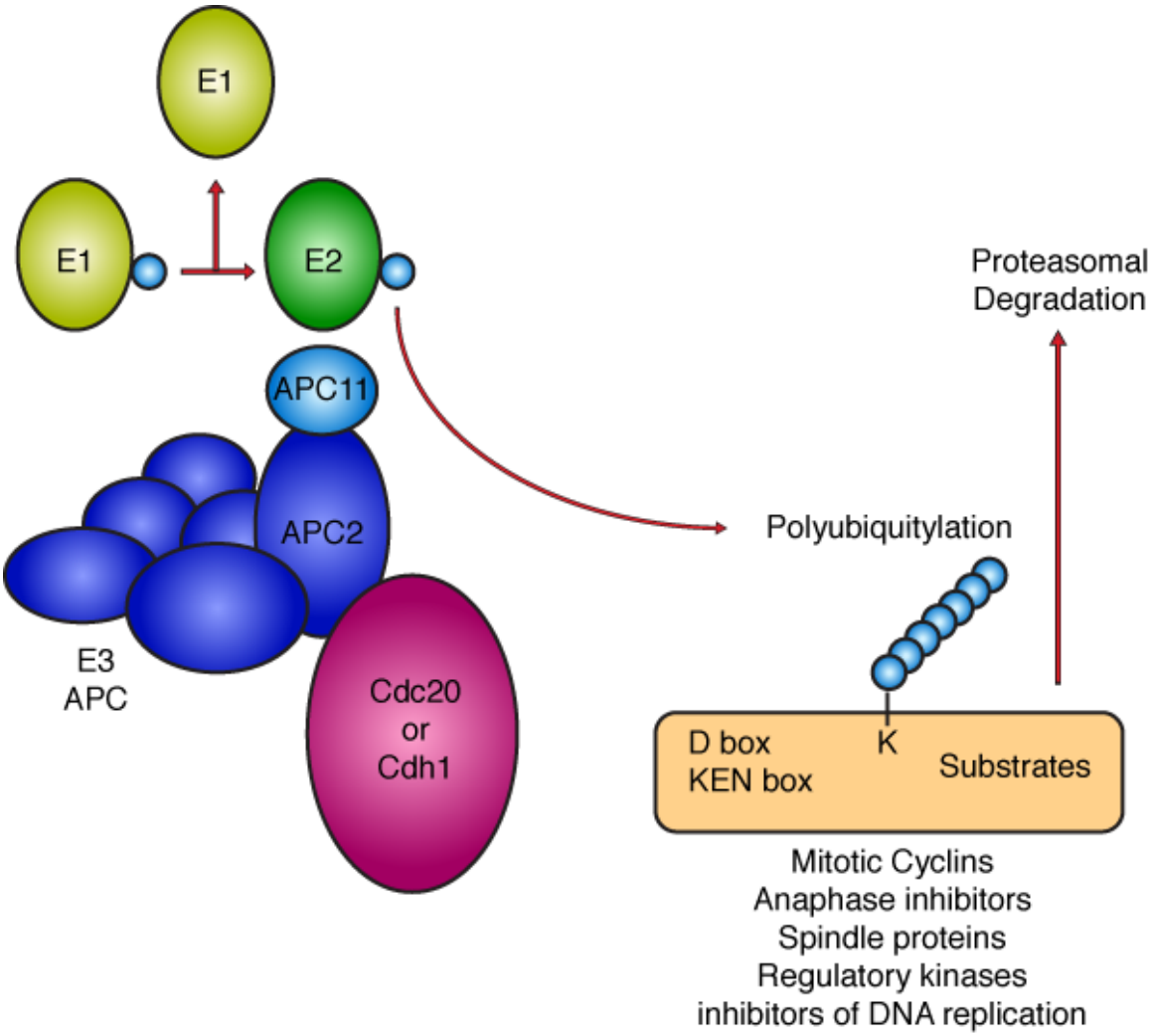

Figure 1.2. The Anaphase Promoting Complex. Cartoon depicting the process of ubiquitylation via the APC. E1 ubiquitin-activating enzyme transfers ubiquitin to E2 ubiquitn-conjugating enzyme. E3 APC activated by Cdc20 or Cdh1 facilitates the transfer ubiquitin to a lysine residue on a D box or KEN box containing substrate, targeting it for degradation by the 26S proteasome.

2007). Other motifs have been recognized, including the A-box and the O-box, though exactly how the APC recognizes its substrates remains a mystery (Simpson-Lavy et al., 2010). At the end of G1, the APC itself is targeted for destruction, ensuring that cyclin levels can rise again to promote S phase.

DNA damage response

DNA damage such as double-stranded breaks may lead to genomic instability if not repaired. Damage may arise spontaneously during cellular processes like replication but may also occur in the presence of DNA damaging agents like ultra violet light or X-rays (Karagiannis and El-Osta, 2004). The classic checkpoint associated with DNA damage and incomplete DNA replication occurs at the G2-M transition in many cell types (including Drosophila, mammalian cells, and fission yeast) as a mechanism to ensure that the correct genetic material is transmitted to daughter cells during mitosis (for review, see Chen and Sanchez, 2004). When DNA damage or incomplete replication is sensed in a cell, the ATM (Ataxia telengiectasia mutated) and ATR (ATM and Rad3-related) kinases are activated and phosphorylate Chk1 and Chk2, which then phosphorylates downstream targets to cause a cell cycle arrest and activate repair. One such target is Cdc25, the phosphatase that removes the inhibitory phosphate group from Cdk1 in order for cells to enter into mitosis.

Chromatin modifications

Within the nucleus, DNA is packaged into chromatin fibers with the help of histone octomer. Two units each of Histones H3, H4, H2A, and H2B make up this

structure around which DNA is wound. This Histone octamer and DNA structure is called a nucleosome and is the first level of DNA packaging within the cell (Bednar et al., 1998). Nucleosomes can be further packaged depending on the needs of the cells and require help from chromatin remodeling complexes like SWI-SNF as well as modifications that occur directly on the histones (Peterson and Tamkun, 1995). For example, highly transcribed regions or sites of DNA damage may be less tightly packaged to allow access to the DNA by the necessary enzymes. In addition, nucleosomes may contain histone variants which are required for specific regions of the chromatin such as the centromere. The histone variant H2AX is commonly found in the region of DNA breaks (Khorasanizadeh, 2004).

During mitosis, very dramatic packing occurs as chromatin is condensed into chromsomes. This step is necessary to ensure sister chromatids can divide into the daughter cells without getting tangled or damaged. During prophase, sister chromatids begin to condense but are not resolved, appearing as a single rod. By metaphase, sister chromatids are fully resolved, each with distinguishable arms. One player in the process of sister chromatid resolution is Topoisomerase II, which aids in the detcatenation or untangling of sister chromatids (Berger and Wang, 1996). Multi-subunit complexes known as Condensins participate in further chromosome condensation (Hirano, 2005). There are two Condensin complexes: Condensin I and Condensin II. In early mitosis, nuclear Condensin II promotes chromosome condensation during prophase. Upon nuclear envelope breakdown, Condensin I, which normally resides in the cytoplasm, gains access to the

condensing chromatin, further resolving the sister chromatids prior to the onset of anaphase, when sister chromatids are separated.

Autosomal Recessive Primary Microcephaly

Microcephaly describes the condition in which an individual's head circumference is four or more standard deviations below the mean (for review, see Kumar et al., 2002; Woods, 2004). Head size is an indicator of brain size because outward pressure of the developing brain causes cranial vault enlargement. Primary microcephaly (occurring by 32 weeks of gestation) is likely caused by increased apoptosis during neuronal development or decreased production of neurons whereas secondary microcephaly (occurring after birth) is due to reduced dendritic connections (Woods, 2004). As a result, individuals with primary microcephaly are born with brains that are architecturally normal but lack several layers of the cerebral cortex (Figure 1.3). Causes of primary microcephaly include environmental (e.g. infection or maternal alcohol consumption) and genetic factors. To date, seven loci have been linked to autosomal recessive forms of primary microcephaly (MCPH), and five have been mapped to genes (*Microcephalin*, *ASPM*, *Cdk5rap2*, *Cenpj,* and *STIL*). All except *STIL* have roles or hypothesized roles in the cell cycle and homologs in Drosophila.

ASPM is the homolog of Drosophila *abnormal spindle* (*asp*), a microtubule-associated protein necessary for centrosomes to function as microtubule organizing centers (do Carmo Avides and Glover, 1999; Ripoll et al., 1985; Saunders et al., 1997). *Cdk5rap2* is the homolog of a core centrosomal component in Drosophila,

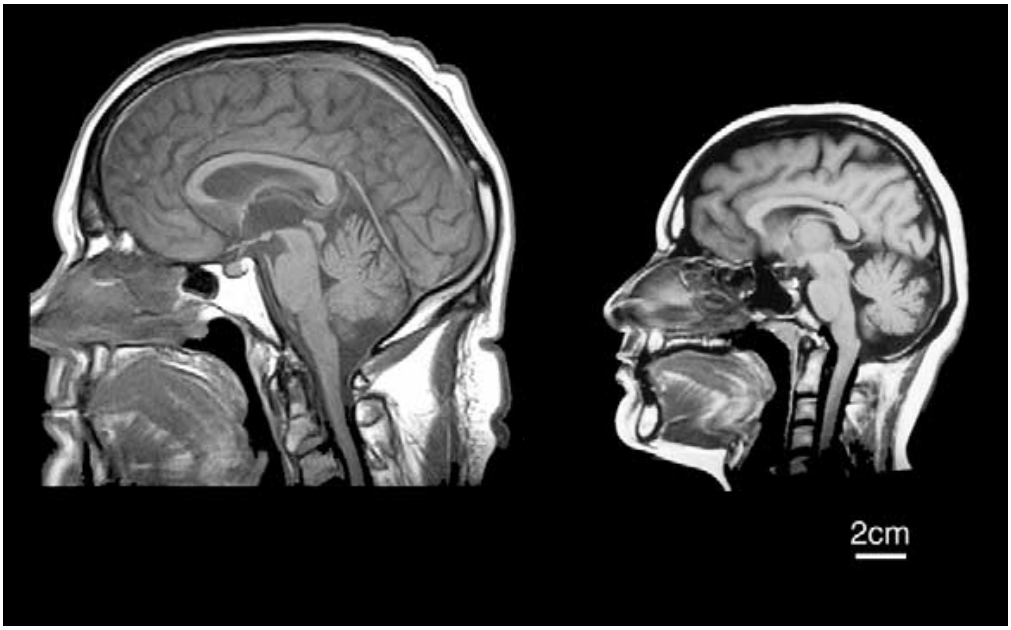

Figure 1.3. Comparison of brain size in subjects with or without primary microcephaly. MRI reveals brain that is much smaller in age- and sex-matched microcephalic patient. Adapted from Ponting and Jackson (2005).

centrosomin, which interacts with the γ-tubulin ring complex (γTuRC) responsible for microtubule nucleation during mitosis (Li and Kaufman, 1996; Megraw et al., 1999; Terada et al., 2003). CENPJ also associates with γTuRC and inhibits microtubule assembly (Hung et al., 2004). *Dsas-4*, the Drosophila homolog of *CENPJ*, is required for centrosome integrity. *Dsas-4* mutants lack centrioles and cilia, displaying defects in their sensory neurons (Basto et al., 2006). Furthermore, approximately 30% of the neuronal precursor asymmetric divisions of the developing Drosophila brain fail. Finally, the zebrafish homolog of human *STIL* encodes a centrosomal protein required for proper spindle formation (Pfaff et al., 2007).

Microcephalin

Members of consanguineous families in northern Pakistan with primary microcephaly were found to have a nonsense mutation in the *microcephalin*, or *MCPH1,* gene resulting in a severe truncation near the amino terminus of the protein (Jackson et al., 2002; Woods et al., 2005). MCPH1 contains three BRCT (BRCA1 C-terminal) domains: one N-terminal and two C-terminal. BRCT domains, which are 80-100 amino acids in length, can bind to double-stranded DNA (dsDNA) breaks and form homo- or hetero-dimers (Huyton et al., 2000). It was reported that BRCT domains preferentially bind to phosphorylated targets of ATM/ATR kinases (Manke et al., 2003). Many BRCT domain-containing proteins are known to participate in the DNA damage response. For example, XRCC1, a DNA repair protein, has a BRCT domain that interacts with DNA ligase III (Taylor et al., 1998), and BRCA1 has

tandem BRCT motifs at its carboxyl terminus that bind to a DNA repair helicase, BACH1 (Yu et al., 2003). Thus, MCPH1 is hypothesized to play a cell cycle role because it contains BRCT domains.

Several groups have now discovered that MCPH1 plays a role in the response to DNA damage. Depletion of MCPH1 in HEK293 or U2OS cells by RNA interference was reported to reduce levels of BRCA1 and Checkpoint kinase 1 (Chk1), thereby affecting intra-S-phase and G2-M checkpoints (Xu et al., 2004; Lin et al., 2005). MCPH1 was further shown to participate within the response to DNA damage functioning directly in the ATR/Chk1 pathway; however, reports conflict on whether MCPH1 functions upstream of ATR or downstream of Chk1. One study, which suggested a downstream role, determined that MCPH1 could bind Chk1 *in vitro*, inhibit Cdc25 activity, and prevent entry into mitosis (Alderton et al., 2006). Additionally, MCPH1 was found to promote inhibitory phosphorylation of Cdk1 independently of ATR and Chk1 (Alderton et al., 2006).

In contrast, several groups have discovered that MCPH1 functions early in the response to DNA damage, localizing to sites of double stranded DNA breaks by binding to phospho-H2AX (Wood et al., 2007; Jeffers et al., 2008). Once recruited, MCPH1 further mediates the damage response. First, MCPH1 binds RPA that in turn recruits ATR-ATRIP, promoting an ATR damage response cascade (Rai et al., 2006). Additionally, MCPH1 brings in the BRCA2-Rad51 complex to initiate repair (Wu et al., 2009). The ability of MCPH1 to localize to dsDNA breaks or irradiation-induced foci is dependent upon its C-terminal BRCT domains (Wood et al., 2007; Jeffers et al., 2008). MCPH1 also acts as a transcriptional regulator of E2F1, promoting the

transcription of many DNA response and repair genes such as Chk1, BRCA1, p73, and Rad51 (Yang et al., 2008).

Patients homozygous for a severely truncating mutation in *MCPH1* exhibit premature chromosome condensation (characterized by an abnormally high percentage of lymphocytes in a prophase-like state), which suggests a role for Microcephalin in the control of cell-cycle timing (Trimborn et al., 2004). In addition to condensing too soon, chromosomes also fail to decondense in a timely manner at the end of mitosis (Trimborn et al., 2004). Further studies revealed that MCPH1 negatively regulates the Condensin II complex to prevent premature condensation (Trimborn et al., 2006). Whereas the C-terminal BRCT domains were found to be important for the DNA damage response role of MCPH1, the N-terminal BRCT domain is required to prevent the condensation defect (Wood et al., 2008; Richards et al., 2009). Thus, MCPH1 appears to have another cell-cycle role distinct from its participation in the DNA damage response. The capacity of MCPH1 to promote changes in chromatin structure, however, has been linked to its capacity to promote DNA repair. MCPH1, together with the Condensin II complex, is required for homologous recombination repair (Wood et al., 2008). In addition, MCPH1 binds directly with the ATP-dependent chromatin remodeling complex, SWI-SNF, in the presence of DNA damage (Peng et al., 2009). This interaction promotes chromatin relaxation and provides increased accessibility for repair enzymes to the damaged DNA. Taken together, these data suggest MCPH1 functions somewhat as a cellular middleman, linking the state of the chromatin to DNA repair.

MCPH1 has been observed to have a role in telomere maintenance as well (Lin and Elledge, 2003; Kim et al., 2009). In addition to the observations of nuclear MCPH1, several groups have localized MCPH1 to centrosomes (Zhong et al., 2006; Brunk et al., 2007; Jeffers et al., 2008; Tibelius et al., 2009). In one study, centrosomal MCPH1 is required to recruit Chk1 to prevent early Cdk1/Cyclin B activation (Tibelius et al., 2009).

One of the hallmarks of cancer is genomic instability, and MCPH1 has been found to be downregulated in several human cancer cell lines (Rai et al., 2006). Interestingly, it has been suggested that too much MCPH1 also leads to a developmental defect in the form of autism (Glancy et al., 2008; Ozgen et al., 2009). Recently, the first MCPH1 mouse models were described and confirmed results from previous studies. In one study, an MCPH1 knockout mouse was created, resulting in severe DNA repair defects (Liang et al., 2010). The mice were retarded in growth and sterile. A second study established a hypomorphic model with defects only in chromosome condensation (Trimborn et al., 2010).

Evolution of *MCPH* genes

Recent reports indicate that *microcephalin* and *ASPM*, another *MCPH* gene, are among the most rapidly evolving genes in higher organisms (Evans et al., 2004; Ponting and Jackson, 2005; Wang and Su, 2004). *microcephalin* and *ASPM* both have high rates of adaptive amino acid changes from early primates to humans. It has been hypothesized that these genes are involved in brain size determination because severe truncation mutations in either of these genes lead to brain sizes

similar to that of early hominids, and they are expressed in the forebrains of fetal mice during a period of extensive neurogenesis. Recently, *Cdk5rap2* and *cenpj*, which have also been identified as *MCPH* genes, were shown to be similarly expressed during mouse brain development (Woods et al., 2005). Thus, it is suggested that these MCPH proteins regulate neurogenic mitoses by controlling microtubule nucleation.

Early Drosophila embryogenesis

Drosophila melanogaster is an ideal model organism for studying the cell cycle in a developmental context. Mutations are easily obtained, the effects of cell cycle mutations are easily observed using fluorescence microscopy, the genome has been sequenced, and there are many tools and techniques available to allow for the rapid mapping and characterization of mutant genes. Early Drosophila embryogenesis consists of thirteen nuclear divisions driven by stockpiles of maternal mRNA and protein that occur in a syncytial blastoderm. The cycles vary from the canonical G1-S-G2-M cycles in that they have no intervening gaps or cytokinesis; instead, they consist of rapidly oscillating cycles of DNA replication and mitosis (~10 minute cycles) (for review, see Edgar and Lehner, 1996; Lee and Orr-Weaver, 2003). These rapid S-M cycles do not depend upon cell growth or zygotic transcription until the fourteenth cycle, at which point cellularization occurs and a G2 phase is introduced (the mid-blastula transition). Cell cycle mutations that are maternal effect-lethal affect the embryos of homozygous females, causing defects during the first thirteen divisions due to a lack of essential cell cycle proteins that

must be provided maternally. The genetic tractability of the fly as well as these early developmental characteristics make it easy to identify genes that are essential for normal S-M cell cycles.

The *Xenopus laevis* model system

Xenopus laevis is an important model system for studying the cell cycle. Unfertilized eggs arrest during meiosis at metaphase II, with high Cdk1-Cyclin B activity but inactive APC-Cdc20. Fertilization or treatment with calcium leads to APC-Cdc20 activation and degradation of Cyclin B, releasing the metaphase II arrest (Draetta *et al.*, 1989; Murray *et al.*, 1989; Ferrell, 1999). Extracts can be made from the eggs to study biological processes in a cell-free, easily manipulated environment. In this dissertation, we activate the APC either by addition of calcium to create APC-Cdc20 extracts, or by addition of Cdh1 to activate APC-Cdh1.

The *Xenopus* embryo is also an important model system for the study of development. Cleavage planes of fertilized, developing embryos give rise to easily identifiable blastomeres that can be manipulated by injection of RNA, drugs, or morpholinos. The first 12 cell cycles of early embryogenesis (~30 minutes each) consist of alternating rounds of DNA replication and mitosis without gap phases. Arrested cells do not undergo apoptosis until after the 13th cycle when cell division slows down and becomes asynchronous, marking the midblastula transition (MBT) (Newport and Kirschner, 1982a, b). Because the basic mechanisms of early embryonic development are highly conserved among vertebrates, data obtained with *Xenopus* may be readily extrapolated to humans.

CHAPTER II

DEVELOPMENTAL REQUIREMENT FOR MCPH1 IN THE EARLY DROSOPHILA EMBRYO

The contents of this chapter have been published (Rickmyre et al., 2007).

INTRODUCTION

Drosophila melanogaster is an ideal model organism for study of the cell cycle during development (reviewed by Foe et al., 1993; Lee and Orr-Weaver, 2003). Drosophila achieves rapid embryogenesis by using a streamlined cell cycle that is not dependent on transcription or growth. The first 13 embryonic cell cycles are nearly synchronous nuclear divisions without cytokinesis occurring in the shared cytoplasm of the syncytial blastoderm. These cycles differ from canonical G1-S-G2-M cycles in that they have no intervening gaps; instead DNA replication and mitosis rapidly oscillate. Maternal RNA and protein stockpiles drive these abbreviated `S-M' cycles (~10 minutes each). In mammalian embryos, rapid peri-gastrulation divisions that occur later in development share many features and have been proposed to be related by evolutionary descent to early embryonic divisions of flies and frogs (O'Farrell et al., 2004). Thus, advances gained from studies of these streamlined cycles in `simple' model organisms likely have relevance for understanding mammalian cell cycles.

In a genetic screen for regulators of embryonic S-M cycles, we identified the *Drosophila* homolog of a human disease gene, *MCPH1* (*microcephalin*). Mutation of human *MCPH1* causes autosomal recessive primary microcephaly, a developmental disorder characterized by severe reduction of cerebral cortex size (Jackson et al., 2002). *Mcph1* is highly expressed in the developing forebrain of fetal mice, consistent with its proposed role in regulating the number neuronal precursor cell divisions and, ultimately, brain size (Jackson et al., 2002). Human MCPH1 protein is predicted to contain three BRCA1 C-terminal (BRCT) domains (reviewed by Glover et al., 2004; Huyton et al., 2000), which mediate phosphorylation-dependent protein-protein interactions in cell-cycle checkpoint and DNA repair functions.

Several studies have implicated human MCPH1 in the cellular response to DNA damage. The DNA checkpoint is engaged at critical cell-cycle transitions in response to DNA damage or incomplete replication and serves as a mechanism to preserve genomic integrity (reviewed by Nyberg et al., 2002). Triggering of this checkpoint causes cell-cycle delay, presumably to allow time for correction of DNA defects. When a cell senses DNA damage or incomplete replication, a kinase cascade is activated. Activated ATM and ATR kinases phosphorylate their targets, including the checkpoint kinase Chk1, which is activated to phosphorylate its targets. The first clue that MCPH1 plays a role in the DNA damage response came from siRNA-mediated knockdown studies in cultured mammalian cells demonstrating a requirement for MCPH1 in the intra-S phase and G2-M checkpoints in response to ionizing radiation (Lin et al., 2005; Xu et al., 2004). Two recent reports have further implicated MCPH1 in the DNA checkpoint, although puzzling discrepancies remain

to be resolved (reviewed by Bartek, 2006). One report indicates that MCPH1 functions far downstream in the pathway, at a level between Chk1 and one of its targets, Cdc25 (Alderton et al., 2006). Another report (Rai et al., 2006) suggests that MCPH1 is a proximal component of the DNA damage response required for radiation-induced foci formation (i.e. recruitment of checkpoint and repair proteins to damaged chromatin).

Additional functions have been reported for MCPH1. *MCPH1*$^{-}$ lymphocytes of microcephalic patients exhibit premature chromosome condensation (PCC) characterized by an abnormally high percentage of cells in a prophase-like state, suggesting that MCPH1 regulates chromosome condensation and/or cell-cycle timing (Trimborn et al., 2004). A possible explanation for the PCC phenotype is that *MCPH1*-deficient cells have high Cdk1-cyclin B activity, which drives mitotic entry; decreased inhibitory phosphorylation of Cdk1 was found to be responsible for elevated Cdk1 activity in *MCPH1*-deficient cells (Alderton et al., 2006). It is not clear whether MCPH1's role in regulating mitotic entry in unperturbed cells is related to its checkpoint function; intriguingly, Chk1 has similarly been reported to regulate timing of mitosis during normal division (Kramer et al., 2004). *MCPH1* (also called *Brit1*) was independently identified in a screen for negative regulators of telomerase, suggesting that it may function as a tumor suppressor (Lin and Elledge, 2003). Further evidence for such a role comes from a study showing that gene copy number and expression of *MCPH1* is reduced in human breast cancer cell lines and epithelial tumors (Rai et al., 2006).

We report here the identification and phenotypic characterization of *Drosophila* mutants null for *mcph1*. We show that syncytial embryos from *mcph1* females exhibit genomic instability and undergo mitotic arrest due to activation of a DNA checkpoint kinase, Chk2. We find that, in contrast to reports of MCPH1 function in human cells, the ATR/Chk1-mediated DNA checkpoint is intact in *Drosophila mcph1* mutants. We propose that *Drosophila* MCPH1, like its human counterpart, is required for proper coordination of cell-cycle events; in early embryos lacking *mcph1*, chromosome condensation prior to completion of DNA replication causes genomic instability and Chk2-mediated mitotic arrest.

METHODS

Drosophila stocks

Flies were maintained at 25°C using standard techniques (Greenspan, 2004). Wild-type stocks used were *y w* or *Oregon-R*. Zuker alleles of *mcph1* are *cn bw* and balanced over *CyO*. Zuker stock designations have been shortened and superscripted to indicate that they are alleles of *mcph1* (e.g. *ZII-1861* becomes $mcph1^{Z1861}$). Deficiency strains, P-element lines for mapping, mutants for complementation testing (grp^{1}, $aurora^{1}$, $wee1^{ES1}$), *nanos-Gal4:VP16* stock, and *mei-41* mutants were from Bloomington Stock Center. *mcph1* P-element insertions were from Bloomington Stock Center (*EY11307*), Kyoto Stock Center (*NP6229-5-1*), or a gift from Steven Hou (*l(2)SH0220*). $tefu^{356}$, mnk^{6006} and grp^{209} stocks were gifts from Mike Brodsky, Bill Theurkauf and Tin Tin Su, respectively.

Identification of new alleles of cell-cycle regulators

A combination of female meiotic recombination, deficiency mapping and direct complementation testing of candidates was used to identify mutants from our screen. Complementation testing with known cell-cycle regulators was performed by assessing fertility of females carrying a Zuker chromosome in trans to a known mutation. We used the following alleles: $wee1^{ES1}$ (Price et al., 2000), grp^{1} (Fogarty et al., 1997), $tefu^{\Delta 356}$ (Oikemus et al., 2004) and aur^{1} (Glover et al., 1995).

Quantification of embryonic hatch rates

For hatch rate assays, embryos (0-4 hours) were collected on grape plates, counted and aged ~40 hours at 25°C. The number of hatched embryos was determined by subtracting the number of unhatched (intact) embryos from the total number collected. Hatch rate is the ratio of hatched to total embryos expressed as a percentage.

Genetic and molecular mapping of *awol*

The *awol* gene was localized by a combination of mapping strategies. We first screened a collection of deficiencies on the second chromosome for non-complementation of the female sterility of $awol^{Z1861}$. We found that females carrying $awol^{Z1861}$ in trans to *Df(2R)BSC39* produced embryos with the awol phenotype; similar results were obtained for $awol^{Z0978}$ and $awol^{Z4050}$. Thus, *awol* lies between the breakpoints of *Df(2R)BSC39* in the polytene interval 48C5-E1, a region that contains ~35 genes. We mapped *awol* by P-element-induced male recombination (Chen et al.,

1998) relative to the following insertion lines: *Mtor*^{k03905}, *ERp60*^{BG01854}, *KG04952*, *otk*^{EP2017} and *CG8378*^{EP2501}. We thereby narrowed *awol* to a region of five genes (including *mcph1*) that lie distal to *ERp60*^{BG01854} and proximal to *KG04952*. The *awol* stock used (*cn ZII-1861 bw/CyO*) has visible flanking markers *cn* and *bw*. The source of transposase was *Delta2-3 Sb*. Multiple independent recombinant chromosomes were recovered for each P-element line tested. Genomic DNA was extracted from whole flies homozygous for *awol* mutations essentially as previously described (Ballinger and Benzer, 1989). *mcph1* coding regions were PCR-amplified from genomic DNA and sequenced.

Generation of *mcph1* excision line

P-element insertions have been identified in the 5'-UTR of *mcph1* (*NP6229-5-1*) and within its largest intron (*l(2)k06612*, *l(2)SH0220* and *EY11307*) (Grumbling and Strelets, 2006). *l(2)k06612* is no longer available from stock centers. We mapped the lethality of line *l(2)SH0220* (Oh et al., 2003) outside of the *mcph1* genomic region (data not shown). We found that *EY11307* homozygous and *EY11307/mcph1*^{Z1861} transheterozygous females are viable, fertile and produce embryos with nearly wild-type levels of MCPH1 protein, indicating that this P-insertion has little effect on *mcph1* transcription; similar results were obtained for *NP6229-5-1* (data not shown). *EY11307* is inserted in the 5'-UTR of *CG13189*, which encodes a putative metal ion transporter, and the largest intron of *mcph1* (Figure 2.2A). All EMS-induced *mcph1* mutations described here lie outside of *CG13189* (including two beyond its 3' end), thereby making it unlikely that decreased

CG13189 activity causes the awol phenotype. We performed imprecise P-element excision of *EY11307* to generate *mcph1*^{Exc21}, which lacks two internal exons and part of the 3'-most exon of *mcph1*; this excision left the 5'-UTR, coding region and 3'-UTR of *CG13189* intact, but probably removed some of its promoter (Figure 2.2A).

Embryo fixation, staining and microscopy

Embryos (1-2 hours unless otherwise indicated) were collected for staining using standard techniques (Rothwell and Sullivan, 2000). For mouse anti-α-tubulin (DM1α, 1:500, Sigma) or rabbit anti-Centrosomin (1:10,000, a gift from W. Theurkauf) staining, embryos were dechorionated in 50% bleach, fixed, and devitellinized by shaking in a mixture of methanol and heptane (1:1). For staining with guinea pig anti-MCPH1 (1:200) or mouse anti-actin (1:400, MP Biomedicals) or co-staining with anti-α-tubulin (YL1/2, Serotec, 1:250) and anti-γ-tubulin (GTU-88, 1:250, Sigma), embryos were fixed fore 20 minutes in a mixture of 3.7% formaldehyde in PBS and heptane (1:1). The aqueous layer containing formaldehyde was removed and embryos devitellinized as described above. Embryos were incubated in primary antibodies at 4°C overnight except for anti-MCPH1 (4°C for three days). Secondary antibodies were conjugated to Cy2 (Jackson ImmunoResearch). Embryos were stained with propidium iodide (Sigma) and cleared as previously described (Fenger et al., 2000). A Nikon Eclipse 80i microscope equipped with a CoolSNAP ES camera (Photometrics) and Plan-Apo (20x, 100x) or Plan-Fluor 40x objectives was used; for confocal images, we used a Zeiss LSM510 microscope equipped with a Plan-Neofluar 100x objective.

Embryo squashes and quantification of DNA bridging

Methanol-fixed embryos (40-80 minutes) were placed in 2-µl drops of 45% acetic acid on coverslips for 1-2 minutes. Slides were lowered onto coverslips, inverted and embryos squashed by hand between blotting paper. Samples were snap-frozen in liquid nitrogen, coverslips removed, and slides immersed in ethanol at –20°C for 10 minutes and air-dried. Vectashield mounting medium with DAPI (Vector Labs) and new coverslips were added to slides. Fluorescence microscopy (100x objective) was used to visualize DNA. Late anaphase and telophase figures (cycle-5 to -7 embryos) were examined. The presence of one or more linkages between DNA masses segregating to opposite poles was scored as a bridging defect.

Live embryo imaging

For analysis of cell-cycle timing, embryos (0-1.5 hours) were dechorionated in 50% bleach, glued (octane extract of tape) to glass-bottomed culture dishes (MatTek Corp.), and covered with halocarbon oil 27 (Sigma). DIC images of dividing embryos at 21.5-22.5°C were captured (20-second intervals) using a Nikon Eclipse TE2000-E inverted microscope with a CoolSNAP HQ CCD camera (Photometrics), Plan-Apo 20x objective, and IPLab image acquisition software (BD Biosciences). Interphase length was determined by counting frame numbers from nuclear envelope formation to breakdown. Mitosis length was determined by counting frame numbers from nuclear envelope breakdown to reformation. Cycle number was determined by nuclear size and density.

mcph1 cDNA clones and transgenes

cDNA clones encoding MCPH1-B (LD43341) or MCPH1-A (LP15451) were from the Drosophila Gene Collection or Drosophila Genomics Resource Center, respectively. MCPH1-B coding region was PCR-amplified from LD43341, subcloned into UASp (Rorth, 1998), and transformed into *y w* flies (Spradling, 1986). To generate IVT constructs, MCPH1-B coding region was subcloned into pCS2. The BRCT domains of MCPH1 were identified using ScanProsite. Descriptions of FlyBase's annotation of *mcph1* were based on version FB2006_01 (Grumbling and Strelets, 2006). GenBank accession number for LP15451 encoding MCPH1-A is EF587234.

Polyclonal antibodies against MCPH1

Maltose-binding protein (MBP) fused to MCPH1-B protein (residues 1-352) was used to produce antibodies. N-terminal MCPH1-B sequence was PCR-amplified from LD43341 and subcloned into pMAL (New England Biolabs). MBP-N-MCPH1-B was made in bacterial cells, purified using amylose beads, and injected into guinea pigs for antibody production (Covance). Anti-MCPH1 antibodies were affinity purified using standard techniques.

Protein extracts and immunoblots

Protein extracts were made by homogenizing either embryos (1-2 hours old unless otherwise indicated) or dissected tissues in urea sample buffer as described previously (Moore et al., 1998). Proteins were transferred to nitrocellulose for

immunoblotting using standard techniques. MCPH1-A and -B (unlabeled proteins) were made by coupled transcription-translation of LP15451 and LD43341, respectively, according to the manufacturer's protocol (Promega). Antibodies were used as follows: guinea pig anti-MCPH1 (1:200-500), mouse anti-Cyclin B (F2F4, 1:200, Developmental Studies Hybridoma Bank), rabbit anti-pY15-Cdk1 (1:1000, Upstate), rabbit anti-Grapes (1:500, a gift from T. T. Su) (Purdy et al., 2005), mouse anti-α-tubulin (DM1α, 1:5000, Sigma), mouse anti-GAPDH (1:1000, Abcam). HRP-conjugated secondary antibodies and chemiluminescence were used to detect primary antibodies.

DNA damage response assays

We used a Mark I cesium-137 irradiator as a source of irradiation (IR). To test the G2-M checkpoint post-IR, we used the method of Brodsky et al. (Brodsky et al., 2000) except that fluorescently coupled secondary antibodies were used. To test the intra-S phase checkpoint post-IR, we used the method of Jaklevic and Su (Jaklevic and Su, 2004) except that larvae were exposed to 40 Gray (4000 Rad). To test sensitivity to irradiation, third instar larvae were untreated or exposed to 10 Gray (1000 Rad), transferred to food, and allowed to pupate and eclose as adults. Mutant chromosomes were balanced over *CyO, arm-GFP* (Sullivan et al., 2000) and homozygotes identified by lack of GFP signal. Numbers of pupae formed and empty pupal cases (due to eclosion) were scored up to 10 days post-IR. Percentage eclosion (measure of survival) is the number of empty pupal cases expressed as a percentage of total pupae. All irradiated larvae formed pupae in these experiments. To test

hydroxyurea (HU) sensitivity, heterozygous adults (ten males and ten virgin females) were added to vials. After embryo collection (48 hours), adults were removed and 500 ml of 20 μM HU in water was added to food 24 hours later. Adult progeny were scored after 2 weeks. HU sensitivity is indicated by preferential loss of a specific genotypic class.

Adult brain immunostaining

Adult brains were fixed, immunostained and examined by confocal microscopy as previously described (Krashes et al., 2007) using mouse anti-Fasciclin II antibodies (1D4, 1:4, Developmental Studies Hybridoma Bank).

RESULTS

Screen for *Drosophila* cell-cycle mutants identifies *absent without leave* (*awol*)

In an effort to identify genes required for S-M cycles of the early embryo, we previously screened (Lee et al., 2003) a maternal-effect lethal subset of a collection of ethylmethanesulfonate (EMS)-mutagenized lines from Charles Zuker's lab (Koundakjian et al., 2004). We screened ~2400 lines by examining DAPI-stained embryos of homozygous females. Because early embryonic development is entirely regulated by maternally deposited mRNA and protein, only the maternal genotype is relevant in this screen. We identified 33 lines (12 chromosome II and 21 chromosome III mutants) representing 26 complementation groups in which the majority of embryos from mutant females arrest at the syncytial blastoderm stage.

We previously identified two alleles of *giant nuclei*, which prevents excessive DNA replication in S-M cycles (Freeman et al., 1986; Renault et al., 2003), from this collection (Lee et al., 2003). We have now identified alleles of four well-known regulators of the cell cycle from the same screen (Table 2.1). All four genes encode protein kinases with conserved roles in cell-cycle regulation. *wee1, grapes, telomere fusion* and *aurora* encode *Drosophila* orthologs of Wee1 (a Cdk1 inhibitory kinase), DNA checkpoint kinases Chk1 and ATM (ataxia telangiectasia mutated), and the mitotic kinase Aurora A, respectively (Fogarty et al., 1997; Glover et al., 1995; Oikemus et al., 2004; Price et al., 2000). Additionally, we identified an allele of *nopo*, an E3 ubiquitin ligase necessary for genomic stability in the early embryo (Merkle et al., 2009). Identification of these alleles of bona fide cell-cycle regulators validates our screen.

We chose for further study the largest complementation group on chromosome II (comprising *ZII-0978, ZII-1861* and *ZII-4050*) identified in our screen. Females homozygous or transheterozygous for any of these mutations are completely sterile, producing embryos that arrest in a metaphase-like state (~90% of embryos) in cycles 1-8 (the majority in cycles 6-8). Unevenly spaced, asynchronously dividing nuclei and centrosome duplication prior to chromosome segregation are often seen (Figure 2.1B-D; Table 2.2); all of these are consistent with failure of nuclear divisions. Tubulin foci are frequently missing from one or both poles of mitotic spindles, which are typically shorter and more barrel-shaped than those of wild type (Figure 2.1E; Table 2.2). Chromosomes are poorly aligned and

Table 2.1. New alleles of known cell-cycle regulators in *Drosophila*

Chromosome	Gene	New alleles	Vertebrate homolog
II	*wee1*	*ZII-2186*	Wee1
	grapes	*ZII-5170*[a]	Chk1
III	*giant nuclei*	*ZIII-0591*[b]	None
		ZIII-3770[b]	
	aurora	*ZIII-2400*	Aurora A
		ZIII-2974	
		ZIII-5137	
	telomere fusion	*ZIII-5190*	ATM

[a]Independently identified as *grapes* allele by LaRocque et al. (2006).
[b]Previously described by Lee et al. (2003).

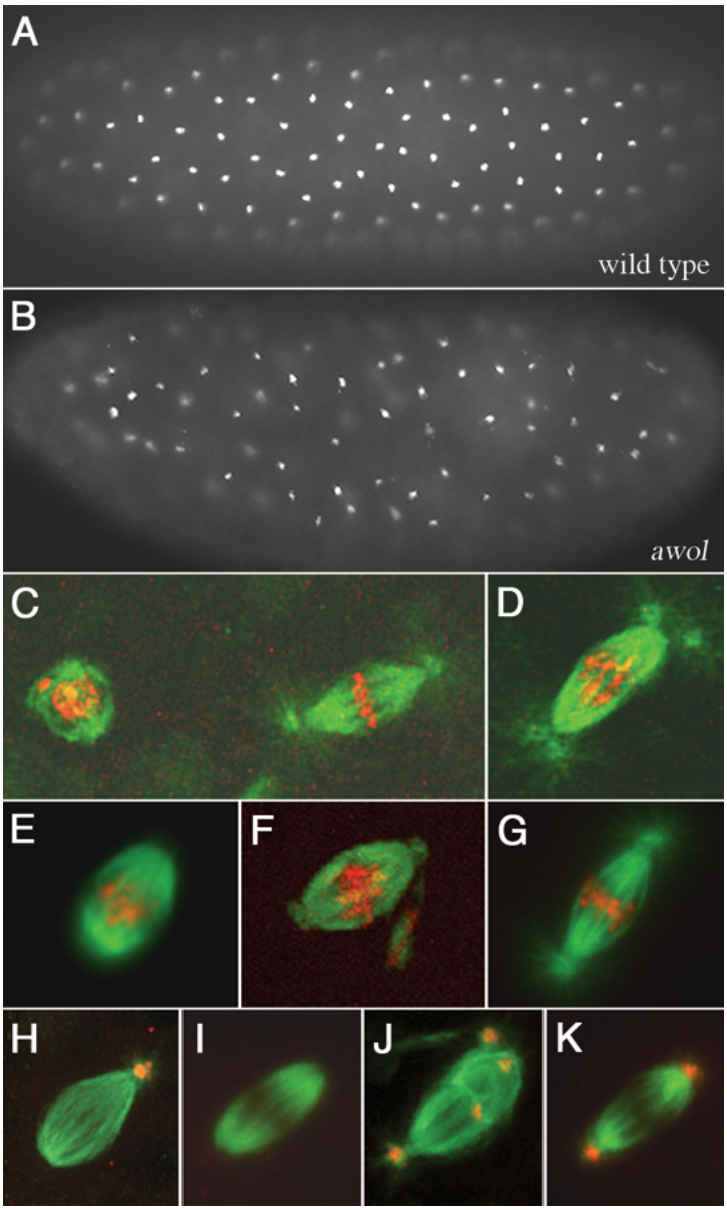

Figure 2.1. The *awol* phenotype. Representative syncytial embryos (A,B) and mitotic spindles (C-K) in embryos from wild-type or *awolZ1861/awolZ0978* females. (A,B) DNA staining of embryos from *awol* females shows arrest with condensed chromosomes and unevenly spaced nuclei (B) compared to wild type (A). (C-G) Microtubules are in green and DNA in red. (C) Asynchronous neighboring nuclei in embryo from *awol* female (left, interphase; right, mitosis). (D) Metaphase spindle with duplicated centrosomes in embryo from *awol* female shows asynchronous nuclear and centrosome cycles (duplication normally occurs in telophase). (E) Shortened, barrel-shaped spindle in embryo from *awol* female. (F) DNA displaced from metaphase plate is tethered by microtubules to spindle pole in embryo from *awol* female. (G) Wild-type spindle. (H-K) Microtubules are in green and centrosomes in red. (H-I) *awol*spindles with missing or ectopic centrosomes. (K) Wild-type spindle. Bars, 20 _m.

Table 2.2. Mitotic spindle defects in *mcph1* embryos and suppression by *mnk*

		Centrosome number (% spindles)[b]		Other spindle defects (% spindles)[b]		
Genotype	**MI[a]**	**Decreased[c]**	**Increased[d]**	**Barrel**	**Interacting[e]**	**Multipolar**
Wild type	54.1	0.2	0.0	0.1	0.0	0.0
mcph1[f]	88.8	43.6	46.0	97.5	0.0	0.2
mnk	54.2	0.2	0.1	0.0	0.2	0.0
mnk *mcph1*^{Z1861}	57.5	0.2	1.2	0.0	15.0	6.0

[a]Mitotic index=% embryos in mitosis/total number of embryos (>100 embryos scored per genotype). The presence of both condensed chromosomes and a mitotic spindle was used as the criterion for scoring mitotic embryos

[b]To quantify spindle defects, >500 spindles from 25 embryos were scored per genotype

[c]Spindles with centrosomal detachment at one or both poles

[d]Spindles with >1 centrosome per pole (one or both poles) or ectopic centrosomes within spindle. Telophase spindles were not scored because centrosome duplication normally occurs at this phase in the early embryo

[e] Two spindles connected by microtubules

[f] *mcph1*^{Z1861}/*mcph1*^{Z0978}

occasionally displaced from the metaphase plate (Figure 2.1F). Staining for Centrosomin, a core centrosomal component (Li and Kaufman, 1996), revealed that lack of tubulin foci at one or both poles in mutant-derived embryos is due to an absence of centrosomes (Figure 2.1H,I; Table 2.2); we occasionally see ectopic centrosomes embedded in spindles (Figure 2.1J; Table 2.2). On the basis of the phenotype of acentrosomal mitotic spindles, we have given the name `*absent without leave*' (`*awol*') to mutants of this complementation group.

awol encodes the *Drosophila* homolog of *MCPH1*

We localized *awol* to a region including five genes by a combination of mapping strategies (see Materials and Methods for details). A candidate in this region was the *Drosophila* homolog of the human disease gene, *MCPH1* (Jackson et al., 2002). Sequencing of PCR-amplified *mcph1* coding region from homozygous mutant genomic DNA revealed that $awol^{Z0978}$ and $awol^{Z4050}$ are distinct missense mutations in *mcph1* causing non-conservative amino acid changes and $awol^{Z1861}$ is a nonsense mutation resulting in severe truncation of the protein (Figure 2.2A). Thus, all three EMS-induced *awol* alleles represent mutations affecting MCPH1 protein. Furthermore, females carrying any of these *awol* alleles in *trans* to a deletion of the *mcph1* genomic locus produce embryos with phenotypes indistinguishable from that of homozygous mutant females (data not shown), suggesting that all three Zuker *awol* alleles behave genetically as nulls.

To confirm that mutation of *mcph1* is responsible for the awol phenotype, we generated a null allele ($mcph1^{Exc21}$) by imprecise P-element excision (Figure 2.2A).

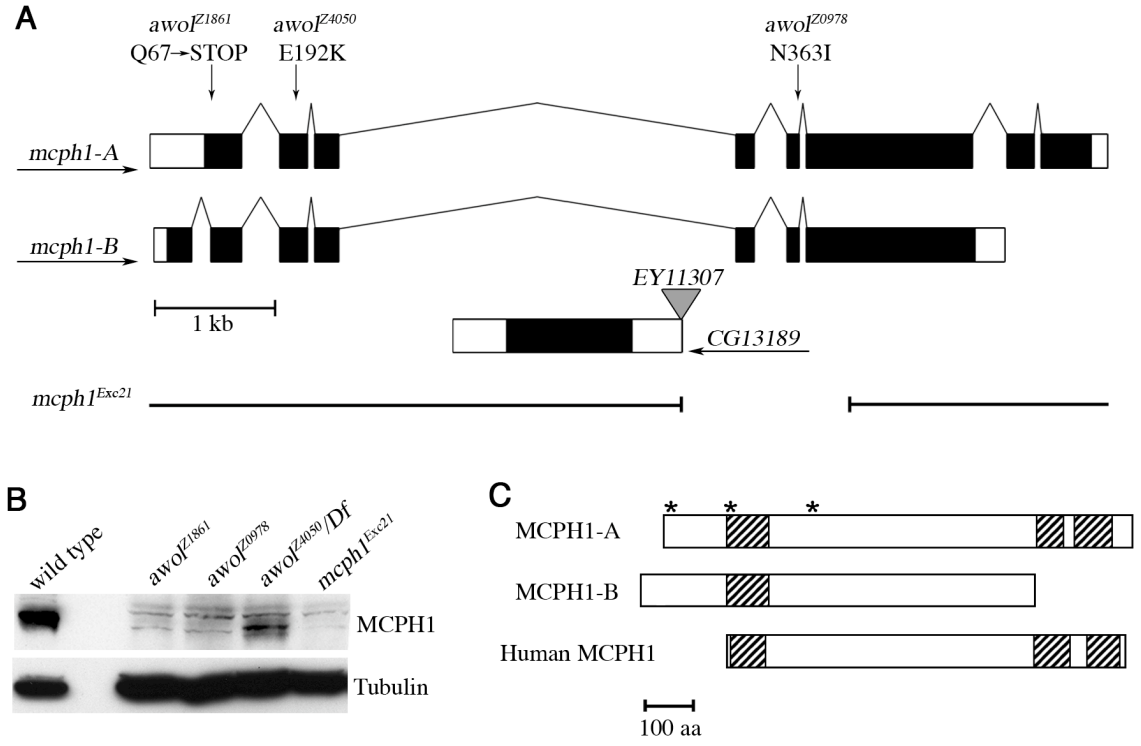

Figure 2.2. *mcph1* is the *awol* gene. (A) The *Drosophila mcph1* gene structure. Exons are represented by filled boxes, 5_- and 3_- UTRs by open boxes, and splicing events by thin lines. The gene *CG13189* lies within the largest intron of *mcph1*. Alternative splicing produces transcript *mcph1-RA* or *-RB*. Arrows below gene or transcript names indicate direction of transcription. Positions of the point mutations in each of the three EMS-induced alleles of *awol* and resulting amino acid changes (numbers refer to MCPH1-B) are indicated above the *mcph1* gene. Imprecise excision of *P*-element *EY11307* (inverted triangle) generated allele *mcph1Exc21* (deleted region indicated by gap). (B) Western analysis reveals trace amounts of or no MCPH1 protein in extracts of *awol* embryos relative to wild type (loading control: anti-_-tubulin). The excision allele (*Exc21*) of *mcph1* serves as negative control. *Df=Df(2R)BSC39*, which removes the *mcph1* genomic locus. (C) Comparison of the BRCT domain content (hatched boxes) of the two *Drosophila* MCPH1 isoforms (MCPH1-A and -B) and human MCPH1 protein (bottom). Positions of the amino acid changes in each of the three EMS-induced alleles of *awol* are indicated by asterisks. A double-sided arrow indicates the region of MCPH1-B used for antibody production.

mcph1^{Exc21} homozygous females produce embryos with the awol phenotype; similar results were obtained for females carrying this excision in *trans* to any of the EMS-induced *awol* alleles or a deletion of the *mcph1* genomic locus (data not shown), further confirming that mutation of *mcph1* causes the awol phenotype. Importantly, expression of transgenic *mcph1* using the UAS-Gal4 system (Brand and Perrimon, 1993; Rorth, 1998) restored fertility to *awol*^{Z0978}/*awol*^{Z4050} females, resulting in a hatch rate of ~40% of their embryos (Table 2.3). Thus, *mcph1* is the *awol* gene. We used the MCPH1 isoform that is most abundant in the early embryo for transgenic rescue; it is possible that full rescue of the maternal-effect lethality of *awol* mutants might additionally require expression of the less abundant isoform (see below for description of MCPH1 isoforms; Figure 2.2A and Figure 2.3B).

To further characterize our *mcph1* alleles, we generated polyclonal antibodies against an MBP-MCPH1 fusion. Anti-MCPH1 antibodies recognize a major band of ~90 kDa, consistent with the predicted size of MCPH1-B, when used to probe immunoblots of wild-type embryo extracts (Figure 2.2B). In contrast, for all *mcph1* alleles identified here, we detect greatly reduced or no MCPH1 protein in mutant-derived embryos. Thus, all of these alleles are null (or nearly null) for MCPH1 protein.

MCPH1 isoforms differ in expression pattern and BRCT domain content

Our genetic data revealed that *mcph1* null alleles are homozygous viable and that *mcph1* is required maternally for early embryonic development. To measure MCPH1 levels throughout *Drosophila* development, we probed immunoblots of

Table 2.3. Effects of maternal overexpression of transgenic *mcph1* on development of *awol* or wild-type embryos

Genotype	Hatch rate (%)	Embryos (n)
Wild type	95.6	139
awol[a]	0	215
awol[a]; *UASp-mcph1*[b]*/nanos-Gal4:VP16*	38.4	164
awol[a]; *UASp-mcph1*[b]*/+*	0.5	193
awol[a]; *nanos-Gal4:VP16/+*	0	230
UASp-mcph1/nanos-Gal4:VP16	86.9	260

[a]*awol*^{Z4050}*/awol*^{Z0978} transheterozygotes.

[b]cDNA encoding MCPH1-B was used to make transgenic construct.

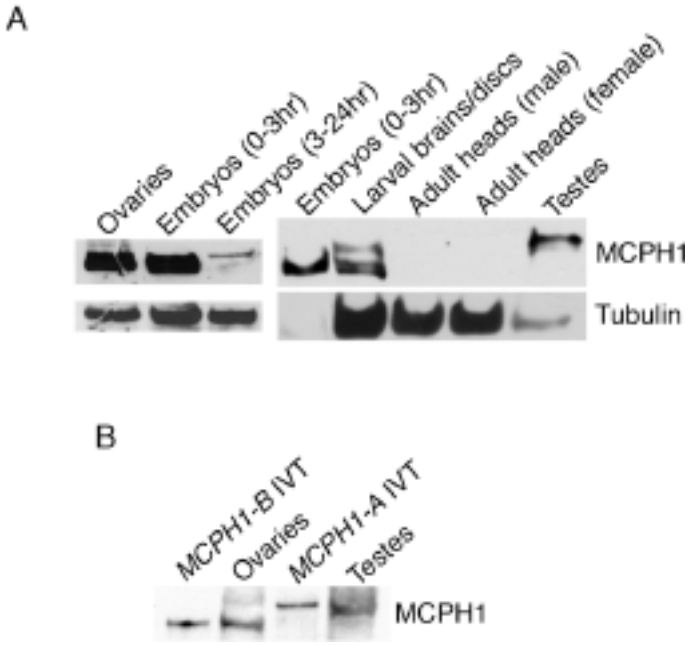

Figure 2.3. Developmental expression of alternate MCPH1 isoforms. (A,B) MCPH1 immunoblots. (A) Developmental western of wild-type extracts shows MCPH1 protein is present in a variety of tissues and at several life-cycle stages. Extracts of embryos and testes were relatively underloaded (loading control: anti-α-tubulin). (B) Type A and B MCPH1 isoforms produced in vitro co-migrate on SDS-PAGE with endogenous MCPH1 isoforms abundant in testes and ovaries, respectively.

extracts from various developmental stages with anti-MCPH1 antibodies (Figure 2.3A). As expected, MCPH1 is abundant in ovaries and early embryos, whereas older embryos under zygotic control have relatively low amounts. MCPH1 is present in larval brains and imaginal discs but undetectable in adult brain extracts. Although high levels of MCPH1 are present in adult testes, it is not required for male fertility (data not shown).

Two major isoforms of MCPH1 were detected by immunoblotting: ~90 kDa (predominant in ovaries and embryos) and ~110 kDa (predominant in testes). Both isoforms were detected in larval tissues. The most recent *mcph1* gene model annotated by FlyBase predicts two splice variants (A and B) differing at their 5'-ends that encode proteins with distinct amino termini (Grumbling and Strelets, 2006). We compared sizes of recombinant MCPH1-A and -B proteins (produced by in vitro transcription-translation reactions) to that of endogenous MCPH1 isoforms by immunoblotting. We found that the gel mobilities of MCPH1-A and -B closely match that of MCPH1 in testes and ovaries, respectively; thus, MCPH1-A is the 110 kDa isoform that is abundant in testes, and MCPH1-B is the ~90 kDa isoform that is abundant in ovaries and early embryos (Figure 2.3B).

We observed a discrepancy between relative sizes of MCPH1-A and -B on our immunoblots (A larger than B; Figure 2.3B) and as predicted by FlyBase [779 versus 826 amino acids, respectively (Grumbling and Strelets, 2006)]. We were unable to find 3'-end sequence data for *mcph1-A* on public databases, so we fully sequenced a representative clone (LP15451) and found it to encode a protein of 981 amino acids, which closely matches our estimated size of 110 kDa for endogenous MCPH1-A.

Furthermore, our sequencing revealed that *mcph1-A* contains coding sequence from both *mcph1* and *CG30038*, a gene predicted to overlap the 3'-end of *mcph1* (Figure 2.2A). Thus, *mcph1-A* and *-B* are alternatively spliced at both ends, producing proteins that differ in their N- and C-terminal regions (Figure 2.2C), and predicted gene *CG30038* comprises alternatively spliced exons of *mcph1-A*.

MCPH1-A and -B proteins both contain BRCT domains (three or one, respectively). The arrangement of BRCT domains within MCPH1-A (one N-terminal and two paired C-terminal) resembles that of human MCPH1 (Figure 2.2C). *Drosophila* and human MCPH1 have highest sequence identity in their BRCT domains (37.6%, 52.5% and 26.8% between the N-terminal, first C-terminal, and second C-terminal domains, respectively). The presence of extended amino termini in both *Drosophila* isoforms relative to human MCPH1 raises the possibility that the reported human sequence (Jackson et al., 2002) may not be full-length.

MCPH1 is a nuclear protein

Because *Drosophila* MCPH1 contains BRCT domains, we hypothesized that it has a nuclear function. In syncytial embryos, MCPH1 signal localizes to interphase nuclei and disappears in mitosis (Figure 2.4). As control for antibody specificity, no MCPH1 signal was detected in interphase nuclei of embryos derived from *mcph1* null females. Because MCPH1 protein is readily detectable throughout the cell cycle (by immunoblotting of extracts from staged embryos; data not shown), the disappearance of MCPH1 signal in mitosis, as observed by immunostaining, is probably due to its dispersal into the cytoplasm upon nuclear envelope breakdown.

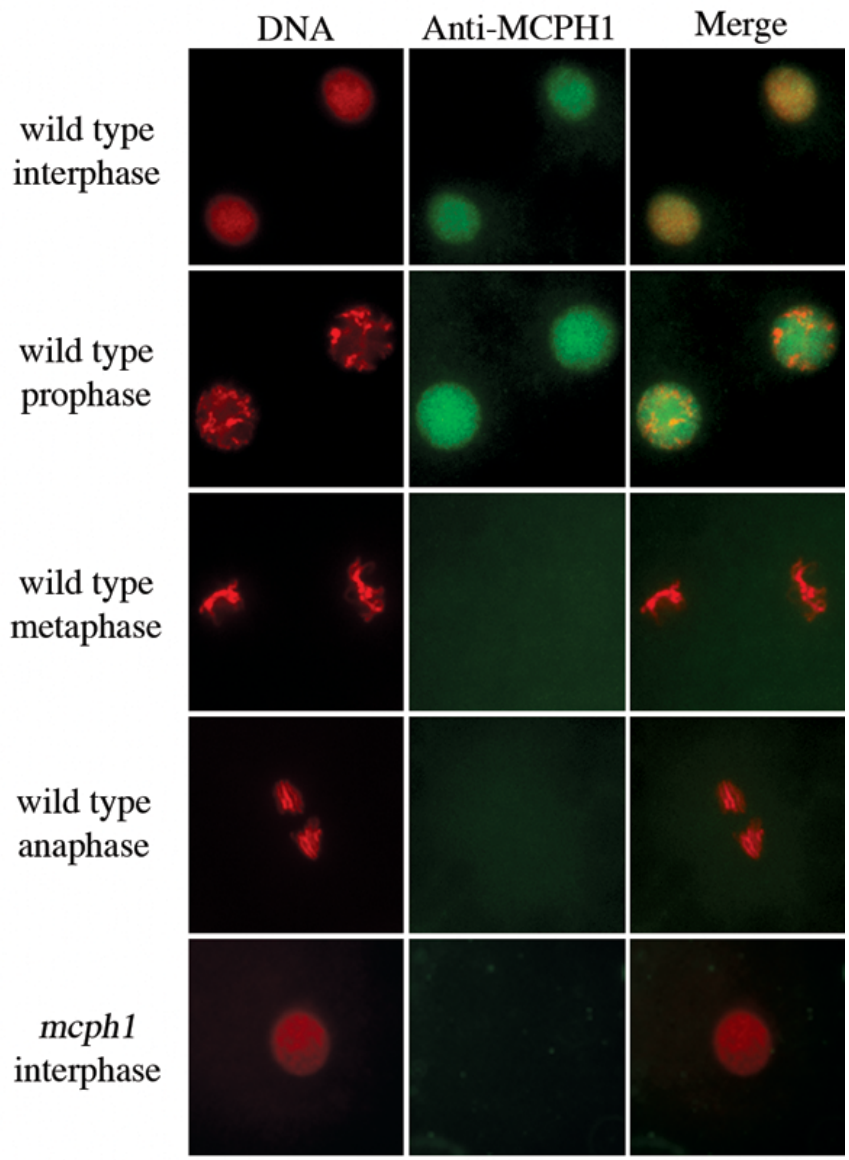

Figure 2.4. MCPH1 is a nuclear protein. Wild-type syncytial embryos were fixed and stained with an antibody against MCPH1 (green) and DNA dye (red). Representative embryos in various cell-cycle stages are shown. MCPH1 localizes to the nucleus during interphase and prophase and is no longer detectable during later stages of mitosis (following nuclear envelope breakdown). No MCPH1 signal is detected in interphase nuclei of *mcph1*^{Z1861} mutants (negative control). Bar, 10 μm.

Human MCPH1 has been reported to localize to the nucleus (Lin et al., 2005) as well as to centrosomes (Jeffers et al., 2007; Zhong et al., 2006); we observe no centrosomal localization for MCPH1 in syncytial embryos of *Drosophila*.

Mitotic arrest in *mcph1* syncytial embryos is a consequence of Chk2 activation

The defective mitotic spindles of embryos derived from *mcph1* females (hereafter referred to as `*mcph1* embryos') exhibit key features reminiscent of Chk2-mediated centrosomal inactivation. In particular, these spindles are short, barrel-shaped, anastral, and associated with poorly aligned chromosomes (Figure 2.1). Late syncytial embryos of *Drosophila* use a two-stage response to DNA damage or replication defects (Sibon et al., 2000). The DNA checkpoint mediated by Meiotic 41 (MEI-41) and Grapes (GRP), the *Drosophila* orthologs of ATR (ATM-Rad3-related) and Chk1 kinases, respectively, delays mitotic entry via inhibitory phosphorylation of Cdk1 to allow repair of DNA damage or completion of replication (Sibon et al., 1999; Sibon et al., 1997). When this checkpoint fails, a secondary damage-control system operating in mitosis is activated; resulting changes in spindle structure block chromosome segregation, presumably to stop propagation of defective DNA (Sibon et al., 2000; Takada et al., 2003). This damage-control system, known as centrosomal inactivation, is mediated by the checkpoint kinase Chk2 (Takada et al., 2003).

Loss of γ-tubulin from centrosomes of mitotic spindles is another characteristic feature of Chk2-mediated centrosomal inactivation. We detected decreased γ-tubulin staining of centrosomes during mitosis in *mcph1* embryos

compared to wild type (Figure 2.5). We typically observe complete detachment of centrosomes from spindles in *mcph1* embryos. High levels of DNA damage induced by intense laser illumination can similarly cause complete centrosomal detachment from spindle poles of wild-type embryos (Takada et al., 2003), suggesting that the spindle changes we observe in *mcph1* embryos represent an extreme form of centrosomal inactivation.

To determine whether mitotic defects in *mcph1* embryos are due to Chk2-mediated centrosomal inactivation, we created lines doubly mutant for *mcph1* and *maternal nuclear kinase* (*mnk*), also known as *loki*, which encodes *Drosophila* Chk2 (Abdu et al., 2002; Brodsky et al., 2004; Masrouha et al., 2003; Xu et al., 2001). A similar approach has been used to demonstrate Chk2-mediated centrosomal inactivation in *grp*, *mei-41* and *wee1* embryos (Stumpff et al., 2004; Takada et al., 2003). Null *mnk* mutants are viable and fertile, but they are highly sensitive to ionizing radiation (Xu et al., 2001). Remarkably, we found that *mnk* suppresses many of the mitotic defects of *mcph1* embryos (Figure 2.6A-D; Table 2.2). Mitotic spindles are restored to near-normality: in contrast to the short, barrel-shaped, anastral spindles of *mcph1* embryos, *mnk mcph1* embryos have elongated spindles with attached centrosomes. Thus, Chk2 activation contributes significantly to the *mcph1* phenotype in syncytial embryos.

In addition to suppressing the mitotic spindle defects of *mcph1* embryos, *mnk* strikingly suppresses their developmental arrest (Figure 2.6G-K). Whereas *mcph1* embryos uniformly (100%) arrest in early to mid-syncytial cycles (cycles 1-8), most (>95%) *mnk mcph1* embryos complete syncytial divisions, cellularize, and cease

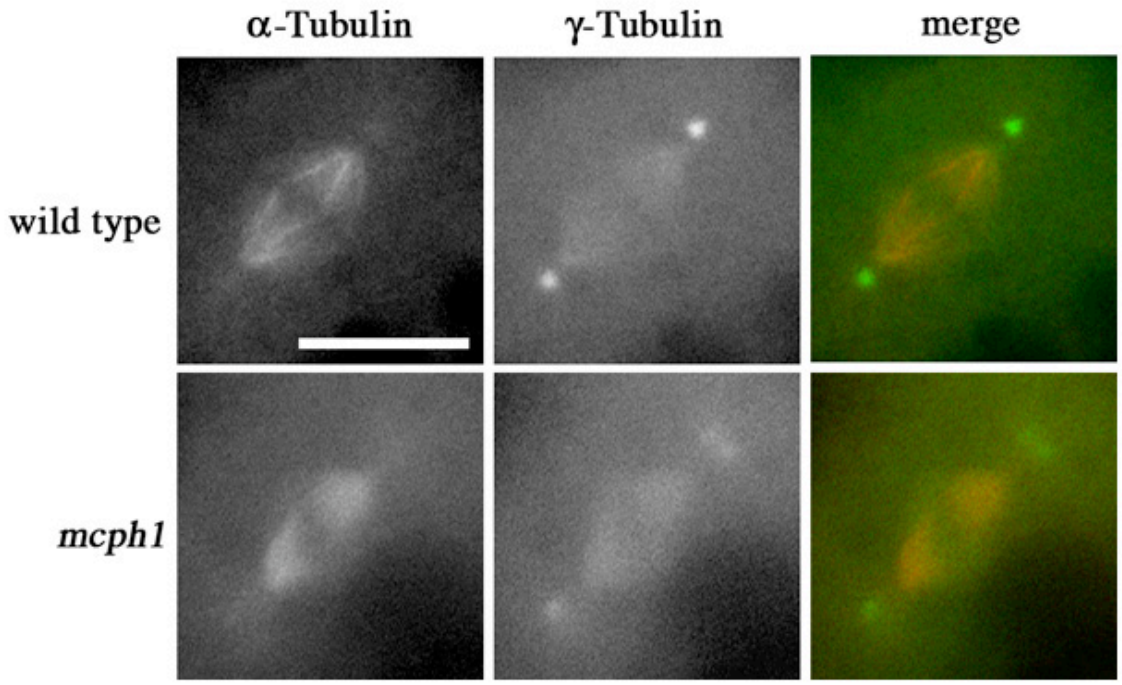

Figure 2.5. Decreased γ-tubulin staining of centrosomes in *mcph1* embryos. Syncytial embryos from wild-type or *mcph1*^{Exc21} females were fixed and co-stained with antibodies against α-tubulin (red) and γ-tubulin (green). Representative mitotic spindles are shown. Bar, 10 μm.

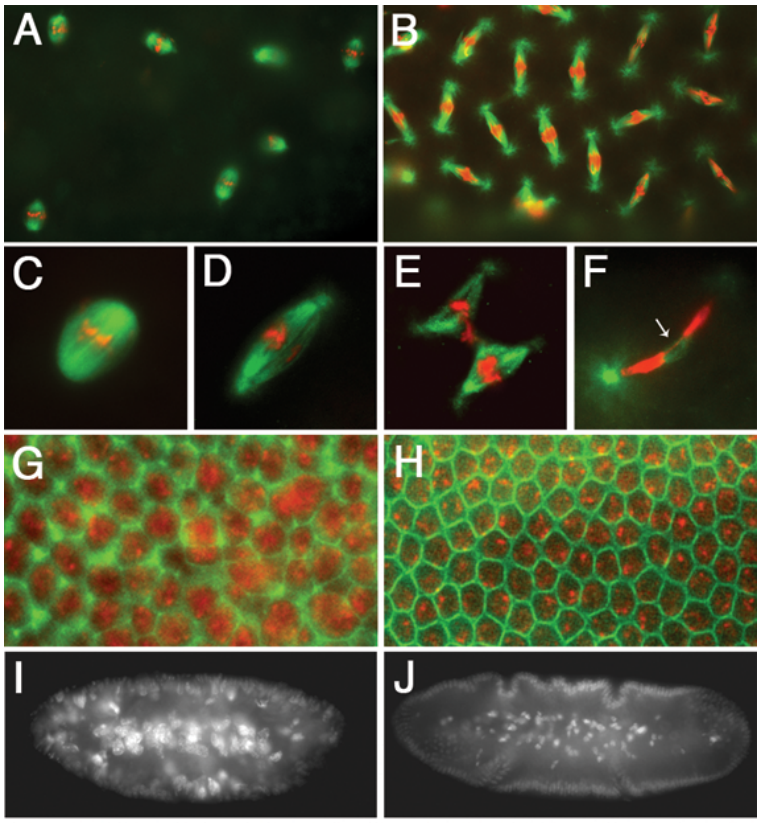

K

Genotype	Gastrulation[a] (% Embryos)	Embryos (n)
wild type	98.6	220
mcph1	0	200
mnk	83.3	180
mnk mcph1	95.9	170

[a]Embryos that initiate gastrulation

Figure 2.6. Suppression of *mcph1* by *Chk2* (*mnk*). (A-J) Representative mitotic spindles in syncytial embryos and whole-mount embryos from *mcph1*^{Z1861}, *mnk mcph1*^{Z1861} and wild-type females. Bars, 20 μm. (A-F) Microtubules are in green and DNA in red; low (A,B) and high (C-F) magnification views. *mcph1* embryos have *awol*-type (barrel-shaped, acentrosomal) spindles (A,C). *awol* phenotype is suppressed in *mnk mcph1* embryos (B,D): note restoration of elongated spindles and attached centrosomes. Other defects are seen in *mnk mcph1* embryos, such as DNA shared by two spindles (E) and DNA bridging (F, arrow). (G,H) Cellularized embryos (2-3 hours) stained for actin (green) and DNA (red). *mnk mcph1* embryos reach gastrulation with irregular cell size and DNA content (G) compared to wild type (H). (I,J) DNA-stained embryos (3-4 hours). *mnk mcph1* embryos (I) arrest peri-gastrulation with aberrant morphology compared to wild type (J). (K) Quantification of suppression of developmental arrest of *mcph1*^{Z1861} embryos by *mnk*.

developing near gastrulation. Thus, Chk2 activation causes *mcph1* embryos to arrest at the syncytial stage. Cellularized *mnk mcph1* embryos show irregularities in cell size and shape and intensity of DNA staining; gastrulation is grossly aberrant. We conclude that mutation of *mnk* removes the `brakes' from *mcph1* embryos, allowing further nuclear divisions and development in the face of DNA defects, which eventually become so severe that embryos die perigastrulation.

mcph1 syncytial embryos exhibit a high frequency of chromatin bridging

We sought to understand the primary defects leading to Chk2 activation in *mcph1* embryos. Known triggers of Chk2-mediated centrosomal inactivation are mitotic entry with incompletely replicated or damaged DNA (Sibon et al., 2000; Takada et al., 2003). Although *mnk* suppresses many of the cell-cycle defects of *mcph1* embryos, we occasionally observe abnormal DNA aggregates shared by more than one spindle and multipolar spindles in *mnk mcph1* embryos that progress beyond the usual *mcph1* arrest point (Figure 2.6E; Table 2.2). These defects are not observed in *mnk* embryos, suggesting that they are due to a lack of *mcph1.* In whole mounts of both *mnk mcph1* and *mcph1* embryos, we frequently observe chromatin bridging, which represents a physical linkage of chromosomes that prevents their segregation to opposite poles at anaphase (Figure 2.6F; data not shown); this bridging could result from mitotic entry with unreplicated, damaged, and/or improperly condensed chromosomes. We were prohibited from quantifying this phenotype, however, as yolk proteins obscure nuclei that lie deep within the interior of early syncytial embryos. We circumvented this problem by adapting a larval brain

squash protocol for this developmental stage that allowed us to more clearly observe chromosomes of early embryos.

Using this approach, we found a high frequency of chromatin bridging in *mcph1* embryos (68% of late anaphase-to-telophase figures) in cycles 4-6, prior to their Chk2-mediated arrest (Figure 2.7). Multiple bridges are often present between segregating chromosomes. Spindle pole-to-pole distances are increased dramatically compared to wild-type figures, presumably due to an extended anaphase B in a failed attempt to separate chromosomes that remain physically linked. All *mcph1* alleles reported here exhibit a similar degree of bridging, whereas this phenotype was rarely observed (<3%) in squashes of wild-type embryos (Figure 2.7 and data not shown). Chromatin bridging probably represents a primary defect of *mcph1* embryos because it occurs at a similar frequency (81%) in *mnk mcph1* embryos that lack the Chk2-mediated checkpoint. We hypothesize that *mcph1* embryos incur chromosomal lesions that cause Chk2-mediated centrosomal inactivation and mitotic arrest as secondary consequences.

We occasionally observe apparent DNA breakage (evidenced by gaps in DAPI staining) along the length of bridging chromatin that is extensively stretched between poles in *mcph1* and *mnk mcph1* embryos (data not shown). We propose that DNA breakage is not a primary defect in *mcph1* embryos but rather occurs secondary to bridging. Our attempts to confirm the presence of DNA breaks in syncytial embryos (*mcph1* or irradiated wild type) by phospho-histone H2Av or TUNEL staining have been unsuccessful.

A

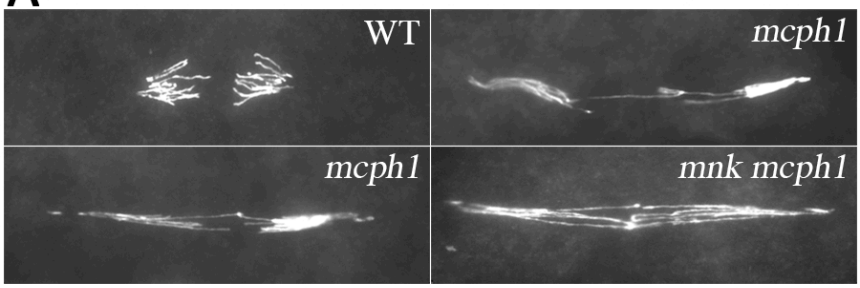

B

Genotype	Chromatin bridging (% A/T[a] figures)	Embryos (n[b])	Late A/T figures (n[b])
wild type	2.9	12	549
mcph1	68.3	14	60
mnk	10.6	6	113
mnk mcph1^{Z1861}	80.8	10	468

[a]A/T represents late anaphase to telophase.
[b]n represents the number of embryos or A/T figures scored.

Figure 2.7. Chromatin bridging in *mcph1* embryos. Syncytial embryos were squashed and the DNA stained. (A) Representative late anaphase-to-telophase figures (images shown at same magnification). DNA bridging and increased pole-to-pole distances are seen in squashes of *mcph1*^{Z1861}/*mcph1*^{Z0978} and *mnk mcph1*^{Z1861} embryos. Bars, 10 µm. (B) Quantification of DNA bridging in *mcph1*^{Z1861}/*mcph1*^{Z0978} and *mnk mcph1*^{Z1861} embryo squashes. Wild-type and *mnk* embryos served as controls.

mcph1 is not required for the DNA checkpoint in *Drosophila*

Chk2-mediated centrosomal inactivation can be triggered in *Drosophila* syncytial embryos by DNA damaging agents, the DNA-replication inhibitor aphidicolin, or mutation of DNA checkpoint components (MEI-41 or GRP) or WEE1, a kinase that prohibits mitotic entry via inhibitory phosphorylation of Cdk1 (Sibon et al., 2000; Stumpff et al., 2004; Takada et al., 2003). Human *MCPH1*-deficient cells show defective G2-M and intra-S phase checkpoint responses following DNA damage (Alderton et al., 2006; Lin et al., 2005; Xu et al., 2004). In light of these studies linking human *MCPH1* to the ATR/Chk1 pathway and our results that *Drosophila mcph1* embryos undergo Chk2-mediated arrest, we sought to determine if MCPH1 is required for the DNA checkpoint in *Drosophila*.

Because MEI-41 and GRP are required during larval stages for the DNA checkpoint (Brodsky et al., 2000; Jaklevic and Su, 2004), we tested whether MCPH1 is required. In response to ionizing radiation (IR), eye-antennal imaginal disc cells of wild-type larvae undergo G2 arrest. We found that *mcph1* larvae also exhibit IR-induced G2 arrest under conditions in which *mei-41* larvae fail to arrest (Figure 2.8A). We next tested the intra-S phase response to IR in larval brain cells. *mcph1* brains exhibited IR-induced intra-S phase arrest similar to that of wild type, whereas no arrest was seen in *mei-41* brains (Figure 2.8B). We also tested sensitivity of *mcph1* larvae to hydroxyurea (HU), which blocks DNA replication. Under conditions in which no *mei-41* larvae survived, *mcph1* larvae were HU resistant, surviving at near-Mendelian ratios (Figure 2.8C). We conclude that MCPH1 is not required for the DNA checkpoint in larval tissues. We also found that *mcph1* larvae, in contrast to

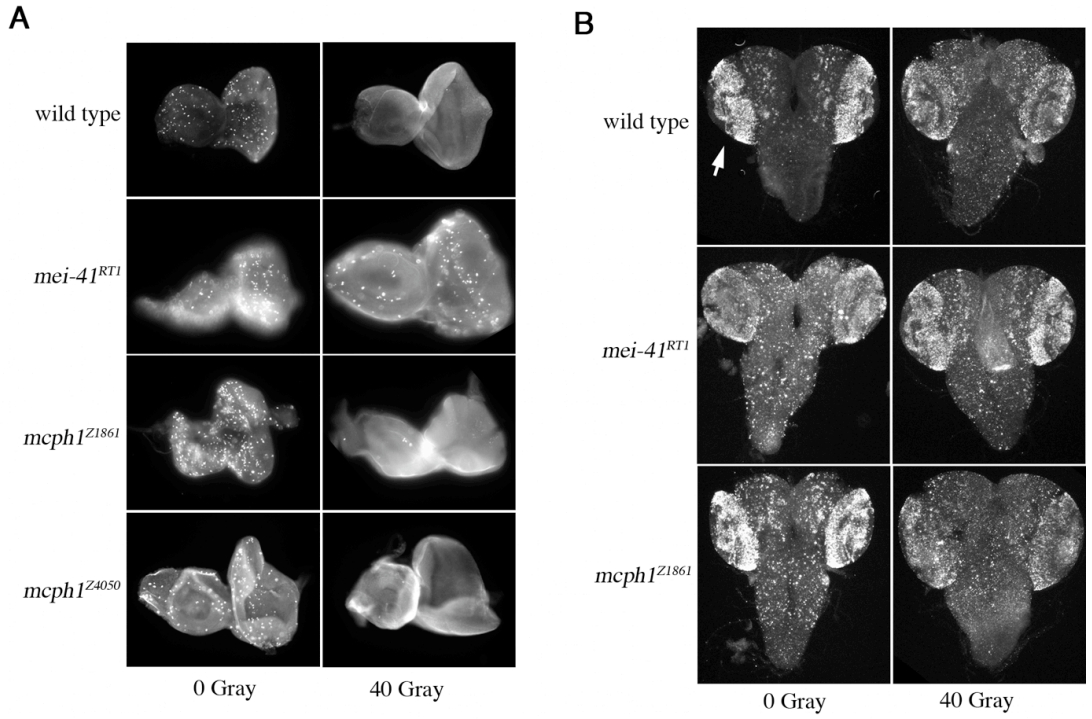

C

Sensitivity to hydroxyurea

Genotype	Percent homozygotes -HU	+HU
mei-41^{RT1}	59.2 (130)	0 (100)
mcph1^{Z1861}/ *mcph1*^{Z0978}	18.4 (163)	22.6 (288)
mcph1^{Exc21}	26.7 (101)	40.6 (101)

D

Eclosion after irradiation

Genotype	Percent eclosion 0 Gray	10 Gray
wild type	86.6 (134)	90.2 (153)
mei-41^{RT1}	79.8 (109)	3.3 (121)
mcph1^{Z1861}	85.1 (114)	82.4 (125)

Figure 2.8. *mcph1* larvae have intact DNA checkpoints and normal sensitivity to DNA-damaging agents. (A,B) Cell-cycle checkpoints in *mcph1* larvae. Bars, 50 µm. (A) G2-M checkpoint. Eye-antennal imaginal disks were dissected from untreated (left) or irradiated (right) larvae, fixed, and stained with antibodies against phosphorylated Histone H3 (anti-PH3), a marker of mitotic cells. Lack of anti-PH3 staining post-IR indicates G2 arrest. Representative disks are shown (with at least twelve discs scored per genotype). (B) Intra-S phase checkpoint. Brains were dissected from untreated (left) or irradiated (right) larvae and labeled with BrdU. Decreased BrdU staining in brain lobes (arrows) post-IR indicates intra-S phase arrest. Representative brains are shown (with at least six brains scored per genotype). (C,D) Survival of *mcph1* larvae following exposure to DNA-damaging agents. (C) Sensitivity to hydroxyurea (HU). Larvae were grown on food minus or plus HU and allowed to develop. For each genotype, the ratio of homozygous mutant to total progeny is expressed as a percentage with total number of adult flies scored shown in parentheses. (D) Sensitivity to IR. Third instar larvae were untreated or exposed to low-dose irradiation and allowed to develop. For each genotype, the ratio of eclosed adults to total pupae is expressed as a percentage with total pupae shown in parentheses.

mei-41, survive normally following low-dose IR exposure (Figure 2.8D), indicating that MCPH1 is not required for DNA repair (Jaklevic and Su, 2004).

The MEI-41/GRP-mediated DNA-replication checkpoint is also developmentally activated at the midblastula transition (MBT) (Sibon et al., 1999; Sibon et al., 1997). Rapid S-M cycles of the early embryo are under maternal genetic control, and the switch to zygotic control occurs at the MBT after cycle 13. During late syncytial cycles (11-13), titration of a maternal DNA-replication factor is thought to induce a *mei-41*/*grp*-dependent checkpoint that causes Cdk1 inhibitory phosphorylation. Mitotic entry is thereby slowed, presumably to allow time to complete replication. Embryos from *mei-41* or *grp* females fail to lengthen interphase in late syncytial cycles and undergo extra S-M cycles (Sibon et al., 1999; Sibon et al., 1997).

We asked if MCPH1 is required for the MEI-41/GRP-dependent DNA-replication checkpoint at the MBT. *mcph1* embryos undergo arrest due to Chk2 activation prior to their reaching cortical divisions (cycles 10-13). Thus, to test whether *mcph1* is required for cell-cycle delay at the MBT, we performed live analysis of cortical divisions in *mnk mcph1* embryos that lack a functional Chk2-mediated checkpoint. We reasoned that any primary defects in cell-cycle timing due to mutation of *mcph1* would still be apparent in *mnk mcph1* embryos. This assumption is strengthened by a recent study showing that *mnk grp* embryos that progress through the MBT due to lack of Chk2-mediated arrest retain the cell-cycle timing defects of *grp* embryos (Takada et al., 2007). We monitored timing of nuclear envelope breakdown and reformation by differential interference contrast

microscopy (DIC) and found no significant differences in interphase or mitosis lengths in *mnk mcph1* and wild-type embryos (Figure 2.9A).

To further confirm that the DNA-replication checkpoint is intact in *mnk mcph1* embryos, we assessed the extent of inhibitory phosphorylation of Cdk1 and found it to be comparable to that of wild type (Figure 2.9B). We also found wild-type levels of Cyclin B and Cyclin A in *mnk mcph1* embryos (Figure 2.9C; data not shown). Low levels of Chk1 protein have been reported in *MCPH1* siRNA human cells (Lin et al., 2005; Xu et al., 2004), but we detected normal levels of Grapes (Chk1) in *mcph1* and *mnk mcph1* embryos (Figure 2.9D). Thus, our data do not support a role for *Drosophila* MCPH1 in control of cell-cycle timing in syncytial embryos via regulation of Cdk1 phosphorylation, Cyclin B, or Grapes levels.

mcph1 cooperates with *mei-41* and *grp* to regulate syncytial divisions

Previous studies of *grp* and *mei-41* embryos largely focused on mitotic defects in cortical nuclear divisions, which are amenable to live analysis (Sibon et al., 2000; Takada et al., 2003). Given the earlier arrest point of *mcph1* embryos, we initially concluded that *mcph1* and *mei-41/grp* must have discrete roles. We subsequently found, however, that a sizeable fraction of embryos (17-33%) from homozygous or hemizygous *grp* females arrest in pre-cortical cycles (1-9) with acentrosomal, barrel-shaped spindles nearly identical to that of *mcph1* (Figure 2.10A). We obtained similar results for all three *grp* alleles tested (Figure 2.10B), including the null grp^{209} (Larocque et al., 2007). Our data and a previous report of defective Cyclin A proteolysis in pre-cortical *grp* embryos (Su et al., 1999) have

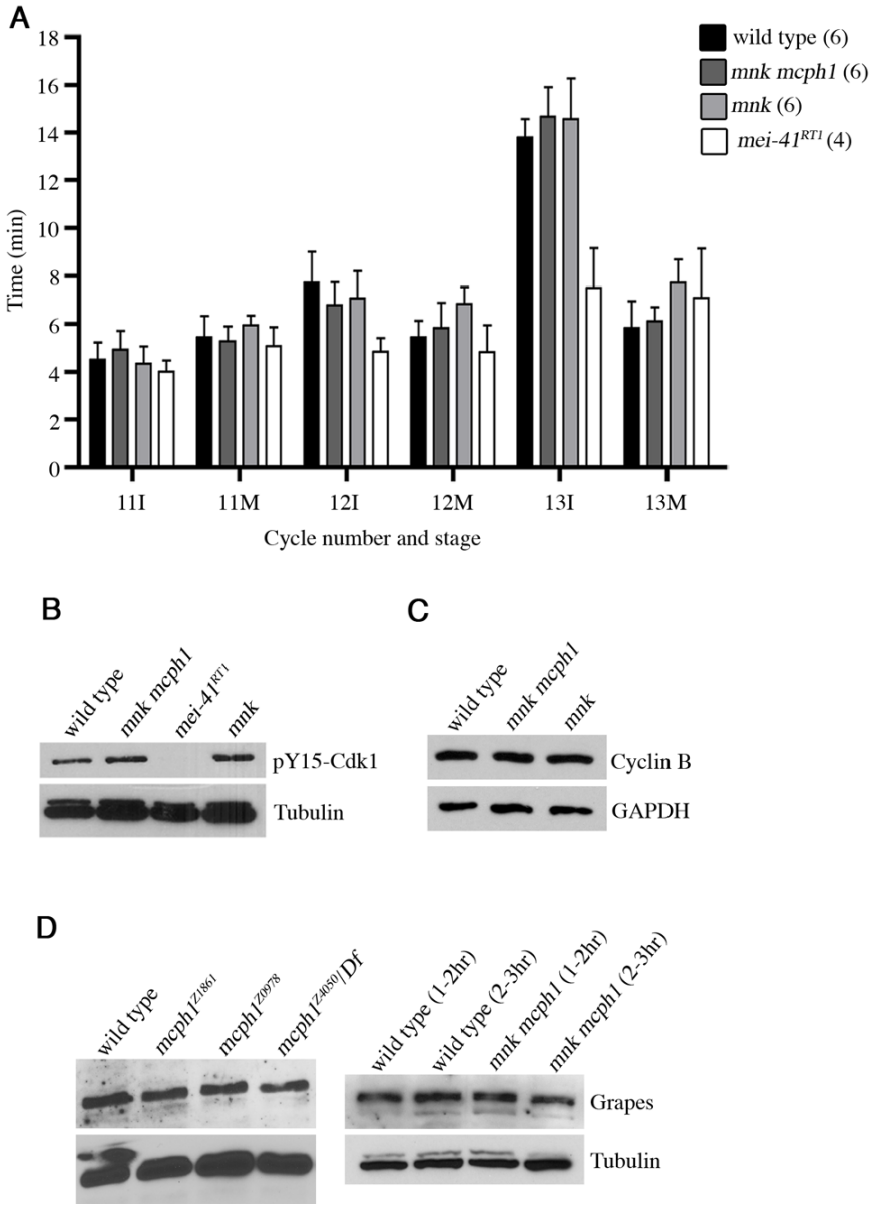

Figure 2.9. Intact DNA-replication checkpoint and normal Cyclin B levels in *mcph1* embryos. (A) Quantification of cell-cycle timing during cortical divisions of early embryogenesis. No significant differences in interphase (I) or mitosis (M) lengths were observed for *mnk mcph1*^{Z1861} embryos compared to wild-type or *mnk* controls, whereas shorter interphases were apparent in *mei-41* embryos (cycles 12 and 13). Average times with standard deviations (error bars) are shown. Numbers of embryos scored for each genotype are shown in parentheses. (B) Western analysis using phospho-specific antibodies against Cdk1 reveals wild-type levels of pY15-Cdk1 in extracts of *mnk mcph1*^{Z1861} embryos (1-2 hours). Control *grp* embryos have reduced pY15-Cdk1 levels. (C) Western analysis reveals normal Cyclin B levels in *mnk mcph1*^{Z1861} embryos (1-2 hours). (D) Western analysis reveals normal GRP levels in *mcph1* and *mnk mcph1*^{Z1861} embryos (1-2 hours unless otherwise indicated). Loading controls: anti-α-tubulin or anti-GAPDH.

A

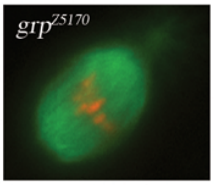

B

Genotype	*mcph1*-like arrest (%)	Embryos (n)
grp^{1}	17.1	152
grp^{1}*/Df(2L)H20*	21.4	234
grp^{Z5170}	21.4	103
grp^{Z1570}*/Df(2L)H20*	32.8	137
grp^{209}*/Df(2L)H20*	27.6	152

C

Genotype	Hatch rate (%)	Embryos (n)
mei-41^{RT1}*/mei-41*^{D5}	22.3	1490
mei-41^{RT1}*/mei-41*^{D5}*; grp*^{1}*/+*	4.4	1441
mei-41^{RT1}*/mei-41*^{D5}*; mcph1*^{Z1861}*/+*	6.9	1774
mcph1^{Z1861}*/+*	90.4	250

D

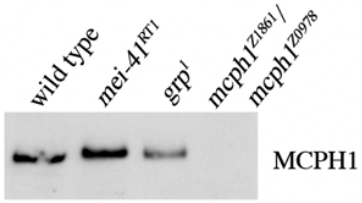

Figure 2.10. *mcph1* cooperates with *mei-41* and *grp* in the early embryo. (A) Mitotic spindle from a pre-cortically arrested *grapes*^{Z5170} embryo resembles *awol*-type spindles of *mcph1* embryos. Microtubules are in green and DNA in red. Scale bar: 10 μm. (B) Quantification of *mcph1*-like arrest in *grp* embryos (2-4 hours). (C) *mcph1* dominantly enhances *mei-41* embryonic lethality. Introduction of one copy of *mcph1*^{Z1861} into a semi-sterile *mei-41* background (*mei-41*^{RT1}*/mei-41*^{D5}) reduces embryonic hatch rate more than threefold. (D) Immunoblotting shows slower gel mobility of MCPH1 in *mei-41*^{RT1} or *grp*^{1} embryos (1-2 hours) relative to wild type.

established a role for *grp* in regulating the cell cycles of early syncytial embryos. We also found that *mcph1* dominantly enhances a weak *mei-41* phenotype to a degree similar to that of *grp* (Figure 2.10C). Intriguingly, by immunoblotting, we consistently observe an upward mobility shift in MCPH1 in *grp* or *mei-41* embryonic extracts (Figure 2.10D). Taken together, these data suggest that MCPH1 cooperates with MEI-41 and GRP to regulate the cell cycles of the early embryo via a mechanism independent of Cdk1 phosphorylation.

mcph1 males exhibit defects in adult brain structure

On the basis of the reduced brain size of patients with mutation of *mcph1*, we tested whether mutation of *Drosophila mcph1* affects brain development. We did not observe an obvious change in overall brain size, but we did observe morphological defects in central brain structures. The mushroom bodies (MBs) of the *Drosophila* adult brain are bilaterally symmetrical structures required for olfactory memory and other complex adaptive behaviors (de Belle and Heisenberg, 1994). MB structure is stereotyped, and gross morphological brain defects often uncover structural defects in MBs. The 2500 intrinsic neurons in each MB can be subdivided into at least three morphologically well-defined subsets (αβ, α'β', or γ) based on bundling of their axonal projections in the region of the MBs called the lobes (Crittenden et al., 1998). Each MB neuron contributing to the αβ subdivision bifurcates and sends one axon branch vertically to the αlobe and one horizontally to the β-lobe. Anti-Fasciclin II (FasII) antibodies strongly label MB neurons that lie in the αβ-lobes (Grenningloh et al., 1991), thereby allowing straightforward

visualization of developmental defects.

Our initial analysis revealed obvious morphological MB defects in brains of *mcph1*^{Z1861} and *mcph1*^{Exc21} male flies (Figure 2.11A). The nature of the MB defects was variable, ranging from missing or malformed lobes to complete absence of lobes, and defects were often asymmetric. For unknown reasons, we never observed MB defects in brains of female *mcph1* flies (data not shown). Quantification revealed defects in 22% of *mcph1*^{Z1861} and 13% of *mcph1*^{Exc21} male brains (Figure 2.11B). We similarly found defects in 11.5% of brains from males carrying *mcph1*^{Z1861} in trans to a deletion of the *mcph1* genomic locus; no defects were found in control heterozygous (*mcph1*^{Z1861}*/+*) male brains. These data establish a role for *mcph1* in *Drosophila* brain development.

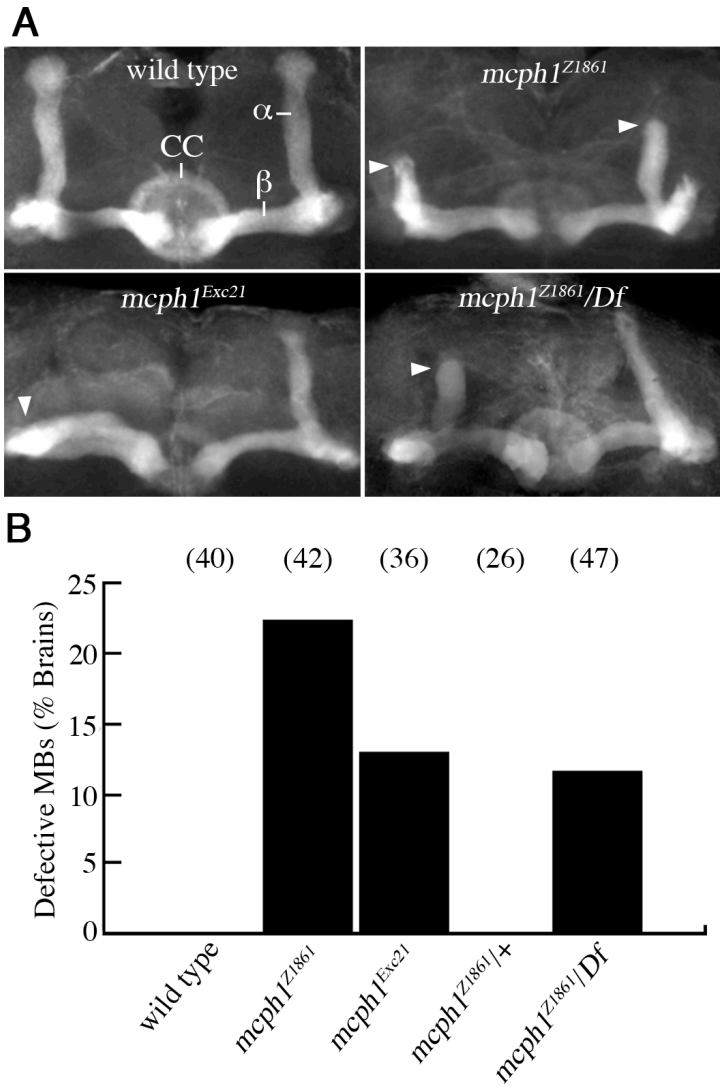

Figure 2.11. Defects in male *mcph1* brains. Adult male brains were stained with anti-FasII antibodies to visualize mushroom body (MB) αβlobes and the ellipsoid body of the central complex (CC). (A) MB αβlobes of wild-type brains are symmetric, whereas MBs of *mcph1* brains are occasionally defective with missing or diminished αβlobes (arrowheads). *Df=Df(2R)BSC39*, which removes the *mcph1* genomic locus. (B) Quantification of brain defects in *mcph1* males. Sample number for each genotype is indicated in parentheses (top).

DISCUSSION

We identified *Drosophila mcph1*, the homolog of the human primary microcephaly gene *MCPH1*, in a genetic screen for cell-cycle regulators and have shown that it is required for genomic stability in the early embryo. Three additional primary microcephaly (*MCPH*) genes have been identified in humans: *ASPM, CDK5RAP2*, and *CENPJ* (reviewed by Cox et al., 2006). Much of our understanding of the biological functions of the proteins encoded by human *MCPH* genes has come from studies of their *Drosophila* counterparts. Mutation of *abnormal spindle* (*asp*), the *Drosophila* ortholog of *ASPM*, results in cytokinesis defects and spindles with poorly focused poles (do Carmo Avides and Glover, 1999; Wakefield et al., 2001). The *Drosophila* ortholog of *CDK5RAP2, centrosomin* (*cnn*), is required for proper localization of other centrosomal components (Li and Kaufman, 1996; Megraw et al., 1999). *Sas-4*, the *Drosophila* ortholog of *CENPJ*, is essential for centriole production, and the mitotic spindle is often misaligned in asymmetrically dividing neuroblasts of *Sas-4* larvae (Basto et al., 2006). Whereas all of these primary microcephaly genes are critical regulators of spindle and centrosome functions, mitotic defects in *Drosophila mcph1* mutants are largely secondary to Chk2 activation in response to DNA defects; thus, *mcph1* probably represents a distinct class of primary microcephaly genes.

MCPH1 is a BRCT domain-containing protein, suggesting that it plays a role in the DNA damage response. Conflicting models of MCPH1 function, however, have emerged from studies of human cells as it has been proposed to function at various

levels in this pathway: upstream, at the level of damage-induced foci formation (Rai et al., 2006) and further downstream, to augment phosphorylation of targets by the effector Chk1 (Alderton et al., 2006). The phenotype of embryos from null *mcph1* females is more severe than that of embryos from null *grp* females, suggesting that enhancement of phosphorylation of GRP (Chk1) substrates is not the sole function of MCPH1. Furthermore, we found both the DNA checkpoint in larval stages and its developmentally regulated use at the MBT to be intact in *mcph1* mutants, suggesting a requisite role for MCPH1 in the DNA checkpoint evolved in higher organisms.

Studies of human cells suggest a role for MCPH1 in regulation of chromosome condensation. Microcephalic patients homozygous for a severely truncating mutation in MCPH1 show increased frequency of G2-like cells displaying premature chromosome condensation (PCC) with an intact nuclear envelope (Alderton et al., 2006; Trimborn et al., 2004). Depletion of Condensin II subunits by RNAi in *MCPH1*-deficient cells leads to reduction in the frequency of PCC, suggesting that MCPH1 is a negative regulator of chromosome condensation (Trimborn et al., 2006). Alderton et al. (Alderton et al., 2006) observed a decreased level of inhibitory phosphates on Cdk1 that correlated with PCC in *MCPH1*-deficient cells. The authors proposed that MCPH1 maintains Cdk1 phosphorylation in an ATR-independent manner because PCC is not seen in cells of patients with Seckel syndrome, which is caused by mutation of *ATR*; residual ATR present in these cells, however, may be sufficient to prevent PCC (O'Driscoll et al., 2003). Furthermore, in several experimental systems, ATR and Chk1 have been implicated in an S-M checkpoint that prevents premature mitotic entry with unreplicated DNA (reviewed by Petermann and Caldecott, 2006).

We have shown that embryos from *grp* (*Chk1*) females occasionally undergo *mcph1*-like arrest in early syncytial cycles, prior to the time at which inhibitory phosphorylation of Cdk1 is thought to control mitotic entry. Thus, decreased signaling through the DNA checkpoint resulting in less Cdk1 phosphorylation is unlikely to explain this *mcph1*-like arrest. In contrast to studies of *MCPH1*-deficient human cells, we detect no decrease in pY15-Cdk1 levels in *mcph1* embryos allowed to progress beyond their normal arrest point by mutation of *mnk* (*Chk2*). Based on these data and the PCC phenotype associated with loss of *MCPH1* in humans, we propose a model in which MEI-41/GRP cooperate with MCPH1 in syncytial embryos in a Cdk1-independent manner to delay chromosome condensation until DNA replication is complete. In the absence of *mcph1*, we hypothesize that embryos condense chromosomes before finishing S phase, resulting in DNA defects (bridging chromatin), Chk2 activation, and mitotic arrest. We were precluded from directly monitoring chromosome condensation in *mnk mcph1* embryos expressing Histone-GFP as previously described (e.g. Brodsky et al., 2000) because we were unable to establish fly stocks carrying this transgene in the *mnk* background. Live imaging of *mcph1* embryos was not technically feasible because they arrest prior to cortical stages, and yolk proteins obscure more interior nuclei in early embryos. *grp* embryos have been reported to initiate chromosome condensation with normal kinetics (Yu et al., 2000), although a subtle PCC phenotype might be difficult to detect.

Support for our model that MCPH1 allows completion of S phase by delaying chromosome condensation comes from the observation that inhibition of DNA

replication in syncytial embryos (via injection of aphidicolin or HU) results in phenotypes similar to those observed in *mcph1* embryos, including chromatin bridging, which is presumably a direct consequence of progressing through mitosis with unreplicated chromosomes (Raff and Glover, 1988), and Chk2 activation (Takada et al., 2003). Alternatively, *mcph1* might be required during S phase for timely completion of DNA synthesis; in this case, *mcph1* embryos would initiate chromosome condensation with normal kinetics prior to completing replication. Coordination of S-phase completion and mitotic entry may be particularly critical in the rapid cell cycles of the early embryo that lack gap phases and may explain why loss of *Drosophila mcph1* is most apparent at this developmental stage. Interestingly, even in the absence of exogenous genotoxic stress, *MCPH1*-deficient human cells also exhibit a high frequency of chromosomal aberrations (Rai et al., 2006), which may be a consequence of PCC.

An evolutionary role for *mcph1* in expansion of brain size along primate lineages has emerged in recent years (reviewed by Woods et al., 2005). In brains of *Drosophila mcph1* males, we find low-penetrance defects in MB structure. Both MCPH1 isoforms are expressed in larval brains, and all *mcph1* mutations described here affect both isoforms, so it is unclear whether MB formation requires one or both isoforms. The lack of MB defects in *mcph1* females is puzzling because both isoforms are found in male and female larval brains (data not shown); other sex-specific factors are probably involved. Larval brains of *mcph1* males show no obvious aneuploidy (data not shown) or spindle orientation defects (Andrew Jackson, personal communication), so the cellular basis for these defects remains to be

determined. It will be interesting to test in future studies whether *mei-41* and *grp*, which cooperate with *mcph1* to regulate early embryogenesis, are similarly required in *Drosophila* males for brain development.

In conclusion, we have demonstrated an essential role for *Drosophila* MCPH1 in maintaining genomic integrity in the early embryo. Our data suggest that, in contrast to the mammalian protein, *Drosophila* MCPH1 is not required for the DNA checkpoint, although its role in regulating other processes (e.g. chromosome condensation) may be conserved. We predict that the early embryo of *Drosophila* will continue to be an important model genetic system for unraveling the biological functions of MCPH1, a critical determinant of brain size in humans.

CHAPTER III

REGULATION OF HUMAN AND DROSOPHILA MCPH1 BY THE ANAPHASE PROMOTING COMPLEX

This work was in collaboration with Danny Liang Yee Ooi, Ph.D., a former graduate student in the Marc Kirschner lab, Harvard Medical School.

INTRODUCTION

Regulated proteolysis is critical for proper cell-cycle timing. The Anaphase-Promoting Complex (APC) is a multisubunit E3 ligase that catalyzes ubiquitin-mediated degradation of key cell-cycle proteins, thereby coordinating orderly progression (reviewed in Harper et al. 2002; Thornton and Toczyski 2006). APC substrates include mitotic cyclins (King et al. 1995) and Securin, an inhibitor of sister-chromatid separation (Shirayama et al. 1999). Cdc20 and Cdh1, which are APC activators, play critical roles in substrate specificity determination and timing of degradation. The APC controls events in mitosis and G1 and influences S-phase events; thus, it affects many aspects of cell-cycle progression.

In Vitro Expression Cloning (IVEC) screening approaches have been used to successfully identify candidate proteins involved in a variety of processes including kinase or protease substrates, and protein binding (reviewed in King et al. 1997). In this approach, pools of radiolabeled proteins generated from cDNA libraries are incubated under the appropriate biochemical conditions and assayed for changes.

Caveats to this approach include clones that may be over- or under-represented within a particular library. Also, inputs are initially unknown requiring progressive subdivision of pools until individual clones can be isolated. A modified IVEC approach in which clones were obtained from the Drosophila Gene Collection has been successfully used to identify substrates of the Pan Gu kinase (Lee et al. 2005). The advantage of this approach, termed "DIVEC" (for "Drosophila IVEC"), is that each clone is fully sequenced, singly represented within the collection, and annotated, thus allowing one to easily identify positives within pools of radiolabeled proteins.

In the previous chapter, we identified MCPH1 in a screen for regulators of early Drosophila embryogenesis. Here, we present the identification of MCPH1 in an independent DIVEC screen for substrates of the APC. Drosophila MCPH1-B contains a functional D box and is targeted by the APC *in vivo*. Furthermore, we find that human MCPH1 is also degraded in an APC-dependent manner. *MCPH1* is a rapidly evolving gene; however, functional APC-mediated regulation has been retained from Drosophila to human. Interestingly, human MCPH1 has evolved to encode an APC recognition sequence, the KEN box, not present within Drosophila MCPH1. Finally, we show that overexpression of MCPH1 in developing Xenopus embryos leads to cell-cycle arrest.

METHODS

Drosophila stocks

Flies were maintained at 25˚C using standard techniques (Greenspan 2004). Wild-type stocks used were *y w*. *nanos-Gal4:VP16* and *fizzy-related* stocks were obtained from the Bloomington Stock Center. *morula* mutant stocks were gifts from Terry Orr-Weaver.

Drosophila *mcph1* cDNA clones and transgenes

cDNA clones encoding MCPH1-B (LD43341) were from the Drosophila Gene Collection or Drosophila Genomics Resource Center. The first putative Dbox (RXXL) was mutated to AXXL using the Stratagene QuikChange II kit. MCPH1-B or MCPH1-B-Dbox coding region was PCR-amplified and subcloned into a UASp (Rorth 1998) derivative encoding six N-terminal Myc tags. UASp-Myc-*MCPH1-B* and UASp-Myc-*MCPH1-B-Dbox* were transformed into *y w* flies as described (Spradling 1986). To generate IVT constructs, MCPH1-B coding region was subcloned into pCS2 or derivatives encoding six N- or C-terminal Myc tags. DeltaN-MCPH1-B (N-terminal 40 amino acids deleted) and DeltaDbox-MCPH1-B (RRPLH at positions 36-40 changed to alanines) were made by PCR-based mutagenesis.

Polyclonal antibodies against Drosophila MCPH1

MBP fused to MCPH1-B (N-terminal 352 amino acids) was used to produce antibodies. N-terminal MCPH1-B sequence was PCR-amplified from LD43341 and

subcloned into pMAL (New England Biolabs). MBP-N-MCPH1-B was made in bacterial cells, purified using amylose beads, and injected into guinea pigs for antibody production (Covance). Anti-MCPH1 antibodies were affinity purified using standard techniques.

Drosophila IVEC screen for APC substrates and APC-mediated degradation assays

Xenopus interphase egg extracts, human Cdh1, and Cyclin B N-terminal peptide were prepared as described (Pfleger and Kirschner 2000). Xenopus mitotic extracts were prepared by supplementing interphase extracts with calcium. Radiolabeled protein pools (1 μl) prepared from the Drosophila Gene Collection as previously described (Lee et al. 2005) were added to Xenopus extracts (5 μl) supplemented with XB buffer, delta90 (non-degradable) Cyclin B (60 μg/ml) (King et al. 1995), or Cdh1 (0.5 nM) (Lorca et al., 1998) and incubated at room temperature. Reaction products were analyzed by SDS-PAGE/autoradiography. For each positive pool, individual clones were identified by testing smaller pools and confirmed by sequencing. Competitive degradation assays were performed by adding Cyclin B N-terminal peptide (100 μM) to Cdh1-supplemented extracts. Radiolabeled MCPH1-A or -B (wild-type, tagged, or mutant) were made by coupled transcription-translation according to the manufacturer's protocol (Promega) and used in degradation assays (as described above for screen).

Subcellular localization of APC substrates in mammalian cells

p71, p78, or p91 (MCPH1-B) coding region was subcloned into a pCS2 derivative encoding an N-terminal GFP tag. The resulting constructs encoding GFP-tagged p71, p78, or p91 were transiently transfected into NIH 3T3 cells using Lipofectamine (Invitrogen) according to the manufacturer's protocol and examined by fluorescence microscopy.

Drosophila protein extracts and immunoblots

Protein extracts were made by homogenizing embryos (1-2 hr unless otherwise indicated) or dissected tissues in urea sample buffer as described (Moore et al. 1998). Proteins were transferred to nitrocellulose for immunoblotting using standard techniques. The method of Edgar et al. (1994) was used to make extracts from staged syncytial embryos (ten cycle-10 embryos per lane). Briefly, Methanol fixed embryos were collected (110-140 minute) and stained using DAPI. After clearing on ice for 1 hour, embryos were observed using a 10X objective and separated based on cycle number and cell-cycle stage. 3X SDS buffer was added (2 µl/embryo), and samples were boiled for 10 minutes. Antibodies were used as follows: guinea pig anti-MCPH1 (1:200-500), mouse anti-Cyclin B (F2F4, 1:200, Developmental Studies Hybridoma Bank), and mouse anti-α-tubulin (DM1α, 1:5000, Sigma). HRP-conjugated secondary antibodies and chemiluminescence were used to detect primary antibodies.

Quantification of embryonic hatch rates

For hatch rate assays, embryos (0-4 hr) were collected on grape plates, counted, and aged ~40 hr at 25°C. The number of hatched embryos was determined by subtracting number of unhatched (intact) embryos from total number collected. Hatch rate is the ratio of hatched to total embryos expressed as a percentage.

Cell culture extracts and immunoblots

HeLa or HEK293 cell extracts were made in 6-well dishes by removing media, washing once with ice-cold PBS, and adding 150 µl of non-denaturing lysis buffer. After 30 minutes, cells were scraped, spun down, and supernatant was collected. Protein concentration was determined by Bradford assay. Lysates containing 10-20 µg of protein were mixed with 3X SDS buffer and analyzed by SDS-PAGE/Western blot. Antibodies were used as follows: rabbit anti-hMCPH1 (2AB1, 1:200-1:500), rabbit anti-Cyclin B (1:500, Santa Cruz), mouse anti-α-Tubulin (DM1α, 1:5000, Sigma), mouse anti-Cdk1 (PSTAIR, 1:1000, Millipore).

Cell synchronization

HeLa cells were plated on a 10 cm dish at 40% confluency and treated with thymidine (2mM) for 24 hours. Cells were washed twice with PBS and treated with nocodazole (0.1µg/ml) for 12-14 hours. After removing the media, plates were firmly tapped to loosen the rounded, mitotic cells from the dish. Cells were collected in 10 ml serum-free media by centrifugation for 5 minutes, and resuspended in fresh serum-free media. This was repeated five times. After the

final wash, cells were resuspended in media containing 10% FBS and plated at 50% confluency in the wells of a 6-well dish. Cells were collected as follows: media was removed and cells washed in PBS. 100 µl 0.25% trypsin-EDTA was added and neutralized with 1 ml media. Cells were collected and washed once in PBS. 25% of each sample was saved for FACS analysis while the remaining cells were resuspended in 50 µl NDLB and analyzed by SDS-PAGE/Western blot. For FACS, cells were fixed in 70% ethanol, stained with propidium iodide, and analyzed using a 5-laser BD LSRII located in the Vanderbilt University Flow Cytometry Core Facility.

***In vivo* ubiquitylation assay**

hMCPH1, hMCPH1-KEN, and hMCPH1-Dbox were subcloned into the CS2+ vector encoding an N-terminal 6-Myc tag and transfected into HEK293 cells using Lipofectamine (Invitrogen) with or without a construct encoding histidine-tagged ubiquitin (PMT107, Treier et al., 1994). 40 hours post-transfection, cells were harvested and washed two times in PBS. Cells were sonicated in Buffer A (6M guanidine-HCl, 0.1M Na2HPO4/NaH2PO4, 10mM imidazole, pH 8.0) and incubated with nickel agarose beads for three hours shaking at 4°C. The beads were washed twice in Buffer A, twice in 1:3 Buffer A/TI, and once in Buffer TI (25 mM Tris-HCl, 20 mM imidazole, pH 6.8). Proteins bound to the beads were then released by boiling in 3X SDS for 10 minutes and analyzed by SDS-PAGE/Western blot.

Capped RNA synthesis

The RNA synthesis reaction was derived from patent 7,074,596. Briefly, 20 µL in vitro transcription reactions contained 40 mM Tris-HCl, pH 7.9, 6 mM $MgCl_2$, 2 mM spermidine, 10 mM DTT, 2 µg BSA, 20 units of RNasin (Promega), 0.5 mM ATP, 0.5 mM CTP, 0.5 mM UTP, 0.1 mM GTP, 1 mM cap analog (GpppG,m7GpppG, m^{73}'dGpppG, or m_2^7,O3'GpppG, New England Biolabs), 1.0 µg DNA, and 20 units of SP6 polymerase (Promega). cDNAs (Mos, GFP, human MCPH1, human MCPH1-KEN, Drosophila MCPH1-B, and Drosophila MCPH1-A) subcloned into CS2+ and linearized with the NotI restriction enzyme were used for DNA source. Human *MCPH1* cDNA clones were obtained from Marc Kirschner's lab (Harvard Medical School).

Xenopus embryo injections

Eggs collected from HCG-injected (800 units/frog) virgin female frogs were spread into a monolayer using forceps with a small section of the male testis. After five minutes, eggs were covered with deionized water (dH_20). After one hour, eggs were dejellied with cysteine (2 g in 100 ml dH_20, pH 7.6-7.8) for 5 minutes, washed twice with dH_20, and placed in 0.1X MMR containing 3% Ficoll. Embryos were injected at the 2- or 4-cell stage with 2ng of RNA. Embryos were fixed in MEMFA (100µM MOPS pH 7.4, 2mM EGTA, 1mM $MgSO_4$, and 3.7% formaldehyde) 4 hours post-injection overnight at 4°C. After fixation, embryos were washed twice in PBS then dehydrated stepwise in 75% PBS/25% methanol, 50% PBS/50% methanol, and 100% methanol. Embryos were stored dehydrated at 4°C until further use.

Live analysis of Xenopus embryos

Immediately after injection, embryos were analyzed using a Zeiss Stemi 2000-CS stereoscope equipped with an Olympus DP72 camera. Images of dividing embryos were captured at 30 second intervals using the Olympus DP2-BSW software.

Immunostaining of Xenopus embryos

MEMFA-fixed embryos were dehydrated and stored in methanol overnight. To remove excess pigment, embryos were bleached in 10% H_2O_2/67% methanol for 8 hours at room temperature. Embryos were then rehydrated stepwise in 50% methanol/50% TBS (155mM NaCl, 10mM Tris-Cl pH 7.5), 25% methanol/75% TBS , and finally 100% TBST (155mM NaCl, 10mM Tris-Cl pH 7.5, 0.1% Triton-X-100) for 1 hour each step on a rocking platform. Embryos were blocked in WMBS (155mM NaCl, 10mM Tris-Cl pH 7.5, 10% fetal bovine serum, 5% DMSO) for one hour on a rocking platform. Primary antibody was added directly to the WMBS (Tubulin, 1:500) as well as RNAse A (1mg/ml) and propidium iodide (2µg/ml). Embryos were incubated overnight at 4°C on a nutator then washed with five 1-hour rinses in TBST. Embryos were then treated using Cy2 conjugated secondary antibodies (1:500) incubated in WMBS plus RNAse A and propidium iodide then washed with five 1-hour rinses in TBST. Embryos were placed in MatTek dishes and imaged using a Leica TCS SP5 inverted confocal microscope.

RESULTS

A screen for substrates of the Anaphase-Promoting Complex identifies Drosophila MCPH1

We independently identified MCPH1 in a Drosophila genome-scale biochemical screen for Anaphase-Promoting Complex (APC) substrates. We used a previously described Drosophila IVEC (*in vitro* expression cloning) approach (Lee et al. 2005) to screen for radiolabeled Drosophila proteins that are degraded and/or phosphorylated in mitosis. Our design was based on previous IVEC screens of Xenopus cDNA libraries (King et al. 1997; Lustig et al. 1997; McGarry and Kirschner 1998; Ayad et al. 2005). APC substrates were identified as bands that decrease in intensity in mitotic or Cdh1-supplemented interphase Xenopus egg extracts. Bands with decreased intensity in either of these reactions represent candidate APC-Cdc20 or APC-Cdh1 substrates, respectively. Mitotic kinase substrates were identified as bands with reduced gel mobility in mitotic extracts (compared to interphase extracts). We screened 5849 cDNA clones (~43% of the fly genome) in this manner. We found a high frequency of mitotic phosphorylation (roughly one positive per pool of 24 clones). In contrast, only three pools had proteins (p91, p78, and p71) that degraded in Cdh1-supplemented extracts; all three exhibited upward mobility shifts in mitotic extracts (Figure 3.1A), suggesting that they are substrates of both the APC-Cdh1 and of mitotic kinases.

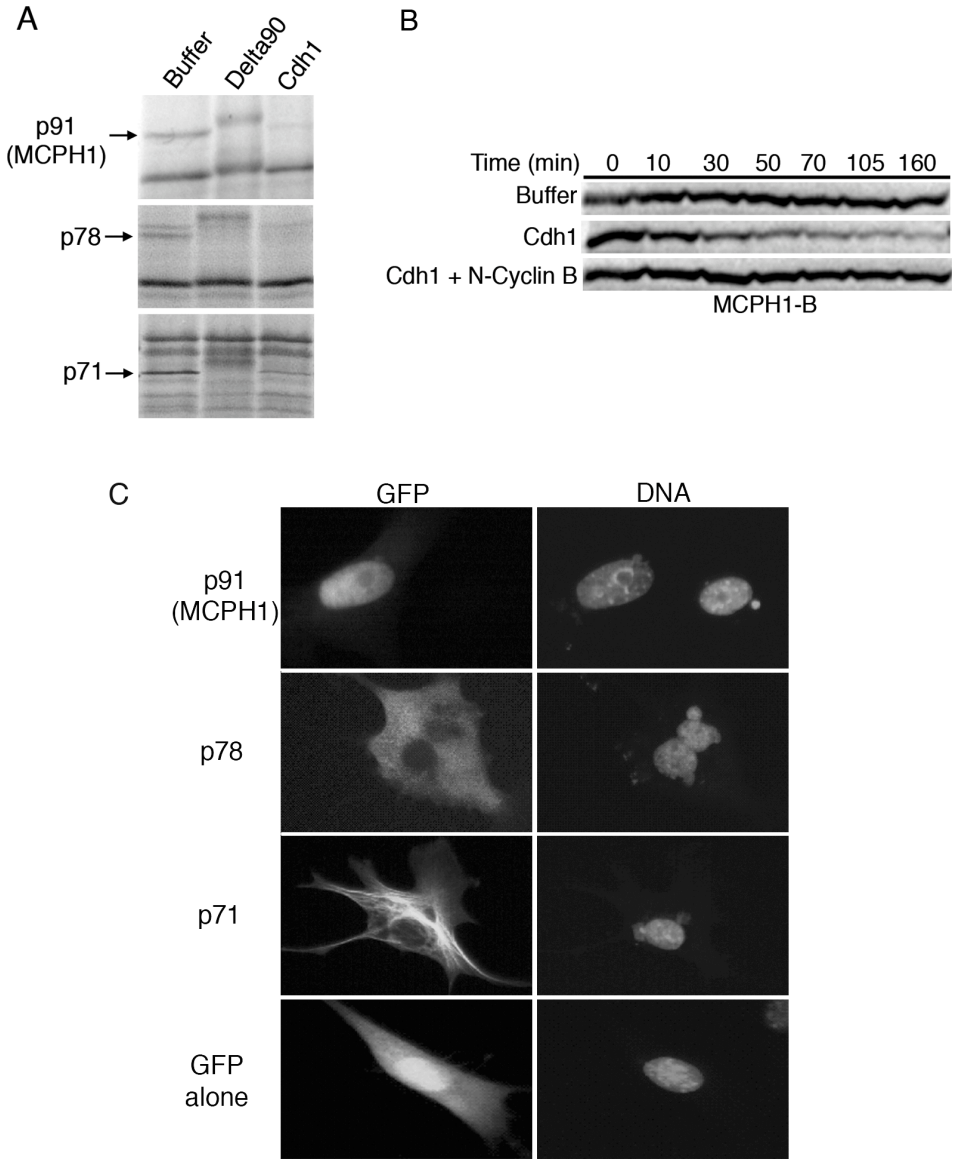

Figure 3.1. Drosophila MCPH1-B is an APC substrate. (A-B) APC-mediated protein degradation assays. Radiolabeled proteins were incubated in Xenopus egg extracts and reaction products analyzed by SDS-PAGE/autoradiography. (A) Candidates from screen for APC substrates. Protein pools were incubated with interphase extracts plus XB buffer, non-degradable Cyclin B ("Delta90"; to create mitotic extracts), or Cdh1 (to activate APC). Three pools contained bands (p91, p78, or p71) showing both an upward mobility shift in mitotic extracts and decreased intensity in Cdh1-supplemented extracts. Clones encoding APC substrates were identified (Supp. Table 3); p91 is MCPH1-B. (B) Competitive degradation assay. Addition of N-terminal Cyclin B peptide to Cdh1-supplemented extracts caused MCPH1-B stabilization. (C) Subcellular localizations of new APC substrates. GFP fusions of Drosophila p91/MCPH1, p78, or p71 were expressed in NIH 3T3 cells. DNA was staining with DAPI. GFP alone was used as control.

Table 3.1. New APC substrates from Drosophila IVEC screen

Protein band	DGC[a] cDNA clone ID	Drosophila gene	Protein description	Subcellular localization[b]	Vertebrate homolog
p91	LD43341[c]	*MCPH1*	BRCT domain[d]	Nucleus	MCPH1
p78	GH13229	*CG32982*	PH domain[e]	Cytoplasm	None
p71	LD21675	*CG3679*	Novel	Microtubules	None

[a]Drosophila Gene Collection
[b]Based on results shown in Figure 3.1C
[c]Encodes isoform B of *MCPH1*
[d]BRCA1 C-Terminal domain
[e]Pleckstrin homology domain

Individual cDNA clones encoding APC substrates were identified within each of the three positive pools (Table 3.1). p91 is identical to MCPH1-B. p78 and p71 are novel proteins, and BLAST searches revealed no obvious vertebrate homologs. For all three, specificity of APC-mediated degradation was shown by Cyclin competition: addition of N-terminal Cyclin B peptide to Cdh1-supplemented extracts blocked their degradation (Figure 3.1B and data not shown). We assessed their subcellular localizations by transfecting plasmids encoding GFP fusions of the Drosophila proteins into mammalian cells. MCPH1-B, p78, and p71 localized to the nucleus, cytoplasm, and microtubules, respectively, of interphase cells (Figure 3.1C).

MCPH1-B contains a functional D box

Two MCPH1 isoforms, splice variants of the same gene, exist in Drosophila. *mcph1-A* encodes a protein that is structurally similar to human Microcephalin with a single N-terminal BRCT domain and paired BRCT domains at the C-terminus. Only the N-terminal BRCT domain is encoded within *mcph1-B* and the protein terminates just before the start of the paired domains. Alternative splicing also results in an extra 40 amino acids at the amino terminus of MCPH1-B (Figure 3.2A). To identify the signal within MCPH1 that mediates its turnover, we looked for sequences that might represent the two major degradation signals recognized by APC-Cdh1: the destruction box (D box) (Glotzer et al. 1991) and the KEN box (Pfleger and Kirschner 2000). MCPH1-B contains several candidate D box sequences (data not shown) but no KEN boxes. We found that MCPH1-A is not significantly degraded in Cdh1-supplemented Xenopus extracts (Figure 3.2B), suggesting that the critical D

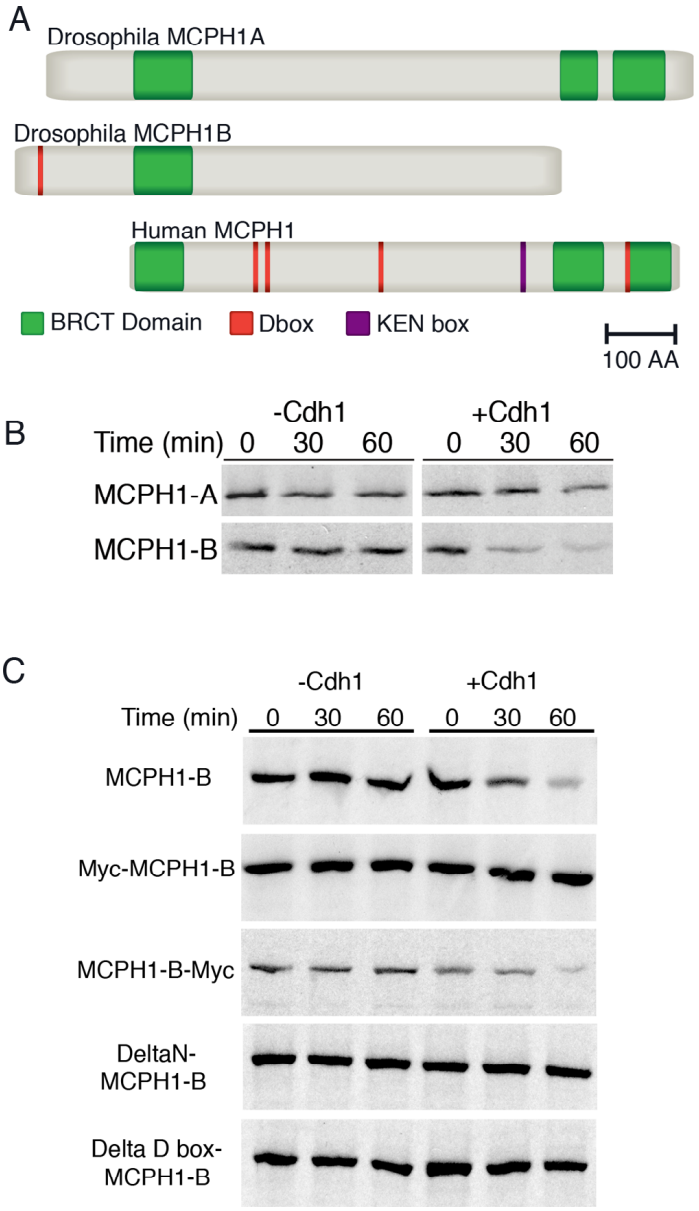

Figure 3.2. Identification of the critical destruction box within MCPH1-B. (A) Comparison of MCPH1 isoforms reveals differences in the N-terminus including the presence (MCPH1-B) or absence (MCPH1-A) of a putative D box sequence. Human MCPH1 contains four putative D boxes as well as a KEN box. (B) Cdh1-supplemented extracts degrade MCPH1-B, but not MCPH1-A. (C) Radiolabeled MCPH1-B (untagged, Myc-tagged, or mutated) was added to Xenopus interphase egg extracts (minus or plus Cdh1) and reaction products analyzed by SDS-PAGE/autoradiography. Cdh1-supplemented extracts degrade full-length, untagged MCPH1-B. MCPH1-B proteins with the following modifications were tested in this assay: Myc-tagged at the amino or carboxy terminus (Myc-MCPH1-B or MCPH1-B-Myc, respectively), N-terminal deletion of 40 amino acids (DeltaN-MCPH1-B), or mutation of destruction box within this N-terminal region (DeltaDbox-MCPH1-B).

box lies in the N- or C-terminal regions of MCPH1-B that differ from MCPH1-A. Myc tagging the amino terminus of MCPH1-B rendered it resistant to APC-Cdh1, whereas tagging the carboxy terminus had no effect on stability (Figure 3.2C). These results suggest that the critical D box lies near the amino terminus of MCPH1-B. Removal of its N-terminal 40 amino acids or specific mutation of a candidate D box in this region resulted in its stabilization in Cdh1-supplemented extracts (Figure 3.2C), confirming that we have identified the critical D box of MCPH1-B.

Drosophila MCPH1-B is an *in vivo* substrate of the Anaphase Promoting Complex

If MCPH1-B were an *in vivo* substrate of APC-Cdh1, its levels should fluctuate in a cell-cycle dependent manner. Immunoblotting of extracts from staged syncytial embryos revealed that MCPH1 levels are lower in interphase than in mitosis (Figure 3.3A). This type of pattern parallels that of the iconic APC substrate, Cyclin B, in syncytial embryos (Edgar et al. 1994). Consistent with our observation that MCPH1 is phosphorylated in Xenopus mitotic extracts, we observe an upward shift in its mobility on immunoblots of early mitotic embryos .

We further used a genetic approach to examine MCPH1 levels in embryos derived from *APC2* (*morula* or *mr*) mutant females. *mr* encodes the Cullin-homology domain subunit of the APC and is essential for ubiquitin ligase function. Similar to a known APC substrate, Cyclin B, MCPH1 levels are higher in 0-1hr embryos derived from *mr* females (Figure 3.3B). These embryos arrest soon after the start of the syncytial divisions, so to test whether this difference in MCPH1 levels is due to the

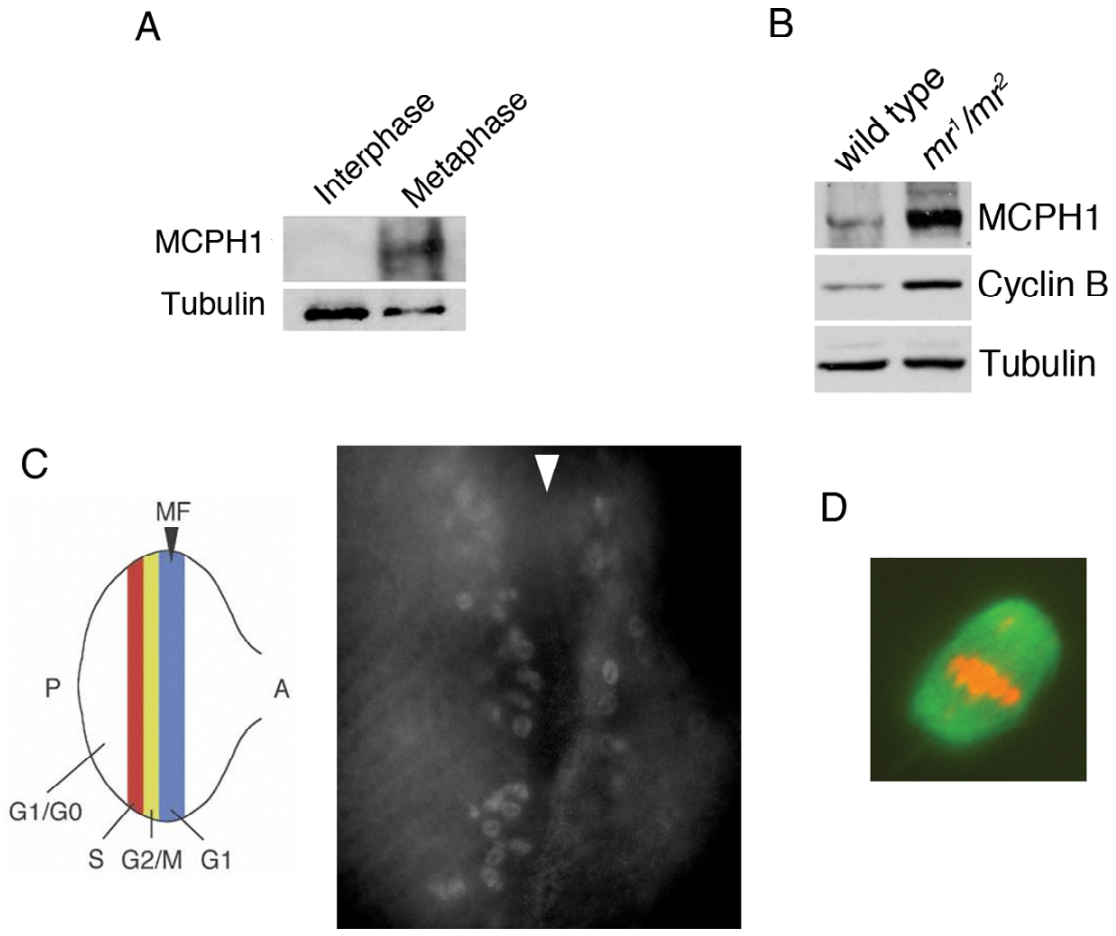

Figure 3.3. **Drosophila MCPH1-B is an *in vivo* APC substrate.** (A-B) MCPH1 immunoblots. (A) A comparison of interphase and metaphase embryo extracts reveals higher levels of MCPH1 during mitosis. (B) Higher MCPH1 and Cyclin B levels are present in *morula* mutant background. (C) Localization of endogenous MCPH1 within wild-type eye imaginal disc by immunofluorescence. Arrowhead indicates morphogenetic furrow. A band of cells at G2/M are visible behind the furrow in the posterior half of the disc. Asynchronously dividing cells are present in front of the furrow in the anterior half. Eye imaginal disc diagram adapted from Araki et al. (2005). (D) Spindle from embryo overexpressing MCPH1. Tubulin (green) and DNA (red).

age of the embryos, we compared MCPH1 levels in wild type embryos over the course of an hour. No differences in MCPH1 levels were observed between 0-15 min, 15-30 min, 30-45 min, and 45-60 min embryos (data not shown).

We also examined MCPH1 localization within the eye imaginal discs of Drosophila third instar larvae. In this system, as the morphogenetic furrow moves in a posterior to anterior direction, cells are synchronized; G1 cells are present within the furrow, followed by stripes of G2/M and S phase cells (Figure 3.3C). APC substrates, because they are degraded during late M and G1, are not observed within the morphogenetic furrow. In wild-type discs, MCPH1 and Cyclin B localize to G2/M cells (Figure 3.3C and data not shown).

To assess the biological importance of MCPH1 oscillations, we generated transgenic flies to express MCPH1-B with an RXXL to AXXL mutation in the D box. This non-degradable MCPH1 is functional because it rescues an *mcph1* mutant with a 95% embryo hatch rate. To determine if stabilization of MCPH1 causes developmental effects, we compared the embryonic hatch rate of several MCPH1 and MCPH1-Dbox transgenic lines. Seven lines each were used; however, hatch rates varied greatly within each group suggesting that the effects of chromosomal insertion mask any developmental effects that exist. We were precluded from making transgenes with the same insertion site because the constructs do not exist for UASp-type vectors. Syncytial embryos expressing high Myc-MCPH1 levels have aberrant spindles resembling those of *mcph1* loss-of-function mutants suggesting proper control of MCPH1 levels during early embryogenesis is critical for cell-cycle

progression (Figure 3.3D). It remains to be determined if the inability of APC to degrade MCPH1 present at more physiological levels affects embryo development.

Human Microcephalin is degraded in a Cdh1-dependent manner

We next sought to determine if APC regulation of MCPH1 is evolutionarily conserved. Human and Drosophila MCPH1 share only 16% identity overall and 38% identity of their N-terminal BRCT domains. Using the same Xenopus extract degradation assay, we found that human MCPH1 is degraded in an APC-Cdh1-dependent manner but remains stable in APC-Cdc20/mitotic extracts (Figure 3.4A). As a control, Cyclin B, a known substrate of both APC-Cdc20 and APC-Cdh1, is degraded in both extracts as expected. Similar to Drosophila MCPH1, a mobility shift occurs in CycBΔ90-supplemented (mitotic) extracts.

APC substrates oscillate in abundance during the cell cycle with levels highest in G2/M and lowest in G1. By Western analysis and using antibodies generated against human MCPH1, we examined MCPH1 over a 24-hour time period in HeLa cells synchronized using a nocodazole block and release. Similar to Cyclin B, MCPH1 levels are highest during mitosis after nocodazole release. Once the cells enter G1 after 3-4 hours, protein levels drop but begin to rise again during S phase 16 hours post-release (Figure 3.4B). To confirm cell synchronization, cells from each time point were fixed and analyzed for DNA content by FACS (data not shown).

Identification of a functional KEN box in human MCPH1

We identified putative destruction sequences, four D boxes and one KEN sequence, within human MCPH1 (Figure 3.2A). Recognition of a KEN sequence is specific to APC-Cdh1, and human MCPH1 degrades in an APC-Cdh1 dependent manner. Thus, we hypothesized that mutation of the KEN sequence to alanines would stabilize the protein. In Xenopus extracts supplemented with Cdh1, the MCPH1 KEN mutant remains stable over time compared to wild type. We also tested the functionality of the first putative D box; however, an RXXL to AXXA mutation does not stabilize the protein nor does it enhance stability when the KEN box is mutated (Figure 3.4A).

MCPH1 is ubiquitinated in human cells

Because mutation of the KEN sequence prevented degradation of MCPH1 within extracts, we hypothesized that we would not observe accumulation of ubiquitin ladders on the protein. HEK293 cells were co-transfected with His-ubiquitin and Myc-tagged MCPH1 constructs. All ubiquitinated proteins were immunoprecipitated using nickel beads and analyzed by SDS-PAGE and Western analysis using antibodies against Myc. Surprisingly, we found that wild-type MCPH1 and MCPH1-KEN constructs are ubiquitinated to the same extent. Because the IVT proteins used for *in vitro* degradation assays could be misfolded so that only the KEN is recognized, we next began to test whether multiple sites are recognized by APC. Constructs in which each D box is mutated singly in combination with the KEN box are also ubiquitinated at levels similar to wild type (Figure 3.4C). Further work

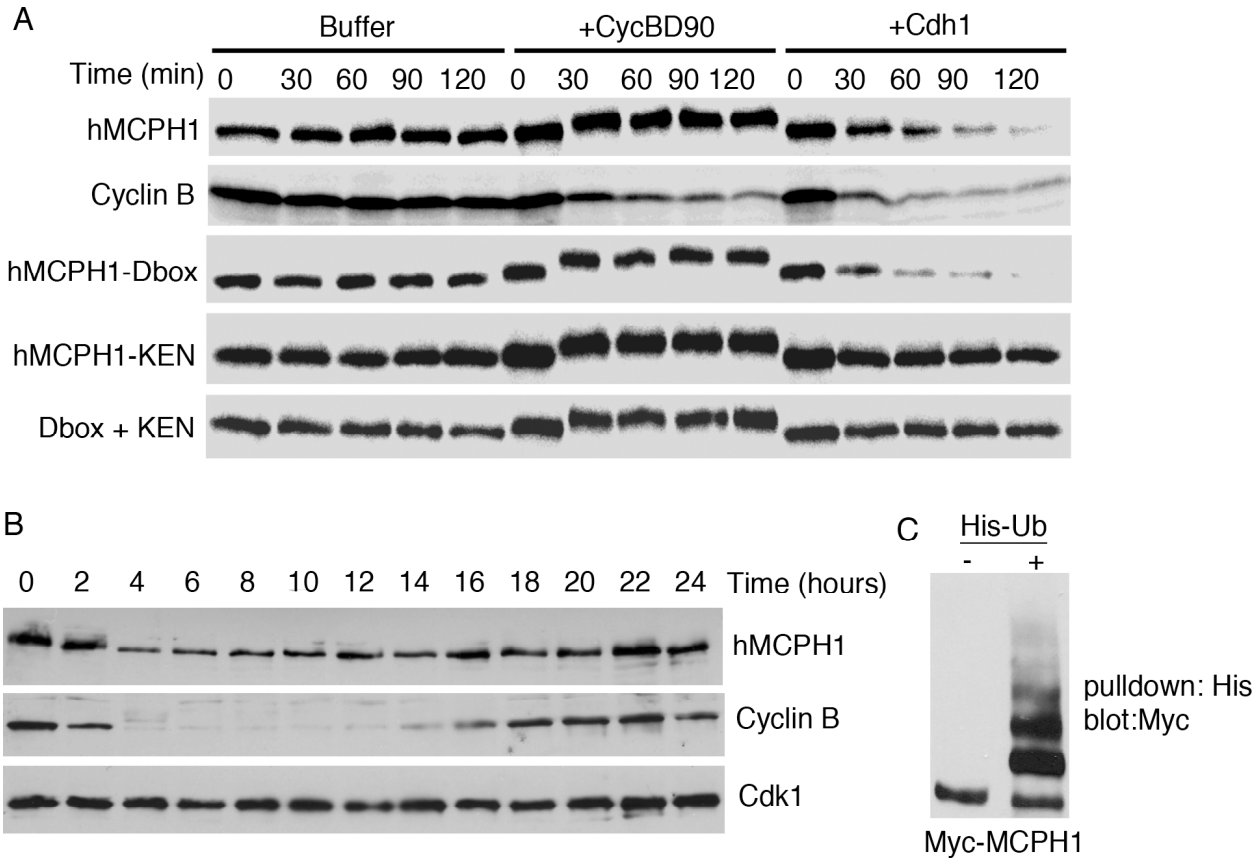

Figure 3.4. Human MCPH1 is an APC substrate. (A) APC-mediated protein degradation assays. Radiolabeled proteins were incubated in Xenopus egg extracts and reaction products analyzed by SDS-PAGE/autoradiography. MCPH1 degrades in a Cdh1-dependent manner while a Cyclin B control degrades in both APC-Cdc20 (+CycBΔ90 extracts) and APC-Cdh1 extracts. Mutation of the KEN degradation box to alanines stabilizes the protein while mutation of the first putative Dbox does not. (B) Endogenous levels of MCPH1 in nocodazole-synchronized HeLa cells over time. Higher protein levels in mitosis after nocodazole release (0-2 hours). Decreased levels are apparent during G1 (hours 4-14) but levels begin to rise again in S through the following G2/M (hours 16-22). A Cyclin B control has a similar pattern. (C) HEK293 cells transfected with Myc-MCPH1 and His-Ub reveal ubiquitylated protein.

is required to determine if mutation of all D boxes and the KEN sequence is required to stabilize MCPH1 *in vivo*.

Overexpression of MCPH1 leads to cell-cycle arrest

Previously, we determined that overexpression of MCPH1 leads to cell-cycle arrest in Drosophila embryos. We next wanted to determine if vertebrate development was also affected in the presence of excess MCPH1. 2- or 4-cell stage Xenopus embryos were injected with MCPH1 in one half of the embryo. As a control, embryos were injected with Mos, a strong inhibitor of Cdk1 function that prevents the injected cells from dividing more than one time (Figure 3.5A). GFP-injected embryos served as a negative control and were indistinguishable from those that were uninjected (Figure 3.5A). Injection of human MCPH1 results in cell-cycle arrest or delay in 92% of embryos (Figure 3.5B). Injection of either Drosophila MCPH1-B or MCPH1-A RNA results in 67% and 30% of embryos with cell-cycle progression defects, respectively (Figure 3.5B). Live imaging of MCPH1-injected embryos revealed cells that appear to divide normally for the first few cell cycles followed by attempted divisions where a cleavage furrow forms but eventually disappears.

The absence of MCPH1 leads to premature chromosome condensation defects in human cells, and in Drosophila, chromatin bridging occurs at anaphase. We hypothesized that the presence of too much MCPH1 also leads to chromosomal aberrations and subsequent cell-cycle arrest. By immunofluorescence, we localized Tubulin as well as DNA within MCPH1-injected embryos fixed four hours post-

injection (Figure 3.6A). Cells derived from uninjected cells appeared normal, undergoing mostly synchronous cycles (Figure 3.6B). Cells within the injected area, however, were largely devoid of DNA and also contained detached centrosomes (Figure 3.6C). Furthermore, any detectable DNA appears to stretch between cells, likely explaining why later cleavages fail to occur.

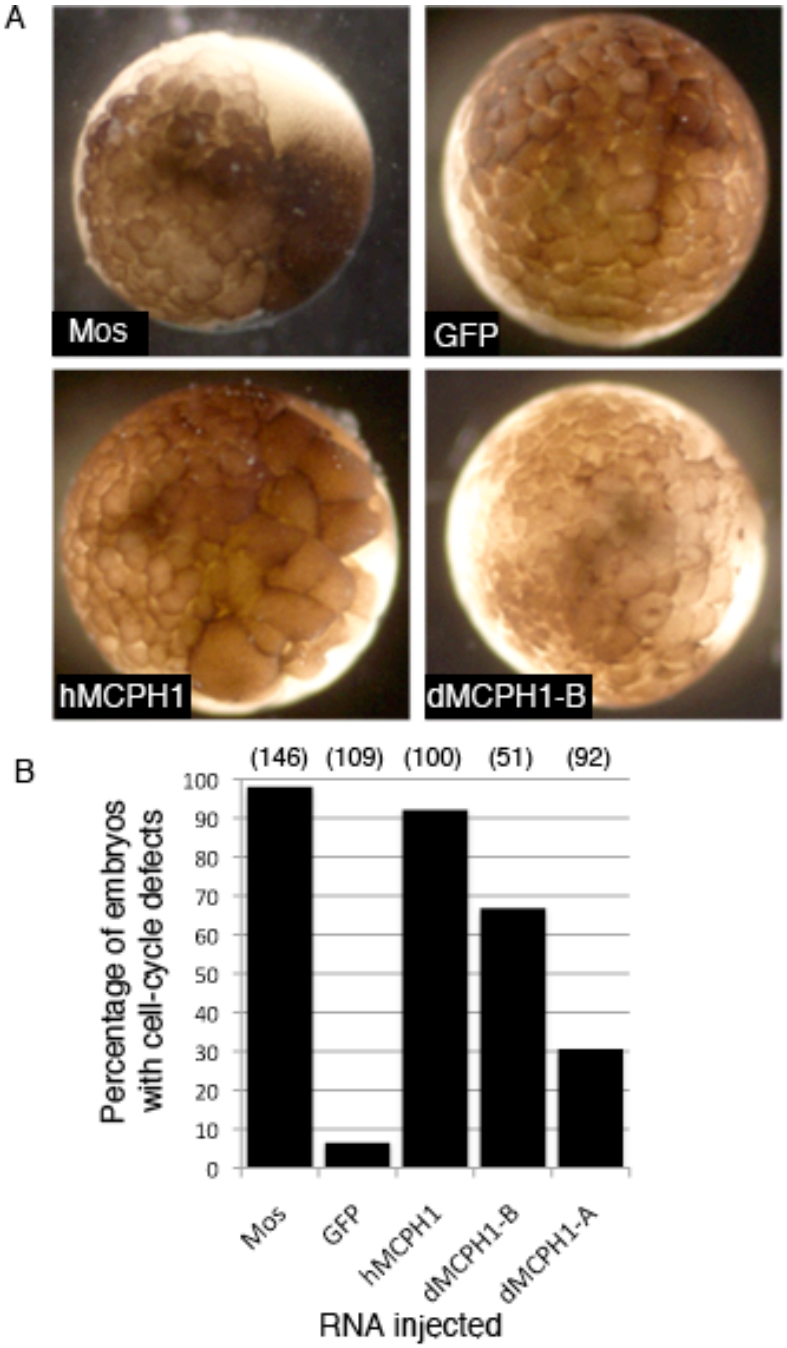

Figure 3.5. MCPH1-injected Xenopus embryos exhibit cell-cycle defects. (A) Examples of embryos injected with 2ng RNA at the 2-cell stage. The injected half is on the right in each image and RNA injected is indicated on the bottom. (B) Quantification of embryos that displayed cell-cycle defects 4 hours post-injection. Total embryo injected is indicated in parentheses (top).

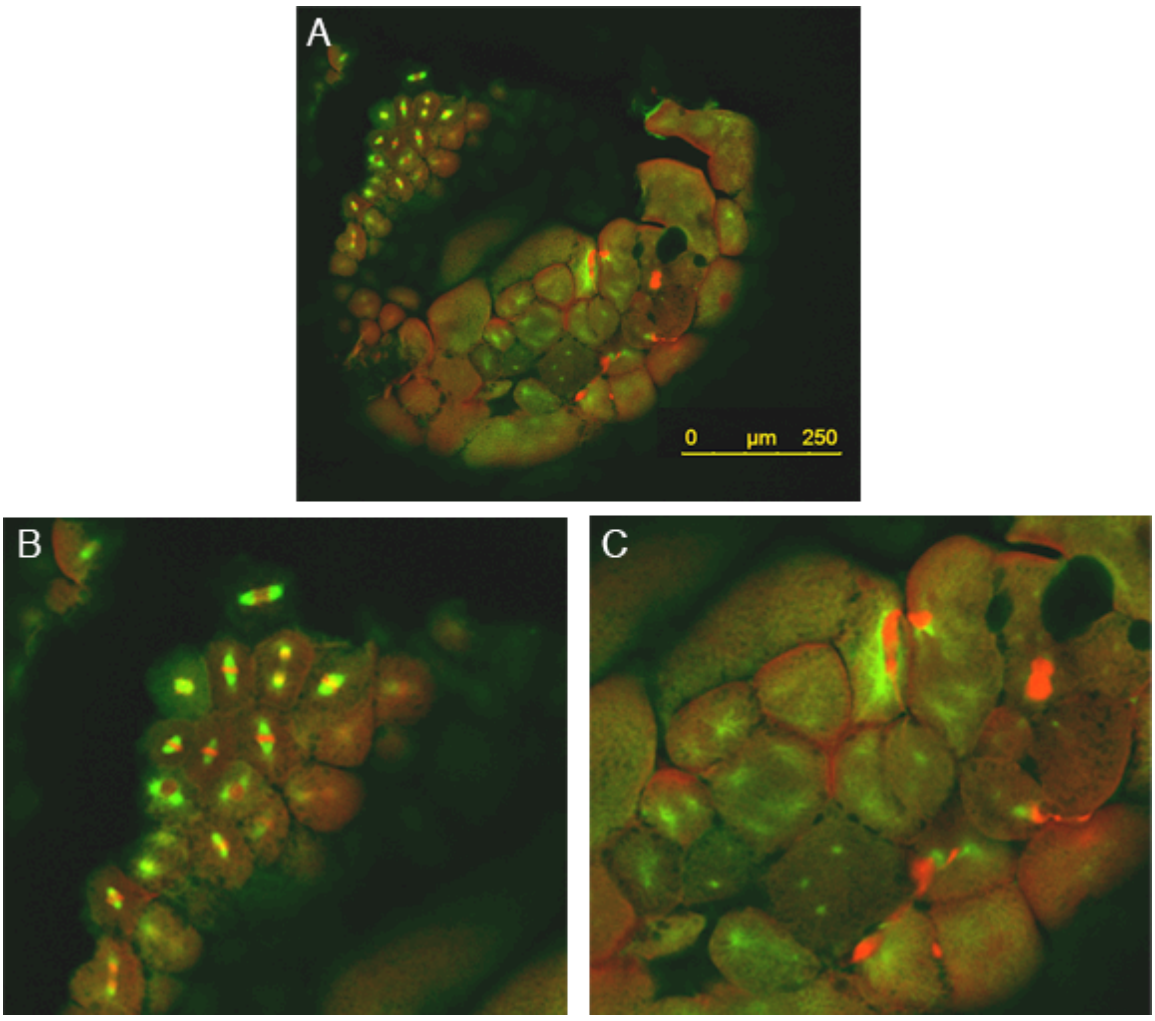

Figure 3.6. **Embryos injected with *MCPH1* RNA exhibit chromatin bridging and centrosomal defects.** (A-C) Images from a representative whole embryo injected with 2ng of *MCPH1* RNA at the 2-cell stage, fixed 4 hours post-injection, and analyzed by immunofluorescence. Microtubules are in green, DNA is in red. (A) Cells derived from the uninjected half are in the upper left and magnified in (B). Cells derived from the *MCPH1*-injected half are in the lower right and magnified in (C).

DISCUSSION

We identified Drosophila MCPH1 as well as two other novel proteins, p78 and p71, in a biochemical DIVEC screen for substrates of the APC. Previous screens for vertebrate substrates of the APC that employed a similar IVEC approach successfully identified key cell-cycle regulators, including Geminin, an inhibitor of DNA replication (McGarry and Kirschner 1998), Securin, an inhibitor of sister-chromatid separation (Zou et al. 1999), Tome-1, a trigger of mitotic entry (Ayad et al. 2003), and Sororin, a mediator of sister-chromatid cohesion (Rankin et al. 2005). Our data indicate that Drosophila MCPH1 degrades in an APC-Cdh1-dependent manner while remaining stable in mitotic extracts when APC-Cdc20 is activated. The first putative D-box within the MCPH1-B protein structure is sufficient for APC-mediated degradation. By genetic analysis, we found that mutations in Drosophila *morula*, which encodes the homolog of the vertebrate APC2 subunit, renders MCPH1 stable. MCPH1 protein also cycles in the early embryo with highest levels in mitosis.

We further discovered that human MCPH1 degrades in a Cdh1-dependent manner, and endogenous protein levels in cultured HeLa cells fluctuate similar to other APC substrates. Mutation of the KEN box alone confers stability in the biochemical extract system; however, this was not the case in an *in vivo* ubiquitination assay or when Myc-tagged constructs were co-transfected with Cdh1. Besides the KEN box, human MCPH1 contains four putative D boxes. Several APC substrates that contain multiple degrons have been identified including Securin, Shugoshin, Cdc6, and Nek2A (Zur and Brandeis, 2001) (Karamysheva et al, 2008)

(Mailand and Diffley, 2005) (Hayes et al. 2006). Thus, it is possible that multiple degrons within human MCPH1 are recognized *in vivo*. Our results indicate that mutation of each D-box singly in addition to the KEN box does not stabilize MCPH1; therefore, a more thorough examination is in order to test every combination of mutated degrons.

Finally, our data indicate that excess levels of MCPH1 cause cell-cycle arrest as evidenced by injection of Xenopus embryos with either human or Drosophila *MCPH1* RNA. Arrested cells contain multiple, free-floating centrosomes, and any DNA present has an appearance of aneuploidy and is strewn between cells. Interestingly, in early Drosophila syncytial embryos, overexpression of MCPH1-B results in cell-cycle arrest similar to the *mcph1* null mutation, though the percentage of arrested embryos seems to be dependent upon the level of overexpression (Rickmyre et al. 2007 and Chapter 2). In each case, triggering of the centrosomal inactivation pathway, a Checkpoint kinase 2-mediated event, appears to be the cause of the mitotic arrest.

Our data is in accordance with previous studies that suggest under- or over-expression of MCPH1 leads to cell-cycle defects. In *MCPH1* null or siRNA-treated cells, premature chromosome condensation defects occur as well as a failure to timely decondense chromatin after mitosis (Trimborn et al., 2004). Additionally, in the presence of DNA damage, in particular, double-stranded DNA breaks, cells are unable to respond properly to initiate repair (Lin et al., 2005; Wu et al., 2009). Interestingly, too much MCPH1 resulting from a chromosomal duplication has been implicated in cases of autism (Glancy et al., 2009; Ozgen et al., 2009). These changes

in MCPH1 levels are detrimental to embryonic development, and our current study indicates that even small fluctuations of MCPH1 protein levels, as caused by regulation of the APC and 26S proteasome, may be important to promote proper cell cycles.

We propose a simple model for APC regulation of MCPH1 levels during the cell cycle. During S and G2, when APC is not active, MCPH1 levels rise to prevent premature chromosome condensation and early activation of Condensin II complexes. During mitosis, we hypothesize inhibitory phospho-regulation of MCPH1 occurs during prophase, allowing Condensin II activity and appropriate chromosome condensation. MCPH1 is not degraded early in an APC-Cdc20 manner because proper decondensation at the end of mitosis also requires MCPH1. Our overexpression studies in Drosophila and Xenopus suggest excessive MCPH1 induces genomic instability; therefore MCPH1 is downregulated in an APC-Cdh1 dependent manner during G1 though never fully degraded. This allows MCPH1 to continue to perform its other function as a genomic scaffold to bring in repair proteins to sites of DNA damage.

From an evolutionary standpoint, our data suggest that APC regulation of MCPH1 is important from Drosophila to human. Intriguingly, humans have evolved an additional APC recognition sequence, the KEN box. A database search for other vertebrate MCPH1 sequences reveals a similarly positioned KEN box within their respective MCPH1 proteins. Unexpectedly, the *C. elegans* homolog of MCPH1 also contains a KEN box, though its location within the protein is not similar to human and other vertebrates. Whether any of these KEN box are functional remains to be

determined; however, the presence of a KEN box sequence within *C. elegans* MCPH1 could represent an independent evolutionary event that occurred to retain functional regulation by the APC.

CHAPTER IV

INDENTIFICATION OF MCPH1 INTERACTORS

INTRODUCTION

We previously identified MCPH1 in two independent screens: one for regulators of the early syncytial cycles in Drosophila and the other for substrates of the Anaphase Promoting Complex or APC. In the absence of MCPH1, embryos arrest with barrel-shaped spindles, lacking centrosomes. This phenotype was due to triggering of centrosomal inactivation, a Checkpoint Kinase 2-mediated response that occurs in the early embryo in the presence of DNA damage or incomplete replication. A primary defect observed in embryos from null *mcph1* females was chromatin bridging after the onset of anaphase. In addition to MCPH1, the Drosophila homologs of Checkpoint Kinase 1 and ATR, or Grapes and Mei-41, respectively, also caused centrosomal inactivation. Studies of human MCPH1 placed the protein within the ATR/Chk1 response to DNA damage. We found no apparent role for Drosophila MCPH1, however, within the ATR/Chk1 pathway. In an effort to understand the role MCPH1 plays during embryogenesis, we performed tandem affinity purification/mass spectrometry of MCPH1 complexes from the early Drosophila embryo.

Tandem affinity purification or TAP provides an effective strategy for the purification of protein complexes under non-denaturing conditions. These

complexes can then be trypsinized and analyzed by liquid chromatography and tandem mass spectrometry (Gould et al. 2004). A typical TAP tag consists of a Calmodulin binding protein (CBP) and two *Staphylococcus aureus* Protein A IgG binding proteins. The Protein A and CBP are separated by a TEV cleavage site allowing two rounds of purification of protein complexes within a reasonable amount of time (Puig et al., 2001). This type of approach was first used in budding yeast due to the ease of culturing large volumes of eukaryotic cells expressing an epitope-tagged protein of interest. TAP has since been adapted for use in a variety of systems, from mammalian cell culture to whole organisms like Drosophila, in which the UAS-Gal4 system was used to express tagged components of the Notch signaling pathway in Drosophila embryos in an effort to identify new pathway components (Veraksa et al. 2005).

Several studies have identified interactors of human MCPH1 through affinity purification/mass spectrometry. Intriguingly, the majority of these reported interactors are involved in chromatin modification. In one study, each subunit of the Condensin II complex, a regulator of chromosome condensation at prophase, was co-purified with MCPH1 (Wood et al., 2008). Another study discovered subunits of SWI-SNF, an ATP-driven chromatin remodeling complex that relaxes chromatin at sites of DNA damage (Peng et al., 2009). Our study would be the first in which MCPH1-containing protein complexes would be purified from a whole organism and at a stage in which MCPH1 is absolutely critical to prevent genomic instability. Thus, we hypothesized that our screen for interactors of Drosophila MCPH1 would yield a subset of proteins not previously reported by other groups.

Here we present the findings from our screen for interactors of MCPH1-B, an isoform of *mcph1* that codes for a single N-terminal BRCT domain in the protein. In contrast, human MCPH1 contains three BRCT domains: one N-terminal and two tandem C-terminal domains. Many of our hits are proteins involved in chromatin modification,. Intriguingly, human MCPH1 studies have reported that the N-terminal BRCT domain is critical to prevent untimely chromosome condensation (Wood et al., 2008; Richards et al., 2009). Our screen has also revealed subsets of proteins involved in RNAi-mediated silencing and spindle integrity that have not previously been reported to interact with MCPH1. Of particular interest, Abnormal Spindle, the Drosophila homolog of another human microcephaly gene, *ASPM*, was identified and confirmed to directly bind MCPH1.

METHODS

Drosophila stocks

Flies were maintained at 25˚C using standard techniques (Greenspan 2004). Wild-type stocks used were *y w*. *nanos-Gal4:VP16* and *actin5C-Gal4* stocks were obtained from the Bloomington Stock Center.

cDNA clones and transgenes

A cDNA clone encoding MCPH1-B (LD43341) was from the Drosophila Gene Collection. A cDNA clone encoding Drosophila Axin was a gift from Ethan Lee. MCPH1-B or Axin coding region was subcloned into a UASp vector (Rorth 1998)

modified with a C-terminal TAP tag or a derivative encoding six N-terminal Myc tags. *UASp-Myc-MCPH1-B*, *UASp-MCPH1-B-TAP*, and *UASp-Axin-TAP* were transformed into *y w* flies as described (Spradling 1986).

Polyclonal antibodies against Drosophila MCPH1

MBP fused to MCPH1-B (N-terminal 352 amino acids) was used to produce antibodies. N-terminal MCPH1-B sequence was PCR-amplified from LD43341 and subcloned into pMAL (New England Biolabs). MBP-N-MCPH1-B was made in bacterial cells, purified using amylose beads, and injected into guinea pigs for antibody production (Covance). Anti-MCPH1 antibodies were affinity purified using standard techniques.

Sucrose density gradient

Embryos expressing Myc-MCPH1 were collected and ground with a pestle in a 2x volume of homogenization buffer. Lysates were centrifuged at 3000 rpm at 4°C for 4 minutes and supernatant was collected. 125 µl of cleared lysates were layered onto a 5% to 30% sucrose gradient (5 ml) and centrifuged at 46000 rpm overnight at 4°C in a sw55ti rotor. 20 fractions of 250 µl each were collected. 30 µl of each fraction was analyzed by SDS-PAGE/Western blot using antibodies against Myc (1:1000, 9E10) or GAPDH (1:1000) for a control. Standards were run in parallel, 7 µg each, on a separate gradient and included Aldolase, Thyroglobulin, Ferritin, and Catalase (Sigma).

Immunostaining and microscopy

Salivary glands from third instar, wandering larvae (those crawling on the sides of the bottle) were dissected in PBS, soaked in 45% acetic acid for 1 minute, and lightly squashed in 15 µl 45% acetic acid on a slide. Slides were immediately frozen in liquid nitrogen and the cover slip was removed. The slide with the tissue was soaked in absolute ethanol at -20°C for 30 minutes. The slide was then washed in PBS-T and stained using anti-mouse Myc (1:500, 9E10, Sigma). Secondary antibodies conjugated to Cy2 were used (1:500) and samples were visualized using a Nikon Eclipse 80j microscope equipped with a PlanFluor 40x objective lens and a Photometrics CoolSnap ES camera.

Quantification of embryonic hatch rates

For hatch rate assays, embryos (0-4 hr) were collected on grape plates, counted, and aged ~40 hr at 25°C. The number of hatched embryos was determined by subtracting number of unhatched (intact) embryos from total number collected. Hatch rate is the ratio of hatched to total embryos expressed as a percentage.

Collection of embryos for TAP

UASp-MCPH1-B-TAP or *UASp-dAxin-TAP* flies were crossed to *nanos-Gal4:VP16* flies in forty bottles each. After 15 days, flies from all of the bottles were divided into two large collection chambers. Styrofoam trays with a grape juice agar and a thin layer of yeast paste were placed in the chambers and used to collect embryos (0-3 hours). For each purification, 1.5 grams of embryos were used.

Tandem affinity purification and mass spectrometry of complexes

This procedure was adapted from Veraksa et al. (2005) and Puig et al. (2001). Embryos were homogenized in 7ml of lysis buffer (6 mM Na_2HPO_4, 4 mM NaH_2PO_4-H_2O, 1% NP-40, 150 mM NaCl, 2 mM EDTA, 50 mM NaF, and protease inhibitors) using a Dounce homogenizer with a tight-fitting pestle. Lysates were spun down at 20,000 x g and the supernatant was collected and incubated with Dynabeads conjugated to rabbit IgG for 1 hour at 4°C, rocking. Beads were separated from the lysate with a magnet and washed three times in IPP150 buffer (10mM Tris-HCl pH 8.0, 150 mM NaCl, 0.1% NP-40). Beads were then washed once in TEV Cleavage Buffer (10 mM Tris-HCl pH 8.0, 150 mM NaCl, 0.1% NP-40, 0.5 mM EDTA, 1.0mM DTT) then incubated in TEV cleavage buffer plus 100U TEV protease (Invitrogen) at 14°C for 2 hours, rocking. After cleavage, the magnet was applied to separate the beads, the lysate was added to a Chromatography Column (0.8 X 4 cm, BioRad) prepared with 200µl calmodulin bead slurry (washed once in calmodulin binding buffer (CBB), 10mM Tris-HCl pH 8.0, 150 mM NaCl, 1 mM Mg^{2+} Acetate, 1mM Imidazole, 20 mM EGTA, 10mM BME), and incubated for 1 hour at 4°C. Unbound complexes were eluted by gravity flow and the column was washed twice with CBB plus 0.1% NP-40. Complexes were eluted with 1ml calmodulin elution buffer (10 mM Tris-HCl pH 8.0, 150 mM NaCl, 0.02% NP-40, 1 mM Mg^{2+} Acetate, 1 mM imidazole, 20mM EGTA, 10mM BME) into a 1.5ml Eppendorf tube on ice. Eluate was split in half and TCA precipitated. One pellet was analyzed by SDS-PAGE and silver stain. The other was resuspended, trypsinized, and analyzed by liquid chromatography/tandem mass spectrometry, a generous gift from Kathy Gould.

RESULTS

A screen for interactors of MCPH1

We examined whether Drosophila MCPH1 exists in a larger molecular weight complex by sucrose density gradient. Myc-tagged MCPH1-B was expressed in early Drosophila embryos. This fusion is functional because it can rescue the null *mcph1* mutation. A peak of low molecular weight (~118 kDa) occurs in fractions 2-5, likely representing Myc-MCPH1 unbound to other proteins (Figure 4.1A). A second prominent peak occurs in fractions 14-15, corresponding to a complex greater than 440 kDa, suggesting that MCPH1 exists in a larger complex of proteins (Figure 4.1A).

In an effort to understand the molecular framework in which MCPH1 participates, we screened for proteins that exist in complex with MCPH1 using a tandem affinity purification/mass spectrometry approach. Similar studies have been performed using human or mouse cells in culture; however, our system is the first in which a whole organism was used, the early Drosophila embryo. The tag used to purify complexes was the C-terminal TAP. We chose a C-terminal tag because our data suggest MCPH1 is a substrate of the Anaphase Promoting Complex, and N-terminally tagging the protein prevents APC from recognizing MCPH1 in our *in vitro* assay. Using the UASp-Gal4 system, we expressed MCPH1-B-TAP in the ovaries and early embryos of Drosophila by driving Gal4 protein synthesis with the *nanos* gene promoter. By Western analysis, we determined that MCPH1-TAP was expressed at a level approximately twice that of wild-type MCPH1 (Figure 4.1B).

Furthermore, expression of this construct was able to fully rescue a null mutation of MCPH1 (84% embryonic hatch rate). A comparison of whole embryo lysates to the final product revealed only TEV-cleaved CBP-MCPH1 was present in the final complexes, thereby validating the tandem purification (Figure 4.1C). Finally, we were able to detect several proteins via SDS-PAGE/silver stain that co-purified with MCPH1 (Figure 4.1D).

To reduce the number of false positives, we performed TAP using an unrelated protein as bait, Axin, and disregarded from further consideration all proteins that were identified in both screens. Axin-TAP was also used to validate our approach because it is a well-studied protein with many known binding partners. Indeed, we were able to co-purify two proteins known to form complexes with Axin: Adenomatous Polyposis Coli-2 and GSK3. In addition, several previously unknown interactors were identified.

In all, 168 unique proteins were identified in complex with MCPH1 after LC-MS/MS analysis. Of those, 76 were ribosomal, metabolic, transport, or heat shock proteins that we have dubbed as false positives despite their absence in the control; however, the total yield of Axin bait was far less than that of MCPH1 within their respective purifications (peptide count of 1434 for MCPH1 versus a total of 25 for Axin). We suspect that in the event of a more robust Axin purification, we could have removed far more false positives from the list. Another 40 uncharacterized proteins were recognized leaving 52 previously studied proteins in our list of hits (Table 4.1). Interactors found in each of the two MCPH1 purifications are

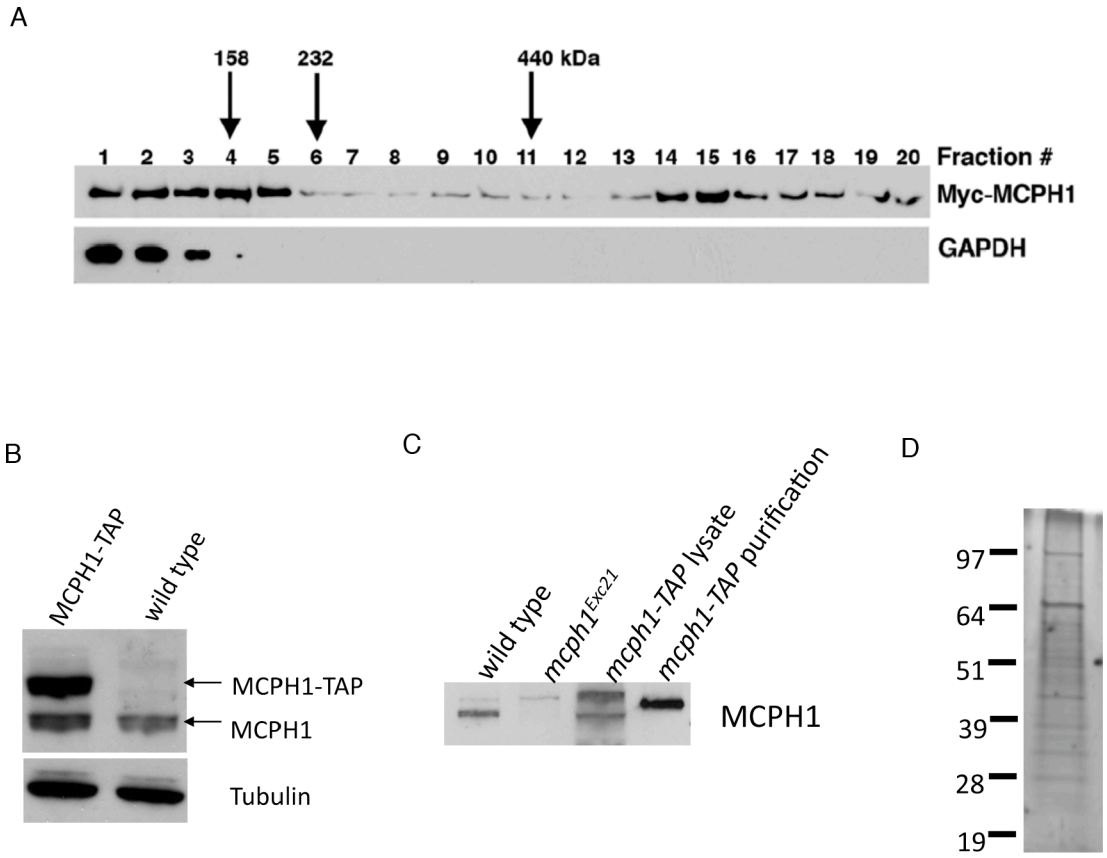

Figure 4.1. MCPH1 exists in a high molecular weight complex. (A) Fractions from a sucrose density gradient reveal MCPH1 exists in a large molecular weight complex, fractions 13-18 (>440 kDa). The first peak, fractions 1-5, likely represent Myc-MCPH1 alone. GAPDH was used as a control for a non-complex forming protein. (B) MCPH1-TAP expresses in early embryos at approximately twice that of endogenous MCPH1. (C) MCPH1 is highly purified after tandem affinity purification. (D) Purified complexes were analyzed by SDS-PAGE and silver stained.

highlighted in green, and a brief description of cellular function is listed for each hit if known (Table 4.1). Our screen for MCPH1-binding proteins revealed several interesting interactors, many of which can be narrowed into one of the following categories of cellular function: chromatin remodeling, RNAi components, DNA damage response and repair, and spindle integrity.

MCPH1-B localizes to euchromatin in Drosophila larval salivary glands

Because many of the MCPH1 interactors were proteins that associate with chromatin, we decided to look more carefully at the cellular localization of MCPH1. Previously, we found that MCPH1 localized to the nucleus in early Drosophila embryos (see figure 2.4). An ideal system for determining if a protein binds to chromatin is the Drosophila larval salivary gland. In this tissue, cells undergo repeated endocycles or rounds of DNA replication and growth without mitotic divisions. As a result, there are approximately 2000 copies of the genomic material within each cell (Urata et al., 1995). Furthermore, the sister chromatids align, and when stained with a DNA dye such as DAPI, bands of highly condensed and less condensed chromatin are apparent, also known as bands and interbands, respectively. In many cases, proteins that associate with the chromatin are easily detectable as there are more surfaces within each cell for interaction. We expressed

Table 4.1. MCPH1 interactors. Results from two purifications/mass spectrometry. Results highlighted in green represent proteins purified from both screens. Results in blue or yellow represent proteins purified from the first and second screens, respectively. Interactors are ordered based upon sequence coverage.

Drosophila protein	Sequence Coverage	Pep Count	Cellular role	References
MCPH1-B	55.20%	2042	genomic stability	(Rickmyre et al., 2007)
Histone H4	35.90%	21	chromatin integrity; nucleosomes	(Khorasanizadeh, 2004)
Histone H3	27.90%	5	chromatin integrity; nucleosomes	(Khorasanizadeh, 2004)
Maternal expression at 31B	24.90%	75	RNAi silencing; component of nuage processing body	(Lim et al., 2009)
Argonaute 2	16.30%	27	associates with RISC, siRNA silencing	(Okamura et al., 2004)
Ballchen/NHK-1	15.30%	75	histone H2A kinase; chromosome structure	(Ivanovska et al., 2005)
Histone H2Av	14.20%	7	Histone H2A variant; becomes phosphorylated at sites of dsDNA breaks	(Ivanovska et al., 2005)
Protein on Ecdysone Puffs	14.10%	38	salivary gland transcription	(Reim et al.,1999)
Rm62	13.50%	21	RNAi silencing; genetic interactor of FMR1	(Cziko et al., 2009)
Otefin	13.00%	8	germline stem cell maintenance; nuclear lamin binding protein	(Jiang et al., 2008)

Drosophila protein	Sequence Coverage	Pep Count	Cellular role	References
Origin recognition complex subunit 4	12.40%	13	Pre-replication complex	(Duncker et al., 2009)
origin recognition complex subunit 1	11.90%	36	Pre-replication complex	(Duncker et al., 2009)
Reptin	11.90%	9	chromatin remodeling	(Jha and Dutta, 2009)
Origin recognition complex subunit 5	10.90%	18	Pre-replication complex	(Duncker et al., 2009)
Topoisomerase II	9.80%	48	chromosome condensation; homologous pairing	(Lupo et al., 2001; Williams et al., 2007)
Replication Factor C subunit 4	9.40%	8	cell cycle checkpoint	(Krause et al., 2001)
Smc2	9.40%	18	Condensin core component	(reviewed in Hirano, 2005)
Abnormal Spindle	9.00%	66	spindle integrity; mcph gene	(do Carmo Avides and Glover, 1999; Riparbelli et al., 2001)
14-3-3epsilon	8.80%	5	DNA damage checkpoint	(Su et al., 2001)
SMC4 (Gluon)	8.60%	20	Condensin core component	(reviewed in Hirano, 2005)
Zn72D	8.20%	11	mRNA binding; splicing	(Worringer and Panning, 2007)
FMR1	8.10%	13	translational repression via miRNA	(reviewed in Zhang and Broadie, 2005)
Origin recognition complex subunit 3	8.00%	7	Pre-replication complex	(Duncker et al., 2009)

Drosophila protein	Sequence Coverage	Pep Count	Cellular role	References
Lodestar	7.80%	15	DNA binding; chromosome integrity	(Girdham and Glover, 1991)
DEAD box protein 73D	7.50%	6	RNA helicase	(Patterson et al., 1992)
Decapping protein 1	7.50%	4	RNAi silencing; component of nuage processing body	(Lim et al., 2009)
Fascetto	7.50%	16	central spindle integrity	(Verni et al., 2004)
La related protein	6.10%	32	syncytial embryo mitosis; male meiosis	(Blagden et al., 2009)
RacGAP50	6.10%	8	central spindle integrity/cytokinesis	(D'Avino et al., 2006)
Suppressor of Variegation 3-7	6.10%	22	heterochromatin silencing	(Bushey and Locke, 2004)
CapG	5.80%	7	Condensin I component	(reviewed in Hirano, 2005)
PAV-KLP protein	5.80%	8	central spindle integrity/cytokinesis	(Delcros et al., 2006)
Pontin	5.70%	8	chromatin remodeling	(Jha and Dutta, 2009)
XRCC1	4.90%	5	DNA repair	(Taylor et al. 2000)
Origin recognition complex subunit 2	4.40%	4	Pre-replication complex	(Duncker et al., 2009)
ATM/Tefu	3.90%	7	DNA damage checkpoint; telomere maintenance	(Silva et al., 2004)

Drosophila protein	Sequence Coverage	Pep Count	Cellular role	References
DISCO interacting protein (DIP1)	3.90%	2	double-stranded RNA binding; mRNA control	(DeSousa et al., 2003)
CapD2	3.60%	16	Condensin I component	(reviewed in Hirano, 2005)
Smaug	3.50%	11	mRNA destabilization	(Tadros et al., 2007)
Ataxin-2	3.30%	2	miRNA silencing	(Satterfield and Pallanck, 2006)
DNA ligase III	3.30%	2	DNA ligase	n/a
No-on-transient A protein form I	3.10%	7	salivary gland transcription; localized to puffs	(Reim et al.,1999)
Slow as Molasses	3.10%	15	mRNA localization; germ cell migration	(Stein et al., 2002)
Aubergine	3.00%	2	piRNA silencing	(reviewed in Klattenhoff and Theurkauf, 2008)
Topoisomerase III	2.90%	3	generates single strand DNA breaks	(Wilson-Sali and Hsieh, 2002)
PIWI	2.60%	7	piRNA silencing	(reviewed in Klattenhoff and Theurkauf, 2008)
Pacman	2.40%	14	RNAi silencing; component of nuage processing body	(Lim et al., 2009)
Ino80	2.30%	6	chomatin remodeling	(Morrison and Shen, 2009)
WOC protein	2.00%	7	transcription factor; telomere maintenance; polytene interbands	(Raffa et al., 2005)

Drosophila protein	Sequence Coverage	Pep Count	Cellular role	References
dMi-2 protein	1.90%	5	chromatin remodeling	(Bouazoune et al., 2002)
Slender lobes	1.70%	4	mushroom body development; nucleolar organization	(Orihara-Ono et al., 2005)
Sallimus	0.10%	2	chromosome structure	(Machado and Andrew, 2000)

UASp-Myc-tagged MCPH1 in Drosophila salivary glands using an Actin-Gal4 promoter. Upon immunostaining for the Myc tag, we found MCPH1 to be specifically localized to the dark bands of polytene chromosomes (Figure 4.2).

Drosophila MCPH1 interacts *in vitro* with Asp

To date, five genes have been identified as primary microcephaly disease (MCPH) genes. Of these, MCPH1 is the only gene that localizes to the nucleus; however, several studies have shown that MCPH1 is also present at the centrosomes, sharing a localization pattern with the remaining MCPH genes (Jeffers et al., 2008; Brunk et al., 2007). Interestingly, our TAP screen revealed MCPH1 is in complex with Abnormal Spindle (Asp), the Drosophila homolog of human ASPM or MCPH5. We tested this interaction *in vitro* by incubating radiolabeled Asp with either a maltose binding protein fusion of MCPH1 (MBP-MCPH1) or MBP alone bound to amylose beads. Asp binds to MBP-MCPH1 but not control beads, and greater than 10% of the Asp input appears to bind (Figure 4.3). Hence, it is plausible that MCPH1 functions with one or more of the other MCPH genes in order to regulate early mitoses of neuronal precursor cells.

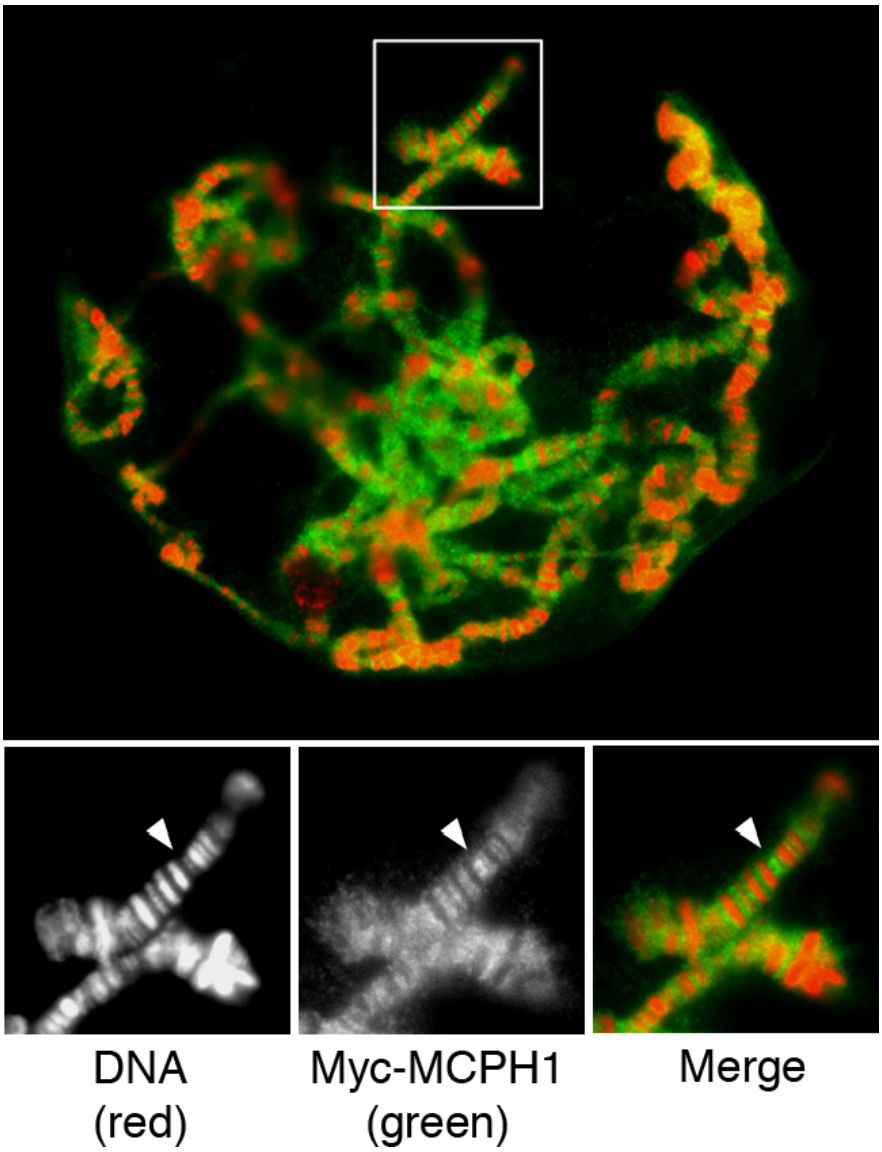

Figure 4.2. MCPH1 localizes to less condensed regions of larval polytene chromosomes. Larval salivary glands were squashed onto a slide and stained for Myc to detect MCPH1 (green) or DNA (red). MCPH1 is primarily localized to the interbands, staining in an opposite pattern to the DNA. Bottom panels are individual channel insets and merge of white-boxed region in top panel.

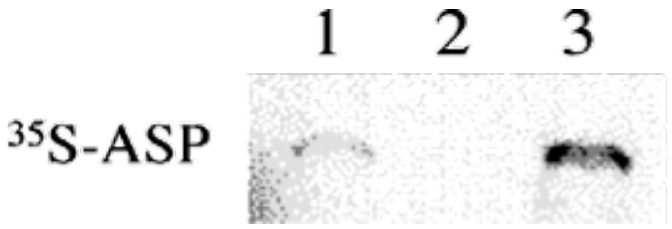

Figure 4.3. Asp directly binds MCPH1. Radiolabeled Asp binds MBP-MCPH1 beads (lane 3) but not control (lane 2). Lane 1 represents 10% of total Asp input.

DISCUSSION

We have performed a screen for interactors of MCPH1 using a tandem affinity purification/mass spectrometry approach. Similar studies have been carried out using human or mouse MCPH1, though full lists of interactors have not been reported. We also discovered that MCPH1 localizes to regions of open chromatin on Drosophila polytene chromosomes. This is intriguing because many of the proteins found in the screen also interact with chromatin. From studies of human MCPH1, one could speculate that MCPH1 plays a role as a genomic director or mediator, bringing together components from multiple pathways, such as chromatin remodeling complexes or repair enzymes, to a common site on the chromatin.

Our study revealed several interactors that have been identified in complex with vertebrate MCPH1 such as components of the Condensin complex, suggesting evolutionary conservation of function between human and Drosophila MCPH1. The difference, however, is that we found Condensin I-specific components, while previous screens identified Condensin II-specific components. We found the core components, SMC2 and SMC4, that are found in both Condensin I and Condensin II, and two out of the three remaining Condensin I components, CapD2 and CapG. In vertebrates, nuclear Condensin II acts early and begins to condense the chromosomes in prophase (reviewed in Hirano, 2005). Drosophila Condensin I has been shown to perform this same function (Oliveira et al., 2007). Furthermore, Drosophila Condensin II appears to be dispensable for this purpose but participates

in the individualization or resolution of sister chromatids prior to the onset of anaphase (Oliveira et al., 2007; Hartl et al., 2008).

In addition to the Condensin I components, we discovered many proteins involved directly in chromatin modifications. Topoisomerase II, an enzyme involved in the decatenation of DNA, was identified in both MCPH1-TAP screens with comparatively high sequence coverage. Also, several other modifiers of chromatin structure such as Pontin, Reptin, and INO80 were found in addition to core components of nucleosomes: H3, H4, and the histone variant H2AV. Taken together, these results confirm previous studies of the involvement of MCPH1 in chromosome condensation and chromatin architecture while adding potential new players.

Our screen also revealed previously undescribed pathways in which MCPH1 may function, including a surprising number of components of RNAi pathways. This includes components of siRNA-, miRNA-, and piRNA-mediated silencing. Two particularly strong hits were Argonaute 2, a core component in siRNA silencing (Okamura et al., 2004) and Maternal Expression at 31B, a component found in RNAi processing centers (Lim et al., 2009). Argonaute-2 is at the core of siRNA silencing, helping to target the heterochromatin protein, HP1 to the heterochromatin in centromeres or telomeres (Djupedal and Ekwall, 2009) Interestingly, our screen also revealed other telomeric proteins such as WOC and Suppressor of Variegation 3-7.

Furthermore, five out of six subunits of the Origin Replication Complex were identified. In Drosophila, ORCs bind chromatin during anaphase when it is hypothesized that they are necessary to begin to set replication origin sites

(Baldinger and Gossen, 2009). In Orc2 and Orc5 mutants, chromosome condensation defects arise as a result of fewer origins (Pflumm and Botchan, 2001). We hypothesize that MCPH1 promotes chromatin relaxation, allowing components, such as the ORCs, access to the chromatin.

We were somewhat surprised to find interactors that are involved in DNA repair because our screen utilized the B isoform of MCPH1 that does not contain tandem BRCT domains in the carboxy terminus. Studies of human MCPH1 have shown that the paired domains are important for MCPH1 localization to sites of DNA damage. We did not find any previously reported interactors such as BRCA2, Rad51, and Chk1 (Wu et al., 2009; Alderton et al., 2006). Our results revealed proteins involved in checkpoints (ATM, 14-3-3ε, and Replication Factor C subunit 4 (RFC4)) and repair (XRCC1 and DNA ligase III). Of these, only RFC4 was a repeated result.

Finally, MCPH1 was found in complex with Abnormal Spindle, the Drosophila homolog of MCPH5. We confirmed that Asp binds directly to MCPH1 *in vitro*. Mutations in MCPH genes give rise to the developmental disorder primary microcephaly, and it is hypothesized that decreased production of neurons or increased apoptosis during neuronal development is the cause. This raises the intriguing possibility that the MCPH genes could function within a common pathway during development, specifically to regulate mitosis in neural precursor cells.

CHAPTER 5

FUTURE DIRECTIONS

Our work represents the first studies of the biological roles of *mcph1* using a genetic model system, *Drosophila melanogaster*. We identified a developmental requirement for the protein during the earliest stages of Drosophila embryogenesis and further found that the Anaphase Promoting Complex (APC) regulates its levels. We also identified many potential new proteins in complex with MCPH1 in an effort to understand the mechanism by which MCPH1 controls cell-cycle progression. Based upon our conclusions, we now propose further studies.

Our screen for interactors of MCPH1 revealed several new possible pathways in which MCPH1 might participate. Quite surprisingly, this includes a potential role in heterochromatin silencing. The Drosophila model system was the first in which position effect variegation was studied. This term simply describes the phenomenon in which the condensed state of the chromatin affects gene transcription. Genes located in less condensed euchromatin are easily transcribed. On the contrary, genes that may have translocated to highly condensed heterochromatin are not expressed due to the limited access to the region by transcription factors and polymerases. Altering the state of the chromatin can allow transcription of masked genes. Mutation of *Argonaute 2*, a core component of siRNA silencing required for heterochromatin silencing in the early Drosophila embryo, leads to decondensed chromatin at the centromere. This prevents CID, a

centromeric protein marker and histone H3 variant, from localizing to the centromere in *argonaute 2* mutants (Deshpande et al., 2005). As a result, defects such as chromatin bridging and floating centrosomes are present, similar to what occurs in *mcph1* mutant embryos (Deshpande et al., 2005; Rickmyre et al., 2007). Suppressor of Variegation 3-7 is also required for heterochromatin silencing. Expression of the *white* gene inserted into heterochromatin is masked again by increasing doses of *Su(var)3-7* (Bushey and Locke, 2004). Both Argonaute2 and Su(var)3-7 are necessary for promoting heterochromatin formation and were found to interact with MCPH1 in our TAP screen. It will be interesting to determine if MCPH1 also affects the state of the chromatin.

As described in Chapter 3, human MCPH1 is never fully degraded when the APC is active. In comparison, Cyclin B is quickly and fully degraded (See Figure 3.B). This raises questions as to how APC might order the destruction of MCPH1. A study by Rape et al. (2008) suggested that different APC substrates could be processed differently. Some are polyubiquitylated for degradation after only binding to APC a few times, and others, known as distributive substrates, are out-competed for binding and therefore take longer to be recognized by the 26S proteasome. It was also suggested that the distributive substrates are further deubiquitylated by DUBs (deubiquitinating enzymes). Because human MCPH1 participates in the DNA damage response, it makes sense that the protein is never fully degraded during G1. It will be interesting to determine the processivity of APC on MCPH1 and if there is a DUB further preventing full degradation by the proteasome.

Finally, mutation of *MCPH1* in humans is responsible for autosomal recessive primary microcephaly, a disorder of brain development. The first vertebrate models with mutation of *MCPH1*, which were published this year, have only confirmed results from cell culture studies that MCPH1 is required for the response to DNA damage (Liang et al., 2010) and to prevent premature chromosome condensation (Trimborn et al., 2010). In addition, we showed that a null mutation of *mcph1* in Drosophila leads to defects in the mushroom bodies, the learning and memory center of the adult fly brain (See Figure 2.11). To date, no study has attempted to understand the role of MCPH1 in brain development using a vertebrate model system. We propose to use the Xenopus embryo, a model that has been used extensively to understand neurulation, in order to study the effects of *MCPH1* knockdown by morpholino injection on vertebrate brain development. Preliminary studies from a graduate student collaborator from Marc Kirschner's lab, Danny Ooi, suggest that loss of MCPH1 leads to smaller brains, similar to what occurs in the human disorder. *MCPH1* transcripts are highly expressed in neural tissues of the developing Xenopus embryo (Figure 5.1A). Injection of morpholinos against *MCPH1* into one cell of a two-cell embryo leads to reduction in head size on the injected side in stage 42 embryos (Figure 5.1B). Furthermore, injection of both cells of a two-cell embryo results in overall smaller head size but not overall body size (Figure 5.1C). Further studies to determine how knockdown of MCPH1 leads to head size defects are in order (e.g. assessment of cell-cycle timing of embryos prior to the mid-blastula transition and analysis of neural marker expression patterns).

These data, together with our proposed studies, will provide a framework to further define the role of MCPH1 in development and disease.

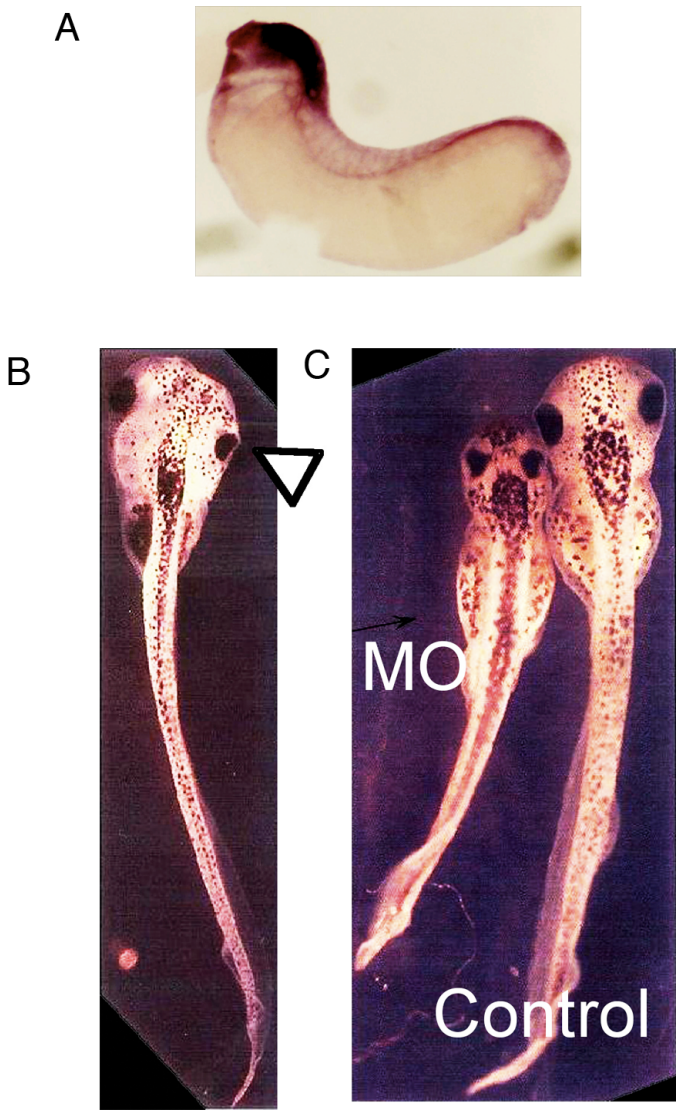

Figure 5.1. Loss of *MCPH1* leads to brain defects in Xenopus embryos. (A) *in situ* hybridization reveals high levels of *MCPH1* transcripts in neural tissues of stage 26 embryo. (B-C) Injection of morpholinos against *MCPH1* into one (B) or both cells (C) of a two-cell embryo leads to brain defects in stage 42 embryos.

BIBLIOGRAPHY

Abdu, U., Brodsky, M., and Schüpbach, T. (2002). Activation of a meiotic checkpoint during Drosophila oogenesis regulates the translation of Gurken through Chk2/Mnk. Curr Biol *12*, 1645-1651.

Alderton, G.K., Galbiati, L., Griffith, E., Surinya, K.H., Neitzel, H., Jackson, A.P., Jeggo, P.A., and O'Driscoll, M. (2006). Regulation of mitotic entry by microcephalin and its overlap with ATR signalling. Nat Cell Biol *8*, 725-733.

Araki, M., Yu, H., and Asano, M. (2005). A novel motif governs APC-dependent degradation of Drosophila ORC1 in vivo. Genes Dev *19*, 2458-2465.

Ayad, N.G., Rankin, S., Murakami, M., Jebanathirajah, J., Gygi, S., and Kirschner, M.W. (2003). Tome-1, a trigger of mitotic entry, is degraded during G1 via the APC. Cell *113*, 101-113.

Ayad, N.G., Rankin, S., Ooi, D., Rape, M., and Kirschner, M.W. (2005). Identification of ubiquitin ligase substrates by in vitro expression cloning. Meth Enzymol *399*, 404-414.

Baldinger, T., and Gossen, M. (2009). Binding of Drosophila ORC proteins to anaphase chromosomes requires cessation of mitotic cyclin-dependent kinase activity. Mol Cell Biol *29*, 140-149.

Ballinger, D.G., and Benzer, S. (1989). Targeted gene mutations in Drosophila. Proc Natl Acad Sci USA *86*, 9402-9406.

Bartek, J. (2006). Microcephalin guards against small brains, genetic instability, and cancer. Cancer Cell *10*, 91-93.

Basto, R., Lau, J., Vinogradova, T., Gardiol, A., Woods, C.G., Khodjakov, A., and Raff, J.W. (2006). Flies without centrioles. Cell *125*, 1375-1386.

Bednar, J., Horowitz, R.A., Grigoryev, S.A., Carruthers, L.M., Hansen, J.C., Koster, A.J., and Woodcock, C.L. (1998). Nucleosomes, linker DNA, and linker histone form a unique structural motif that directs the higher-order folding and compaction of chromatin. Proc Natl Acad Sci USA *95*, 14173-14178.

Berger, J.M., and Wang, J.C. (1996). Recent developments in DNA topoisomerase II structure and mechanism. Curr Opin Struct Biol *6*, 84-90.

Blagden, S.P., Gatt, M.K., Archambault, V., Lada, K., Ichihara, K., Lilley, K.S., Inoue, Y.H., and Glover, D.M. (2009). Drosophila Larp associates with poly(A)-binding protein

and is required for male fertility and syncytial embryo development. Dev Biol *334*, 186-197.

Bouazoune, K., Mitterweger, A., Längst, G., Imhof, A., Akhtar, A., Becker, P.B., and Brehm, A. (2002). The dMi-2 chromodomains are DNA binding modules important for ATP-dependent nucleosome mobilization. EMBO J *21*, 2430-2440.

Brand, A.H., and Perrimon, N. (1993). Targeted gene expression as a means of altering cell fates and generating dominant phenotypes. Development *118*, 401-415.

Brodsky, M.H., Sekelsky, J.J., Tsang, G., Hawley, R.S., and Rubin, G.M. (2000). mus304 encodes a novel DNA damage checkpoint protein required during Drosophila development. Genes Dev *14*, 666-678.

Brodsky, M.H., Weinert, B.T., Tsang, G., Rong, Y.S., McGinnis, N.M., Golic, K.G., Rio, D.C., and Rubin, G.M. (2004). Drosophila melanogaster MNK/Chk2 and p53 regulate multiple DNA repair and apoptotic pathways following DNA damage. Mol Cell Biol *24*, 1219-1231.

Brunk, K., Vernay, B., Griffith, E., Reynolds, N.L., Strutt, D., Ingham, P.W., and Jackson, A.P. (2007). Microcephalin coordinates mitosis in the syncytial Drosophila embryo. J Cell Sci *120*, 3578-3588.

Buschhorn, B.A., and Peters, J.-M. (2006). How APC/C orders destruction. Nat Cell Biol *8*, 209-211.

Bushey, D., and Locke, J. (2004). Mutations in Su(var)205 and Su(var)3-7 suppress P-element-dependent silencing in Drosophila melanogaster. Genetics *168*, 1395-1411.

Cardozo, T., and Pagano, M. (2004). The SCF ubiquitin ligase: insights into a molecular machine. Nat Rev Mol Cell Biol *5*, 739-751.

Chen, B., Chu, T., Harms, E., Gergen, J.P., and Strickland, S. (1998). Mapping of Drosophila mutations using site-specific male recombination. Genetics *149*, 157-163.

Chen, Y., and Sanchez, Y. (2004). Chk1 in the DNA damage response: conserved roles from yeasts to mammals. DNA Repair (Amst) *3*, 1025-1032.

Cox, J., Jackson, A.P., Bond, J., and Woods, C.G. (2006). What primary microcephaly can tell us about brain growth. Trends Mol Med *12*, 358-366.

Crittenden, J.R., Skoulakis, E.M., Han, K.A., Kalderon, D., and Davis, R.L. (1998). Tripartite mushroom body architecture revealed by antigenic markers. Learn Mem *5*, 38-51.

Cziko, A.-M.J., McCann, C.T., Howlett, I.C., Barbee, S.A., Duncan, R.P., Luedemann, R., Zarnescu, D., Zinsmaier, K.E., Parker, R.R., and Ramaswami, M. (2009). Genetic modifiers of dFMR1 encode RNA granule components in Drosophila. Genetics *182*, 1051-1060.

D'Avino, P.P., Savoian, M.S., Capalbo, L., and Glover, D.M. (2006). RacGAP50C is sufficient to signal cleavage furrow formation during cytokinesis. J Cell Sci *119*, 4402-4408.

de Belle, J.S., and Heisenberg, M. (1994). Associative odor learning in Drosophila abolished by chemical ablation of mushroom bodies. Science *263*, 692-695.

Dej, K.J., and Spradling, A.C. (1999). The endocycle controls nurse cell polytene chromosome structure during Drosophila oogenesis. Development *126*, 293-303.

Delcros, J.-G., Prigent, C., and Giet, R. (2006). Dynactin targets Pavarotti-KLP to the central spindle during anaphase and facilitates cytokinesis in Drosophila S2 cells. J Cell Sci *119*, 4431-4441.

Deshpande, G., Calhoun, G., and Schedl, P. (2005). Drosophila argonaute-2 is required early in embryogenesis for the assembly of centric/centromeric heterochromatin, nuclear division, nuclear migration, and germ-cell formation. Genes Dev *19*, 1680-1685.

DeSousa, D., Mukhopadhyay, M., Pelka, P., Zhao, X., Dey, B.K., Robert, V., Pélisson, A., Bucheton, A., and Campos, A.R. (2003). A novel double-stranded RNA-binding protein, disco interacting protein 1 (DIP1), contributes to cell fate decisions during Drosophila development. J Biol Chem *278*, 38040-38050.

Dienstbier, M., Boehl, F., Li, X., and Bullock, S.L. (2009). Egalitarian is a selective RNA-binding protein linking mRNA localization signals to the dynein motor. Genes Dev *23*, 1546-1558.

Djupedal, I., and Ekwall, K. (2009). Epigenetics: heterochromatin meets RNAi. Cell Res *19*, 282-295.

do Carmo Avides, M., and Glover, D.M. (1999). Abnormal spindle protein, Asp, and the integrity of mitotic centrosomal microtubule organizing centers. Science *283*, 1733-1735.

Draetta, G., Luca, F., Westendorf, J., Brizuela, L., Ruderman, J., and Beach, D. (1989). Cdc2 protein kinase is complexed with both cyclin A and B: evidence for proteolytic inactivation of MPF. Cell *56*, 829-838.

Duncker, B.P., Chesnokov, I.N., and McConkey, B.J. (2009). The origin recognition complex protein family. Genome Biol *10*, 214.

Ebert, A., Lein, S., Schotta, G., and Reuter, G. (2006). Histone modification and the control of heterochromatic gene silencing in Drosophila. Chromosome Res *14*, 377-392.

Edgar, B.A., and Lehner, C.F. (1996). Developmental control of cell cycle regulators: a fly's perspective. Science *274*, 1646-1652.

Edgar, B.A., Sprenger, F., Duronio, R.J., Leopold, P., and O'Farrell, P.H. (1994). Distinct molecular mechanism regulate cell cycle timing at successive stages of Drosophila embryogenesis. Genes Dev *8*, 440-452.

Evans, P.D., Anderson, J.R., Vallender, E.J., Choi, S.S., and Lahn, B.T. (2004). Reconstructing the evolutionary history of microcephalin, a gene controlling human brain size. Hum Mol Genet *13*, 1139-1145.

Feine, O., Zur, A., Mahbubani, H., and Brandeis, M. (2007). Human Kid is degraded by the APC/C(Cdh1) but not by the APC/C(Cdc20). Cell Cycle *6*, 2516-2523.

Fenger, D.D., Carminati, J.L., Burney-Sigman, D.L., Kashevsky, H., Dines, J.L., Elfring, L.K., and Orr-Weaver, T.L. (2000). PAN GU: a protein kinase that inhibits S phase and promotes mitosis in early Drosophila development. Development *127*, 4763-4774.

Ferrell, J.E. (1999). Xenopus oocyte maturation: new lessons from a good egg. Bioessays *21*, 833-842.

Fogarty, P., Campbell, S.D., Abu-Shumays, R., Phalle, B.S., Yu, K.R., Uy, G.L., Goldberg, M.L., and Sullivan, W. (1997). The Drosophila grapes gene is related to checkpoint gene chk1/rad27 and is required for late syncytial division fidelity. Curr Biol *7*, 418-426.

Freeman, M., Nüsslein-Volhard, C., and Glover, D.M. (1986). The dissociation of nuclear and centrosomal division in gnu, a mutation causing giant nuclei in Drosophila. Cell *46*, 457-468.

García-Planells, J., Paricio, N., Palau, F., and de Frutos, R. (2000). Dnop56, a Drosophila gene homologous to the yeast nucleolar NOP56 gene. Genetica *109*, 275-282.

Girdham, C.H., and Glover, D.M. (1991). Chromosome tangling and breakage at anaphase result from mutations in lodestar, a Drosophila gene encoding a putative nucleoside triphosphate-binding protein. Genes Dev *5*, 1786-1799.

Glancy, M., Barnicoat, A., Vijeratnam, R., de Souza, S., Gilmore, J., Huang, S., Maloney, V.K., Thomas, N.S., Bunyan, D.J., Jackson, A.*, et al.* (2009). Transmitted duplication of 8p23.1-8p23.2 associated with speech delay, autism and learning difficulties. Eur J Hum Genet *17*, 37-43.

Glover, D.M., Leibowitz, M.H., McLean, D.A., and Parry, H. (1995). Mutations in aurora prevent centrosome separation leading to the formation of monopolar spindles. Cell *81*, 95-105.

Glover, J.N.M., Williams, R.S., and Lee, M.S. (2004). Interactions between BRCT repeats and phosphoproteins: tangled up in two. Trends Biochem Sci *29*, 579-585.

Gould, K.L., Ren, L., Feoktistova, A.S., Jennings, J.L., and Link, A.J. (2004). Tandem affinity purification and identification of protein complex components. Methods *33*, 239-244.

Greenspan, R. (2004). Fly pushing: the theory and practice of Drosophila genetics. booksgooglecom.

Grenningloh, G., Rehm, E.J., and Goodman, C.S. (1991). Genetic analysis of growth cone guidance in Drosophila: fasciclin II functions as a neuronal recognition molecule. Cell *67*, 45-57.

Grumbling, G., and Strelets, V. (2006). FlyBase: anatomical data, images and queries. Nucleic Acids Res *34*, D484-488.

Harper, J.W., Burton, J.L., and Solomon, M.J. (2002). The anaphase-promoting complex: it's not just for mitosis any more. Genes Dev *16*, 2179-2206.

Hartl, T.A., Sweeney, S.J., Knepler, P.J., and Bosco, G. (2008). Condensin II resolves chromosomal associations to enable anaphase I segregation in Drosophila male meiosis. PLoS Genet *4*, e1000228.

Hawley, R.S., and Gilliland, W.D. (2006). Sometimes the result is not the answer: the truths and the lies that come from using the complementation test. Genetics *174*, 5-15.

Hayes, M.J., Kimata, Y., Wattam, S.L., Lindon, C., Mao, G., Yamano, H., and Fry, A.M. (2006). Early mitotic degradation of Nek2A depends on Cdc20-independent interaction with the APC/C. Nat Cell Biol *8*, 607-614.

Hemerly, A.S., Prasanth, S.G., Siddiqui, K., and Stillman, B. (2009). Orc1 controls centriole and centrosome copy number in human cells. Science *323*, 789-793.

Hirano, T. (2005). Condensins: organizing and segregating the genome. Curr Biol *15*, R265-275.

Hung, L.-Y., Chen, H.-L., Chang, C.-W., Li, B.-R., and Tang, T.K. (2004). Identification of a novel microtubule-destabilizing motif in CPAP that binds to tubulin heterodimers and inhibits microtubule assembly. Mol Biol Cell *15*, 2697-2706.

Huyton, T., Bates, P.A., Zhang, X., Sternberg, M.J., and Freemont, P.S. (2000). The BRCA1 C-terminal domain: structure and function. Mutat Res *460*, 319-332.

Ivanovska, I., Khandan, T., Ito, T., and Orr-Weaver, T.L. (2005). A histone code in meiosis: the histone kinase, NHK-1, is required for proper chromosomal architecture in Drosophila oocytes. Genes Dev *19*, 2571-2582.

Jackson, A.P., Eastwood, H., Bell, S.M., Adu, J., Toomes, C., Carr, I.M., Roberts, E., Hampshire, D.J., Crow, Y.J., Mighell, A.J.*, et al.* (2002). Identification of microcephalin, a protein implicated in determining the size of the human brain. Am J Hum Genet *71*, 136-142.

Jacobs, H., Richter, D., Venkatesh, T., and Lehner, C. (2002). Completion of mitosis requires neither fzr/rap nor fzr2, a male germline-specific Drosophila Cdh1 homolog. Current Biology *12*, 1435-1441.

Jaklevic, B.R., and Su, T.T. (2004). Relative contribution of DNA repair, cell cycle checkpoints, and cell death to survival after DNA damage in Drosophila larvae. Curr Biol *14*, 23-32.

Jeffers, L.J., Coull, B.J., Stack, S.J., and Morrison, C.G. (2008). Distinct BRCT domains in Mcph1/Brit1 mediate ionizing radiation-induced focus formation and centrosomal localization. Oncogene *27*, 139-144.

Jha, S., and Dutta, A. (2009). RVB1/RVB2: running rings around molecular biology. Mol Cell *34*, 521-533.

Jiang, X., Xia, L., Chen, D., Yang, Y., Huang, H., Yang, L., Zhao, Q., Shen, L., Wang, J., and Chen, D. (2008). Otefin, a nuclear membrane protein, determines the fate of germline stem cells in Drosophila via interaction with Smad complexes. Dev Cell *14*, 494-506.

Kalderon, D. (2004). Hedgehog signaling: Costal-2 bridges the transduction gap. Curr Biol *14*, R67-69.

Karagiannis, T.C., and El-Osta, A. (2004). Double-strand breaks: signaling pathways and repair mechanisms. Cell Mol Life Sci *61*, 2137-2147.

Karamysheva, Z., Diaz-Martinez, L.A., Crow, S.E., Li, B., and Yu, H. (2008). Multiple Anaphase-promoting Complex/Cyclosome Degrons Mediate the Degradation of Human Sgo1. Journal of Biological Chemistry *284*, 1772-1780.

Kent, D., Bush, E.W., and Hooper, J.E. (2006). Roadkill attenuates Hedgehog responses through degradation of Cubitus interruptus. Development *133*, 2001-2010.

Khorasanizadeh, S. (2004). The nucleosome: from genomic organization to genomic regulation. Cell *116*, 259-272.

Kim, H., Lee, O.-H., Xin, H., Chen, L.-Y., Qin, J., Chae, H.K., Lin, S.-Y., Safari, A., Liu, D., and Songyang, Z. (2009). TRF2 functions as a protein hub and regulates telomere maintenance by recognizing specific peptide motifs. Nat Struct Mol Biol *16*, 372-379.

King, R.W., Deshaies, R.J., Peters, J.M., and Kirschner, M.W. (1996). How proteolysis drives the cell cycle. Science *274*, 1652-1659.

King, R.W., Jackson, P.K., and Kirschner, M.W. (1994). Mitosis in transition. Cell *79*, 563-571.

King, R.W., Lustig, K.D., Stukenberg, P.T., McGarry, T.J., and Kirschner, M.W. (1997). Expression cloning in the test tube. Science *277*, 973-974.

King, R.W., Peters, J.M., Tugendreich, S., Rolfe, M., Hieter, P., and Kirschner, M.W. (1995). A 20S complex containing CDC27 and CDC16 catalyzes the mitosis-specific conjugation of ubiquitin to cyclin B. Cell *81*, 279-288.

Klattenhoff, C., and Theurkauf, W. (2008). Biogenesis and germline functions of piRNAs. Development *135*, 3-9.

Koundakjian, E.J., Cowan, D.M., Hardy, R.W., and Becker, A.H. (2004). The Zuker collection: a resource for the analysis of autosomal gene function in Drosophila melanogaster. Genetics *167*, 203-206.

Krämer, A., Mailand, N., Lukas, C., Syljuåsen, R.G., Wilkinson, C.J., Nigg, E.A., Bartek, J., and Lukas, J. (2004). Centrosome-associated Chk1 prevents premature activation of cyclin-B-Cdk1 kinase. Nat Cell Biol *6*, 884-891.

Krashes, M.J., Keene, A.C., Leung, B., Armstrong, J.D., and Waddell, S. (2007). Sequential use of mushroom body neuron subsets during drosophila odor memory processing. Neuron *53*, 103-115.

Krause, S.A., Loupart, M.L., Vass, S., Schoenfelder, S., Harrison, S., and Heck, M.M. (2001). Loss of cell cycle checkpoint control in Drosophila Rfc4 mutants. Mol Cell Biol *21*, 5156-5168.

Kumar, A., Markandaya, M., and Girimaji, S.C. (2002). Primary microcephaly: microcephalin and ASPM determine the size of the human brain. J Biosci *27*, 629-632.

Lai, C., McMahon, R., Young, C., Mackay, T.F., and Langley, C.H. (1998). quemao, a Drosophila bristle locus, encodes geranylgeranyl pyrophosphate synthase. Genetics *149*, 1051-1061.

LaRocque, J.R., Jaklevic, B., Su, T.T., and Sekelsky, J. (2007). Drosophila ATR in double-strand break repair. Genetics *175*, 1023-1033.

Lee, L.A., Lee, E., Anderson, M.A., Vardy, L., Tahinci, E., Ali, S.M., Kashevsky, H., Benasutti, M., Kirschner, M.W., and Orr-Weaver, T.L. (2005). Drosophila genome-scale screen for PAN GU kinase substrates identifies Mat89Bb as a cell cycle regulator. Dev Cell *8*, 435-442.

Lee, L.A., and Orr-Weaver, T.L. (2003). Regulation of cell cycles in Drosophila development: intrinsic and extrinsic cues. Annu Rev Genet *37*, 545-578.

Lee, L.A., Van Hoewyk, D., and Orr-Weaver, T.L. (2003). The Drosophila cell cycle kinase PAN GU forms an active complex with PLUTONIUM and GNU to regulate embryonic divisions. Genes Dev *17*, 2979-2991.

Li, K., and Kaufman, T.C. (1996). The homeotic target gene centrosomin encodes an essential centrosomal component. Cell *85*, 585-596.

Liang, Y., Gao, H., Lin, S.-Y., Peng, G., Huang, X., Zhang, P., Goss, J.A., Brunicardi, F.C., Multani, A.S., Chang, S.*, et al.* (2010). BRIT1/MCPH1 is essential for mitotic and meiotic recombination DNA repair and maintaining genomic stability in mice. PLoS Genet *6*, e1000826.

Lim, A.K., Tao, L., and Kai, T. (2009). piRNAs mediate posttranscriptional retroelement silencing and localization to pi-bodies in the Drosophila germline. J Cell Biol *186*, 333-342.

Lin, S.-Y., Rai, R., Li, K., Xu, Z.-X., and Elledge, S.J. (2005). BRIT1/MCPH1 is a DNA damage responsive protein that regulates the Brca1-Chk1 pathway, implicating checkpoint dysfunction in microcephaly. Proc Natl Acad Sci USA *102*, 15105-15109.

Lin, S.Y., and Elledge, S.J. (2003). Multiple tumor suppressor pathways negatively regulate telomerase. Cell *113*, 881-889.

Liu, Q.-X., Jindra, M., Ueda, H., Hiromi, Y., and Hirose, S. (2003). Drosophila MBF1 is a co-activator for Tracheae Defective and contributes to the formation of tracheal and nervous systems. Development *130*, 719-728.

Lorca, T., Castro, A., Martinez, A.M., Vigneron, S., Morin, N., Sigrist, S., Lehner, C., Dorée, M., and Labbé, J.C. (1998). Fizzy is required for activation of the APC/cyclosome in Xenopus egg extracts. EMBO J *17*, 3565-3575.

Lupo, R., Breiling, A., Bianchi, M.E., and Orlando, V. (2001). Drosophila chromosome condensation proteins Topoisomerase II and Barren colocalize with Polycomb and maintain Fab-7 PRE silencing. Mol Cell *7*, 127-136.

Lustig, McGarry, T., King, R., Kuang, J., and Kirschner, M. (1997). Systematic identification of mitotic phosphoproteins. Current Biology.

Machado, C., and Andrew, D.J. (2000). D-Titin: a giant protein with dual roles in chromosomes and muscles. J Cell Biol *151*, 639-652.

Mailand, N., and Diffley, J.F.X. (2005). CDKs promote DNA replication origin licensing in human cells by protecting Cdc6 from APC/C-dependent proteolysis. Cell *122*, 915-926.

Manke, I.A., Lowery, D.M., Nguyen, A., and Yaffe, M.B. (2003). BRCT repeats as phosphopeptide-binding modules involved in protein targeting. Science *302*, 636-639.

Mansfield, J.H., Wilhelm, J.E., and Hazelrigg, T. (2002). Ypsilon Schachtel, a Drosophila Y-box protein, acts antagonistically to Orb in the oskar mRNA localization and translation pathway. Development *129*, 197-209.

Masrouha, N., Yang, L., Hijal, S., Larochelle, S., and Suter, B. (2003). The Drosophila chk2 gene loki is essential for embryonic DNA double-strand-break checkpoints induced in S phase or G2. Genetics *163*, 973-982.

Megraw, T.L., Li, K., Kao, L.R., and Kaufman, T.C. (1999). The centrosomin protein is required for centrosome assembly and function during cleavage in Drosophila. Development *126*, 2829-2839.

Merkle, J.A., Rickmyre, J.L., Garg, A., Loggins, E.B., Jodoin, J.N., Lee, E., Wu, L.P., and Lee, L.A. (2009). no poles encodes a predicted E3 ubiquitin ligase required for early embryonic development of Drosophila. Development *136*, 449-459.

Moore, D.P., Page, A.W., Tang, T.T., Kerrebrock, A.W., and Orr-Weaver, T.L. (1998). The cohesion protein MEI-S332 localizes to condensed meiotic and mitotic centromeres until sister chromatids separate. J Cell Biol *140*, 1003-1012.

Morrison, A.J., and Shen, X. (2009). Chromatin remodelling beyond transcription: the INO80 and SWR1 complexes. Nat Rev Mol Cell Biol *10*, 373-384.

Murray, A.W., Solomon, M.J., and Kirschner, M.W. (1989). The role of cyclin synthesis and degradation in the control of maturation promoting factor activity. Nature *339*, 280-286.

Newport, J., and Kirschner, M. (1982). A major developmental transition in early Xenopus embryos: II. Control of the onset of transcription. Cell *30*, 687-696.

Nyberg, K.A., Michelson, R.J., Putnam, C.W., and Weinert, T.A. (2002). Toward maintaining the genome: DNA damage and replication checkpoints. Annu Rev Genet *36*, 617-656.

O'Driscoll, M., Ruiz-Perez, V.L., Woods, C.G., Jeggo, P.A., and Goodship, J.A. (2003). A splicing mutation affecting expression of ataxia-telangiectasia and Rad3-related protein (ATR) results in Seckel syndrome. Nat Genet *33*, 497-501.

O'Farrell, P.H., Stumpff, J., and Su, T.T. (2004). Embryonic cleavage cycles: how is a mouse like a fly? Curr Biol *14*, R35-45.

Oh, S.-W., Kingsley, T., Shin, H.-h., Zheng, Z., Chen, H.-W., Chen, X., Wang, H., Ruan, P., Moody, M., and Hou, S.X. (2003). A P-element insertion screen identified mutations in 455 novel essential genes in Drosophila. Genetics *163*, 195-201.

Oikemus, S.R., McGinnis, N., Queiroz-Machado, J., Tukachinsky, H., Takada, S., Sunkel, C.E., and Brodsky, M.H. (2004). Drosophila atm/telomere fusion is required for telomeric localization of HP1 and telomere position effect. Genes Dev *18*, 1850-1861.

Okamura, K., Ishizuka, A., Siomi, H., and Siomi, M.C. (2004). Distinct roles for Argonaute proteins in small RNA-directed RNA cleavage pathways. Genes Dev *18*, 1655-1666.

Oliveira, R.A., Heidmann, S., and Sunkel, C.E. (2007). Condensin I binds chromatin early in prophase and displays a highly dynamic association with Drosophila mitotic chromosomes. Chromosoma *116*, 259-274.

Ono, T., Losada, A., Hirano, M., Myers, M.P., Neuwald, A.F., and Hirano, T. (2003). Differential contributions of condensin I and condensin II to mitotic chromosome architecture in vertebrate cells. Cell *115*, 109-121.

Orihara-Ono, M., Suzuki, E., Saito, M., Yoda, Y., Aigaki, T., and Hama, C. (2005). The slender lobes gene, identified by retarded mushroom body development, is required for proper nucleolar organization in Drosophila. Dev Biol *281*, 121-133.

Ozgen, H., van Daalen, E., Bolton, P., Maloney, V., Huang, S., Cresswell, L., Van Den Boogaard, M., Eleveld, M., Van 'T Slot, R., Hochstenbach, R.*, et al.* (2009). Copy

number changes of the microcephalin 1 gene (MCPH1) in patients with autism spectrum disorders. Clin Genet *76*, 348-356.

Pasyukova, E.G., Roshina, N.V., and Mackay, T.F.C. (2004). Shuttle craft: a candidate quantitative trait gene for Drosophila lifespan. Aging Cell *3*, 297-307.

Patterson, L.F., Harvey, M., and Lasko, P.F. (1992). Dbp73D, a Drosophila gene expressed in ovary, encodes a novel D-E-A-D box protein. Nucleic Acids Res *20*, 3063-3067.

Peng, G., Yim, E.-K., Dai, H., Jackson, A.P., Burgt, I.v.d., Pan, M.-R., Hu, R., Li, K., and Lin, S.-Y. (2009). BRIT1/MCPH1 links chromatin remodelling to DNA damage response. Nat Cell Biol *11*, 865-872.

Petermann, E., and Caldecott, K.W. (2006). Evidence that the ATR/Chk1 pathway maintains normal replication fork progression during unperturbed S phase. Cell Cycle *5*, 2203-2209.

Peterson, C.L., and Tamkun, J.W. (1995). The SWI-SNF complex: a chromatin remodeling machine? Trends Biochem Sci *20*, 143-146.

Pfaff, K.L., Straub, C.T., Chiang, K., Bear, D.M., Zhou, Y., and Zon, L.I. (2007). The zebra fish cassiopeia mutant reveals that SIL is required for mitotic spindle organization. Mol Cell Biol *27*, 5887-5897.

Pfleger, C.M., and Kirschner, M.W. (2000). The KEN box: an APC recognition signal distinct from the D box targeted by Cdh1. Genes Dev *14*, 655-665.

Pflumm, M.F., and Botchan, M.R. (2001). Orc mutants arrest in metaphase with abnormally condensed chromosomes. Development *128*, 1697-1707.

Pinto, B.S., Wilmington, S.R., Hornick, E.E.L., Wallrath, L.L., and Geyer, P.K. (2008). Tissue-specific defects are caused by loss of the Drosophila MAN1 LEM domain protein. Genetics *180*, 133-145.

Ponting, C., and Jackson, A.P. (2005). Evolution of primary microcephaly genes and the enlargement of primate brains. Curr Opin Genet Dev *15*, 241-248.

Price, D., Rabinovitch, S., O'Farrell, P.H., and Campbell, S.D. (2000). Drosophila wee1 has an essential role in the nuclear divisions of early embryogenesis. Genetics *155*, 159-166.

Puig, O., Caspary, F., Rigaut, G., Rutz, B., Bouveret, E., Bragado-Nilsson, E., Wilm, M., and Séraphin, B. (2001). The tandem affinity purification (TAP) method: a general procedure of protein complex purification. Methods *24*, 218-229.

Purdy, A., Uyetake, L., Cordeiro, M.G., and Su, T.T. (2005). Regulation of mitosis in response to damaged or incompletely replicated DNA require different levels of Grapes (Drosophila Chk1). J Cell Sci *118*, 3305-3315.

Raff, J.W., and Glover, D.M. (1988). Nuclear and cytoplasmic mitotic cycles continue in Drosophila embryos in which DNA synthesis is inhibited with aphidicolin. J Cell Biol *107*, 2009-2019.

Raffa, G.D., Cenci, G., Siriaco, G., Goldberg, M.L., and Gatti, M. (2005). The putative Drosophila transcription factor woc is required to prevent telomeric fusions. Mol Cell *20*, 821-831.

Rai, R., Dai, H., Multani, A.S., Li, K., Chin, K., Gray, J., Lahad, J.P., Liang, J., Mills, G.B., Meric-Bernstam, F*., et al.* (2006). BRIT1 regulates early DNA damage response, chromosomal integrity, and cancer. Cancer Cell *10*, 145-157.

Rai, R., Phadnis, A., Haralkar, S., Badwe, R.A., Dai, H., Li, K., and Lin, S.-Y. (2008). Differential regulation of centrosome integrity by DNA damage response proteins. Cell Cycle *7*, 2225-2233.

Rankin, S., Ayad, N.G., and Kirschner, M.W. (2005). Sororin, a substrate of the anaphase-promoting complex, is required for sister chromatid cohesion in vertebrates. Mol Cell *18*, 185-200.

Rape, M., Reddy, S.K., and Kirschner, M.W. (2006). The processivity of multiubiquitination by the APC determines the order of substrate degradation. Cell *124*, 89-103.

Reim, I., Mattow, J., and Saumweber, H. (1999). The RRM protein NonA from Drosophila forms a complex with the RRM proteins Hrb87F and S5 and the Zn finger protein PEP on hnRNA. Exp Cell Res *253*, 573-586.

Remillieux-Leschelle, N., Santamaria, P., and Randsholt, N.B. (2002). Regulation of larval hematopoiesis in Drosophila melanogaster: a role for the multi sex combs gene. Genetics *162*, 1259-1274.

Renault, A.D., Zhang, X.-H., Alphey, L.S., Frenz, L.M., Glover, D.M., Saunders, R.D.C., and Axton, J.M. (2003). giant nuclei is essential in the cell cycle transition from meiosis to mitosis. Development *130*, 2997-3005.

Richards, M.W., Leung, J.W.C., Roe, S.M., Li, K., Chen, J., and Bayliss, R. (2010). A pocket on the surface of the N-terminal BRCT domain of Mcph1 is required to prevent abnormal chromosome condensation. J Mol Biol *395*, 908-915.

Rickmyre, J., DasGupta, S., Ooi, D., and Keel, J. (2007). The Drosophila homolog of MCPH1, a human microcephaly gene, is required for genomic stability in the early embryo. J Cell Sci *120*, 3565-3577.

Riparbelli, M.G., Callaini, G., Glover, D.M., and Avides, M.d.C. (2002). A requirement for the Abnormal Spindle protein to organise microtubules of the central spindle for cytokinesis in Drosophila. J Cell Sci *115*, 913-922.

Ripoll, P., Pimpinelli, S., Valdivia, M.M., and Avila, J. (1985). A cell division mutant of Drosophila with a functionally abnormal spindle. Cell *41*, 907-912.

Rørth, P. (1998a). Gal4 in the Drosophila female germline. Mechanisms of development *78*, 113-118.

Rørth, P. (1998b). Gal4 in the Drosophila female germline. Mechanisms of development.

Satterfield, T.F., and Pallanck, L.J. (2006). Ataxin-2 and its Drosophila homolog, ATX2, physically assemble with polyribosomes. Hum Mol Genet *15*, 2523-2532.

Saunders, R.D., Avides, M.C., Howard, T., Gonzalez, C., and Glover, D.M. (1997). The Drosophila gene abnormal spindle encodes a novel microtubule-associated protein that associates with the polar regions of the mitotic spindle. J Cell Biol *137*, 881-890.

Shirayama, M., Tóth, A., Gálová, M., and Nasmyth, K. (1999). APC(Cdc20) promotes exit from mitosis by destroying the anaphase inhibitor Pds1 and cyclin Clb5. Nature *402*, 203-207.

Sibon, O.C., Kelkar, A., Lemstra, W., and Theurkauf, W.E. (2000). DNA-replication/DNA-damage-dependent centrosome inactivation in Drosophila embryos. Nat Cell Biol *2*, 90-95.

Sibon, O.C., Laurençon, A., Hawley, R., and Theurkauf, W.E. (1999). The Drosophila ATM homologue Mei-41 has an essential checkpoint function at the midblastula transition. Curr Biol *9*, 302-312.

Sibon, O.C., Stevenson, V.A., and Theurkauf, W.E. (1997). DNA-replication checkpoint control at the Drosophila midblastula transition. Nature *388*, 93-97.

Silva, E., Tiong, S., Pedersen, M., Homola, E., Royou, A., Fasulo, B., Siriaco, G., and Campbell, S.D. (2004). ATM is required for telomere maintenance and chromosome stability during Drosophila development. Curr Biol *14*, 1341-1347.

Simpson-Lavy, K.J., Oren, Y.S., Feine, O., Sajman, J., Listovsky, T., and Brandeis, M. (2010). Fifteen years of APC/cyclosome: a short and impressive biography. Biochem Soc Trans *38*, 78-82.

Stein, J.A., Broihier, H.T., Moore, L.A., and Lehmann, R. (2002). Slow as molasses is required for polarized membrane growth and germ cell migration in Drosophila. Development *129*, 3925-3934.

Stumpff, J., Duncan, T., Homola, E., Campbell, S.D., and Su, T.T. (2004). Drosophila Wee1 kinase regulates Cdk1 and mitotic entry during embryogenesis. Curr Biol *14*, 2143-2148.

Su, T.T., Campbell, S.D., and O'Farrell, P.H. (1999). Drosophila grapes/CHK1 mutants are defective in cyclin proteolysis and coordination of mitotic events. Curr Biol *9*, 919-922.

Su, T.T., Parry, D.H., Donahoe, B., Chien, C.T., O'Farrell, P.H., and Purdy, A. (2001). Cell cycle roles for two 14-3-3 proteins during Drosophila development. J Cell Sci *114*, 3445-3454.

Sullivan, K.M., Scott, K., Zuker, C.S., and Rubin, G.M. (2000). The ryanodine receptor is essential for larval development in Drosophila melanogaster. Proc Natl Acad Sci USA *97*, 5942-5947.

Tadros, W., Goldman, A.L., Babak, T., Menzies, F., Vardy, L., Orr-Weaver, T., Hughes, T.R., Westwood, J.T., Smibert, C.A., and Lipshitz, H.D. (2007). SMAUG is a major regulator of maternal mRNA destabilization in Drosophila and its translation is activated by the PAN GU kinase. Dev Cell *12*, 143-155.

Takada, S., Kelkar, A., and Theurkauf, W.E. (2003). Drosophila checkpoint kinase 2 couples centrosome function and spindle assembly to genomic integrity. Cell *113*, 87-99.

Taylor, R.M., Moore, D.J., Whitehouse, J., Johnson, P., and Caldecott, K.W. (2000). A cell cycle-specific requirement for the XRCC1 BRCT II domain during mammalian DNA strand break repair. Mol Cell Biol *20*, 735-740.

Terada, Y., Uetake, Y., and Kuriyama, R. (2003). Interaction of Aurora-A and centrosomin at the microtubule-nucleating site in Drosophila and mammalian cells. J Cell Biol *162*, 757-763.

Thornton, B.R., and Toczyski, D.P. (2006). Precise destruction: an emerging picture of the APC. Genes Dev *20*, 3069-3078.

Tibelius, A., Marhold, J., Zentgraf, H., Heilig, C.E., Neitzel, H., Ducommun, B., Rauch, A., Ho, A.D., Bartek, J., and Krämer, A. (2009). Microcephalin and pericentrin regulate mitotic entry via centrosome-associated Chk1. J Cell Biol *185*, 1149-1157.

Tolias, P.P., and Stroumbakis, N.D. (1998). The Drosophila zygotic lethal gene shuttle craft is required maternally for proper embryonic development. Dev Genes Evol *208*, 274-282.

Treier, M., Staszewski, L.M., and Bohmann, D. (1994). Ubiquitin-dependent c-Jun degradation in vivo is mediated by the delta domain. Cell *78*, 787-798.

Trimborn, M., Bell, S.M., Felix, C., Rashid, Y., Jafri, H., Griffiths, P.D., Neumann, L.M., Krebs, A., Reis, A., Sperling, K.*, et al.* (2004). Mutations in microcephalin cause aberrant regulation of chromosome condensation. Am J Hum Genet *75*, 261-266.

Trimborn, M., Ghani, M., Walther, D.J., Dopatka, M., Dutrannoy, V., Busche, A., Meyer, F., Nowak, S., Nowak, J., Zabel, C.*, et al.* (2010). Establishment of a mouse model with misregulated chromosome condensation due to defective Mcph1 function. PLoS ONE *5*, e9242.

Trimborn, M., Schindler, D., Neitzel, H., and Hirano, T. (2006). Misregulated chromosome condensation in MCPH1 primary microcephaly is mediated by condensin II. Cell Cycle *5*, 322-326.

Urata, Y., Parmelee, S.J., Agard, D.A., and Sedat, J.W. (1995). A three-dimensional structural dissection of Drosophila polytene chromosomes. J Cell Biol *131*, 279-295.

Vernì, F., Somma, M.P., Gunsalus, K.C., Bonaccorsi, S., Belloni, G., Goldberg, M.L., and Gatti, M. (2004). Feo, the Drosophila homolog of PRC1, is required for central-spindle formation and cytokinesis. Curr Biol *14*, 1569-1575.

Wakefield, J.G., Bonaccorsi, S., and Gatti, M. (2001). The drosophila protein asp is involved in microtubule organization during spindle formation and cytokinesis. J Cell Biol *153*, 637-648.

Wang, Y.-Q., and Su, B. (2004). Molecular evolution of microcephalin, a gene determining human brain size. Hum Mol Genet *13*, 1131-1137.

Williams, B.R., Bateman, J.R., Novikov, N.D., and Wu, C.-T. (2007). Disruption of topoisomerase II perturbs pairing in drosophila cell culture. Genetics *177*, 31-46.

Wood, J.L., Liang, Y., Li, K., and Chen, J. (2008). Microcephalin/MCPH1 associates with the Condensin II complex to function in homologous recombination repair. J Biol Chem *283*, 29586-29592.

Wood, J.L., Singh, N., Mer, G., and Chen, J. (2007). MCPH1 functions in an H2AX-dependent but MDC1-independent pathway in response to DNA damage. J Biol Chem *282*, 35416-35423.

Woods, C.G. (2004). Human microcephaly. Curr Opin Neurobiol *14*, 112-117.

Woods, C.G., Bond, J., and Enard, W. (2005). Autosomal recessive primary microcephaly (MCPH): a review of clinical, molecular, and evolutionary findings. Am J Hum Genet *76*, 717-728.

Worringer, K.A., and Panning, B. (2007). Zinc finger protein Zn72D promotes productive splicing of the maleless transcript. Mol Cell Biol *27*, 8760-8769.

Wu, X., Mondal, G., Wang, X., Wu, J., Yang, L., Pankratz, V.S., Rowley, M., and Couch, F.J. (2009). Microcephalin regulates BRCA2 and Rad51-associated DNA double-strand break repair. Cancer Res *69*, 5531-5536.

Xu, J., Xin, S., and Du, W. (2001). Drosophila Chk2 is required for DNA damage-mediated cell cycle arrest and apoptosis. FEBS Lett *508*, 394-398.

Xu, X., Lee, J., and Stern, D.F. (2004). Microcephalin is a DNA damage response protein involved in regulation of CHK1 and BRCA1. J Biol Chem *279*, 34091-34094.

Yang, S.-Z., Lin, F.-T., and Lin, W.-C. (2008). MCPH1/BRIT1 cooperates with E2F1 in the activation of checkpoint, DNA repair and apoptosis. EMBO Rep *9*, 907-915.

Yu, K.R., Saint, R.B., and Sullivan, W. (2000). The Grapes checkpoint coordinates nuclear envelope breakdown and chromosome condensation. Nat Cell Biol *2*, 609-615.

Yu, X., Chini, C.C.S., He, M., Mer, G., and Chen, J. (2003). The BRCT domain is a phospho-protein binding domain. Science *302*, 639-642.

Zhang, Y.Q., and Broadie, K. (2005). Fathoming fragile X in fruit flies. Trends Genet *21*, 37-45.

Zhong, X., Pfeifer, G.P., and Xu, X. (2006). Microcephalin encodes a centrosomal protein. Cell Cycle *5*, 457-458.

Zur, A., and Brandeis, M. (2001). Securin degradation is mediated by fzy and fzr, and is required for complete chromatid separation but not for cytokinesis. EMBO J *20*, 792-801.